NITRIC OXIDE-INDUCED CARDIOMYOCYTE CELL DEATH

by

SHAUN SCOTT KLASSEN

B.Sc., University of British Columbia, 2001

A THESIS SUBMITTED IN PARTIAL FULFILLMENT OF
THE REQUIREMENTS FOR THE DEGREE OF

MASTER OF SCIENCE

in

THE FACULTY OF GRADUATE STUDIES

(Experimental Medicine)

THE UNIVERSITY OF BRITISH COLUMBIA

December 2006

© Shaun Scott Klassen, 2006

ABSTRACT

Nitric oxide (NO), a regulator of diverse cardiovascular functions, modifies cardiac cell viability through mechanisms that remain uncertain. Several pathways were studied to understand these effects. The possibility that the protein p53 is involved in the cardiomyocyte response to the NO donor s-nitrosoglutathione (GSNO) or the peroxynitrite donor 3-morpholinosydnonimine (SIN-1) was explored. These donors induced a concentration-dependent increase of cell death in cultured embryonic chick cardiomyocytes. Expression of p53 protein was increased in response to GSNO, specifically in the nucleus. GSNO also caused DNA damage, but pifithrin, an inhibitor of p53 transactivation activity, did not alter the extent of this damage or cell death. Therefore, the role of increased nuclear p53 in response to NO and NO-induced DNA damage may not be specifically operative in NO-induced cell death. The action of GSNO also appears independent of mitochondrial pathways in cell death, as there was no association of p53 with the mitochondria. Neither GSNO- or SIN-1-induced cell death was altered by cyclosporin A, suggesting that permeability transition pore opening is not operative in these modes of induction of death. In contrast to SIN-1, GSNO did not reduce mitochondrial transmembrane potential, implying separate mechanisms of cell death. Immunocytochemistry demonstrated increased amounts of nitrotyrosine in response to GSNO or SIN-1, confirmed by Western blot following SIN-1. FeTPPS, an isomerase that converts peroxynitrite into the less toxic nitrate, produced a significant reduction of SIN-1-induced cell death and cellular protein nitration. FeTPPS did not reduce cell death from GSNO alone, but did from the combination of GSNO and hydrogen peroxide, a condition which promotes the generation of peroxynitrite. In summary, NO-induced cardiomyocyte cell death is due in part to the disruption of normal cellular functions by nitration of key proteins. Peroxynitrite decomposition reduces protein nitration and cell death, while p53 appears functions independent of the mitochondria or gene transactivation and may act in other pathways, such as cell repair.

TABLE OF CONTENTS

ABSTRACT ii

TABLE OF CONTENTS iii

LIST OF TABLES vi

LIST OF FIGURES vii

LIST OF ABBREVIATIONS viii

ACKNOWLEDGEMENTS ix

1.0 INTRODUCTION 1

1.1 Cell death 1

1.2 Nitric oxide 2

1.2.1 What is nitric oxide? 2

1.2.2 Nitric oxide synthesis 3

1.2.3 Nitric oxide causes DNA damage 4

1.2.4 Nitric oxide modifies protein structure and function 4

1.2.5 Nitric oxide and necrosis 6

1.2.6 Nitric oxide and apoptosis 7

1.2.6.1 Nitric oxide induces mitochondrial-based apoptotic effects 7

1.2.6.2 Nitric oxide modifies extrinsic apoptotic pathway mechanisms 8

1.2.6.3 Nitric oxide modifies caspase activation 8

1.2.6.4 Nitric oxide modifies cGMP signaling 9

1.2.7 Relationship of NO to the cardiovascular system 10

1.3 Tumor Suppressor p53 12

1.3.1 What is p53? 12

1.3.2 Negative regulators of p53 13

1.3.3 Positive regulators of p53 14

1.3.4 p53 causes apoptosis via transcriptional regulation 15

1.3.5 p53 mediates apoptosis through transcription-independent events 18

1.3.6 p53 causes cell cycle arrest 20

1.3.7 p53 regulates DNA repair 21

1.4 Nitric oxide induces p53-dependent mechanisms 22

Tables 24

2.0 AIM, HYPOTHESES, AND RATIONALE 25

3.0 EXPERIMENTAL MATERIALS AND METHODS 27

3.1 Materials 27

3.2 Embryonic chick cardiomyocyte culture 27

3.3 MTT Assay 28

3.4 Western Blots 29

3.5 Comet Assay 30

3.6 Microscopy - DePsipher™ Staining 32

3.7 Microscopy – Wright Giemsa Staining 32

3.8 Microscopy – Immunocytochemistry 33

3.9 Griess Assay 33
3.10 Data Analysis 33
4.0 RESULTS 34
4.1 GSNO releases NO 34
4.2 GSNO induces cell death 34
4.3 GSNO causes morphological changes 34
4.4 GSNO causes an increase in p53 expression 35
4.5 GSNO does not produce p53 translocation from cytosol to mitochondria 35
4.6 GSNO does not cause major cytochrome c release from mitochondria 36
4.7 GSNO does not cause a change in mitochondrial potential 36
4.8 Cyclosporin A does not reduce GSNO-induced cell death 36
4.9 GSNO causes nuclear p53 accumulation 37
4.10 p53 inhibition does not reduce GSNO-induced cell death 37
4.11 Pifithrin does not reduce GSNO-induced DNA fragmentation 38
4.12 SIN-1 causes nitrite accumulation in solution 38
4.13 SIN-1 induces cell death 39
4.14 SIN-1-induced cell death is increased by H_2O_2 39
4.15 FeTPPS reduces cell death caused by SIN-1 and SIN-1 / H_2O_2 40
4.16 FeTPPS reduces cell death induced by the combination of GSNO and H_2O_2 41
4.17 FeTPPS reduces H_2O_2-induced cell death 41
4.18 Pifithrin does not reduce SIN-1-induced cell death 42
4.19 Cyclosporin A does not reduce SIN-1-induced cell death 42
4.20 SIN-1 causes a reduction of mitochondrial transmembrane potential 42
4.21 Protein tyrosine nitration 43
Figures 45
5.0 DISCUSSION 75
5.1 GSNO 75
5.2 SIN-1 76
5.3 Griess reaction results 77
5.4 GSNO induces cardiac cell death 79
5.5 SIN-1 induces cardiac cell death 79
5.6 H_2O_2 enhances GSNO-induced cell death 80
5.7 FeTPPS 81
5.8 FeTPPS reduces SIN-1-induced and GSNO plus H_2O_2-induced cell death 82
5.9 FeTPPS reduces H_2O_2-induced cell death 83
5.10 GSNO produces an increase in p53 expression in the cell 84

5.11 GSNO produces an accumulation of p53 in the nucleus 84
5.12 NO-induced cell death was not altered by pifithrin 85
5.13 GSNO induces DNA fragmentation 86
5.14 GSNO-induced DNA damage is not altered by pifithrin 87
5.15 GSNO does not induce cell death through the mitochondrial death pathway 88
5.16 SIN-1 causes a reduction of mitochondrial transmembrane potential 91
5.17 NO increases cellular protein tyrosine nitration 92
5.18 Limitations of the study 93
5.19 Summary 95
Figures 98
REFERENCES 104

LIST OF TABLES

FIGURE	TITLE	PAGE
1	Nitric oxide and relevant derivatives	24

LIST OF FIGURES

FIGURE	TITLE	PAGE
1	GSNO releases NO in solution	45
2	GSNO induces cell death	46
3	GSNO causes changes in cellular morphology	47
4	GSNO causes an increase in p53 expression	48
5	GSNO causes a time-dependent increase in p53 expression	49
6	GSNO causes no p53 translocation from cytosol to mitochondria	50
7	GSNO causes no cytochrome c translocation from mitochondria to cytosol	51
8	GSNO does not alter mitochondrial membrane potential	52
9	Cyclosporin A does not affect GSNO-induced cell death	53
10	GSNO causes nuclear p53 accumulation	54
11	Pifithrin does not reduce GSNO-induced cell death	55
12	Pifithrin reduces adriamycin-induced p53-dependent DNA and cellular damage	57
13	GSNO causes DNA fragmentation that is not modified by pifithrin	59
14	SIN-1 releases NO in solution	61
15	SIN-1 induces cell death	62
16	H_2O_2 enhances SIN-1-induced cell death	63
17	FeTPPS reduces SIN-1-induced cell death	64
18	Nitrite in solution	65
19	FeTPPS reduces SIN-1/H_2O_2-induced cell death	66
20	FeTPPS reduces GSNO + H_2O_2-induced cell death, but not GSNO-induced cell death	67
21	FeTPPS reduces H_2O_2-induced cell death	68
22	Pifithrin does not affect SIN-1-induced cell death	69
23	Cyclosporin A does not reduce SIN-1-induced cell death	70
24	SIN-1 causes a reduction of mitochondrial transmembrane potential	71
25	FeTPPS reduces SIN-1-induced protein nitration	72
26	FeTPPS reduces SIN-1-induced mitochondrial tyrosine nitration	73
27	FeTPPS reduces SIN-1- and GSNO-induced tyrosine nitration	74
28	S-transnitrosylation mechanism	98
29	SIN-1 decomposition mechanism	99
30	S-transnitrosylation by peroxynitrite	100
31	Thiol oxidation by peroxynitrite	101
32	The Griess reaction	102
33	FeTPPS-mediated peroxynitrite isomerization	103

LIST OF ABBREVIATIONS

ABBREVIATION	DEFINITION
AhR	Aryl hydrocarbon receptor
ANT	Adenine nucleotide translocase
Apaf-1	Apoptotic peptidase activating factor-1
ATM	Ataxia telangiectasia mutated
Bax	Bcl2-associated X protein
Bid	BH3 interacting domain death agonist
CcOx	Cytochrome c oxidase
cGMP	Cyclic guanosine monophosphate
FeTPPS	5,10,15,20-tetrakis(4-sulfonatophenyl)porphyrinato iron (III) chloride
FITC	Fluorescein isothiocyanate
GAPDH	Glyceraldehyde-3-phosphate dehydrogenase
GSNO	S-nitrosoglutathione
H_2O_2	Hydrogen peroxide
HRP	Horseradish peroxidase
$\Delta\Psi_m$	Mitochondrial transmembrane potential
MAPK	Mitogen-activated protein kinase
MDM2	Murine double minute 2
mtNOS	Mitochondrial nitric oxide synthase
NO	Nitric oxide
NOS1	Neuronal nitric oxide synthase
NOS2	Inducible nitric oxide synthase
NOS3	Endothelial nitric oxide synthase
NOXA	For "damage"
PARP	Poly ADP-ribose polymerase
PI3K	Phosphoinositide-3 kinase
PKG	Protein kinase G
PTP	Permeability transition pore
PUMA	p53 upregulated modulator of apoptosis
ROS	Reactive oxygen species
sGC	Soluble guanylate cyclase
SIN-1	3-morpholinosydnonimine
TBS	Tris-buffered saline
TBST	Tris-buffered saline-Tween
VDAC	Voltage-dependent anion channel
YB1	Y-box binding protein 1

ACKNOWLEDGEMENTS

The author would like to thank the following people:

Dr. Simon W. Rabkin – for allowing the author to study in his laboratory, and for giving his time, support, and guidance throughout the project.

Dr. Sammy Chan and Dr. Kuo-Hsing Kuo – for being on the author's supervisory committee and offering valuable suggestions and support for the project.

Dr. Cathy Pang – for being the author's external examiner on short notice, and providing valuable questions and comments.

Michael Luong and Parth Lodhia – for their valuable assistance in running and maintaining the lab.

1.0 INTRODUCTION

1.1 Cell death

Ironically, a critical component of the normal functioning and health of both the organs and the organism as a whole is death at the cellular level. Comparable to the adage of 'survival of the fittest,' the removal of dead or damaged cells ensures that only the healthiest cells comprise the organ, and thus allows the organ to function at maximal capability. Conversely, if damaged cells were allowed to accumulate, as in some disease states, the efficiency of the organ would be reduced, potentially leading to harmful systemic effects of the whole organism. Cell death also plays an important role in developmental stages and in remodeling, particularly in the heart [1]. Thus, mechanisms have evolved to produce cell death and to serve these valuable functions. Unfortunately, in some organs such as the heart, the loss of cells through cell death impairs the function.

Cell death can occur by several mechanisms with different accompanying morphologies, leading to a diverse set of classifications [2]. Historically, apoptosis and necrosis are two of the most studied types of cell death, among others such as autophagy, excitotoxicity, and anoikis [2]. Necrosis involves the general, and oftentimes described as uncontrolled, destruction of the cell, associated with ATP depletion and an inability of the cell to maintain equilibrium and membrane integrity [3], with the release of intracellular contents into the local environment sufficient to cause a local inflammatory response and damage. By contrast, apoptosis occurs in an ATP-dependent manner, and follows a strict set of cellular execution programs that lead to controlled degradation of the cell, without the inflammatory side effects of necrosis. It is further subdivided into extrinsic receptor-mediated apoptosis and intrinsic mitochondria-mediated apoptosis, capable of responding to different stimuli but converging to bring about the same eventual outcome.

These cell death pathways play a crucial role in maintaining the health of the organism throughout its lifetime. However, their activation at inappropriate times can consequently have hugely deleterious effects. As these pathways are highly complex and tightly integrated with one another, ongoing experimentation into the players and their roles is providing us with a greater understanding of the intricacies that underlie this phenomenon.

1.2 Nitric oxide

1.2.1 What is nitric oxide?

Nitric oxide (NO) is an important messenger molecule that plays critical biochemical roles and has a large impact on cellular functions. Consisting merely of an oxygen and nitrogen atom, it is a small molecule and has no net charge, features that facilitate its ease of passing through cell membranes [4]. Its multifunctional capabilities include its use in the macrophage arsenal against host infection [5], production of vasodilation and modulation of vascular tone [6], and of particular interest to this project, it is involved in both necrotic and apoptotic forms of cell death in cardiac myocytes [7]. However, while an involvement in these and other processes has been described, the diversity of mechanisms governing these actions are, in many cases, incomplete and warrant further investigation.

The reactions involving NO are numerous, due in no small part to its many metabolite derivatives (Table 1). NO can directly react with its targets, or it can be converted into a number of other compounds, collectively known as reactive nitrogen species (RNS), each with their own particular cellular effects and chemistries leading to a diverse set of cellular interactions that can derive from NO. In general, the degree of oxidation of the nitrogen atom determines the species and its associated chemistry. For example, it can take on the forms of nitroxyl anion (NO^-), NO, nitrosonium cation (NO^+), nitrite (NO_2^-), or nitrate (NO_3^-) [8].

Also of significance is the formation of peroxynitrite from the reaction of NO and superoxide anion. This reaction occurs very rapidly [4], suggesting that this may be a dominant species in oxidative environments. Peroxynitrite is a strong oxidizer of sulfhydryl groups [9], as well as a nitrating agent of proteins and DNA [10, 11], all of which can have serious effects on the cell. NO can also react with oxygen to form the strong nitrosylating agent nitrous anhydride, N_2O_3, which is a source of potently reactive nitrosonium ions (NO^+) [12]. In activated macrophages, it was found that approximately half of the synthesized NO was present as N_2O_3 and half was peroxynitrite [13]. Nitrite itself can also form the highly reactive nitrogen dioxide radical, which is involved in nitration reactions [14]. As these RNS can have a wide range of cellular targets, this demonstrates the complexity and diversity of NO chemistry and its biological effects.

1.2.2 Nitric oxide synthesis

NO is synthesized in vivo by several different isoforms of nitric oxide synthase (NOS) enzymes, each with different properties and cellular distributions [15]. These are commonly known as NOS1 (neuronal), NOS2 (inducible), and NOS3 (endothelial). Accumulating research also suggests that there may be a mitochondrial NOS (mtNOS) as well [16-18]. These enzymes all catalyze the liberation of NO from L-arginine [19, 20]. NOS1, the first to be discovered, is primarily, although not exclusively, found in neuronal cells [21-23], and has the requirement of Ca^{2+} and calmodulin for it to be constitutively active [24, 25]. NOS3 has predominantly been described in endothelial cells of blood vessels. It is also constitutively active and requires Ca^{2+} and calmodulin [26], yet unlike NOS1, it can associate with the cell membrane to localize it to that part of the cell, perhaps to optimize its extracellular release [27]. By contrast, NOS2 is inducible by cytokines to cause a rapid increase in cellular NO levels [28, 29] and does not have a requirement of Ca^{2+} or calmodulin [30]. Interestingly, NO feeds back to negatively regulate

the NOS enzymes and inhibit excessive NO production, which becomes cytotoxic at higher levels [31].

1.2.3 Nitric oxide causes DNA damage

One of the consequences of heightened NO concentrations is damage to the DNA. A number of mechanisms have been described to account for this observation. Primary amines within the DNA bases are targets for nitrosylation by N_2O_3 [32]. These modified bases are then prone to spontaneous hydrolytic deamination, resulting in errors in DNA repair or replication [32-34], whereby cytosine is converted to uracil, guanine to xanthine, and adenine to hypoxanthine [35]. As an important consequence of deamination, xanthine spontaneously depurinates in DNA to leave an abasic site, which may be cleaved by endonucleases to give a strand break [34]. The conversion of guanine to xanthine occurs more rapidly than any other NO-induced base modification [32]. Peroxynitrite is also a major inducer of DNA damage, able to induce DNA strand breaks more efficiently than NO itself [34]. Peroxynitrite can induce depurinations and formation of abasic sites similarly to N_2O_3, but it also can cause this result via nitration of guanine to yield 8-nitroguanine, which also spontaneously depurinates [36]. Furthermore, it can oxidize DNA bases into oxo-derivatives [37, 38], which themselves react with peroxynitrite for further modification and degradation [39], or it can additionally target the sugar backbone of the DNA strand to induce strand breaks [34, 40]. Similarly, nitroxyl anions are also responsible for causing DNA breakage and base oxidation [41].

1.2.4 Nitric oxide modifies protein structure and function

The cellular effects of NO are also mediated by NO-induced modifications of proteins. Cysteine residues are the predominant amino acids involved in these reactions, as they react much more rapidly than other amino acids with NO [42]. RNS reactions via S-nitrosylation with

thiol groups leads to nitrosothiol (RSNO) formation. This is a spontaneous and reversible reaction, although the specificity towards certain residues may be attributed to adjacent motif sequences, or to subcellular distribution of NOS and local concentrations of NO [43]. Owing to the reactivity of thiol groups on proteins, and their involvement in countless reactions, modification at this point by NO plays a crucial role in protein function, in a manner that is comparable to phosphorylation [43]. This property makes nitrosothiols valuable components to processes like signaling and transcription regulation [44, 45]. For example, caspases contain a reactive cysteine residue in their active site that can be nitrosylated to modulate the caspase apoptotic signaling cascade [46].

Similarly, tyrosine residues are targets for nitration by the irreversible, non-enzymatic addition of an NO_2 (nitro) group to one of the *ortho* carbons of their aromatic ring. This is not the result of a single pathway, but rather is the end product of a variety of different reactions [47, 48]. The specificity of this reaction is generally dependent on the proximity of the protein to the site of generation of the nitrating species [47], the local sequence [49], and the position and degree of exposure of the tyrosine residue within the protein [49]. However, there are several exceptions that have been observed [50, 51]. Tyrosine nitration also plays a role in modulating protein function and signaling [52, 53], also acting as a marker or predictor of inflammatory processes or diseases [48].

While cysteine and tyrosine residues are principal amino acid targets, NO also has affinity for metal centers of proteins. As with amino acid modifications, alterations in the structures of these metal centers by NO results in a change of their functions. Heme moieties of several proteins strongly bind NO [54, 55]. For example, NO binding to the heme moiety of soluble guanylate cyclase [56], cytochrome c oxidase [57], and cytochrome p450 [58, 59] causes structural realignments that result in a modification of their activities. Non-heme metal centers

are also targets for NO, including metallothionein [60], superoxide dismutase [61], and aconitase [62].

1.2.5 Nitric oxide and necrosis

Among the many processes that are under the influence of NO are those involved in necrosis. Rather than necrosis being a largely uncontained and uncontrolled procedure, recent data suggests that active mechanisms may indeed be involved, such as mitochondrial failure [63, 64]. Inhibition of ATP synthesis by NO leads to decreased ATP stores, which contributes to the initiation of necrosis [65, 66]. The electron transport system is regulated at multiple points by NO. Cytochrome c oxidase (CcOx), the terminal electron acceptor at complex IV, is a significant target. CcOx can be reversibly inhibited by NO, which causes a congestion of the electron transport chain [67]. NO competes with oxygen for binding to CcOx, so the physical association of mtNOS with CcOx may allow for fine-tuned regulation without leading to excessive or toxic NO concentrations [68]. Complexes I (NADH dehydrogenase), II (succinate dehydrogenase), and III (cytochrome bc1) are also inhibited by NO to varying degrees [69, 70]. Cytochrome c is a target, as it contains a reactive thiol group which, when nitrosylated by NO, reduces mitochondrial respiratory function [71]. Glycolysis is also dampened, whereby glyceraldehyde-3-phosphate dehydrogenase (GAPDH) is inhibited by NO at its active site [72, 73]. NO also reduces aconitase activity and inhibit the Krebs cycle [74]. Combining respiration inhibition with glucose deprivation following NO treatment resulted in total depletion of ATP and 80-100% necrosis [75]. NO also activates poly(adenosine 5'-diphosphoribose) synthetase, which catalyzes the addition of ADP-ribose on to nuclear proteins, thus leading to further depletion of ATP stores [76]. With hindered capacity to synthesize new ATP, and reduced ATP stores, normal cellular processes cannot operate properly, and necrotic death ensues.

In addition to energy modulation, NO modifies cysteine residues of caspases to inhibit apoptosis and switch the mode of death to necrosis [77]. This effect occurred after prolonged exposure to NO and was associated with a dramatic increase in poly ADP-ribose polymerase (PARP) activity and subsequent ATP depletion in neonatal rat cardiomyocytes [78]. Interestingly, this PARP activation was a result of a preceding caspase activation earlier in the response [78]. Inactivation of PARP retains ATP stores and favours the apoptotic response [79]. This demonstrates that NO-mediated necrosis is dependent, in part, on changes in energy metabolism that ultimately lead to ATP depletion.

1.2.6 Nitric oxide and apoptosis

1.2.6.1 Nitric oxide induces mitochondrial-based apoptotic effects

The intrinsic apoptotic pathway involves the convergence of a wide range of signaling pathways at the mitochondria, is regulated by Bcl-2 family proteins, and results in pro-apoptotic factor release and caspase activation leading to degradation of the cell [80]. This pathway has been observed in connection with NO in several different studies. One process where NO has been implicated is in the regulation of the permeability transition pore (PTP). The PTP is proposed to be composed of adenine nucleotide translocator (ANT) on the inner mitochondrial membrane, voltage-dependent anion channel (VDAC) on the outer mitochondrial membrane, and cyclophilin D in the matrix [81]. In some instances, NO has been observed to oxidize critical thiols of ANT, resulting in a change in the interaction of ANT with ADP and ATP, leading to the opening of the PTP [82, 83]. Upon PTP opening, ions equilibrate across the membrane, leading to loss of mitochondrial membrane potential and cessation of the electron transport chain's ATP production capacity [84, 85]. In addition, opening of the PTP provides a non-specific channel for leakage of pro-apoptotic inducers into the cytosol, such as cytochrome

c, Smac/DIABLO, and AIF [86]. Regulation of the PTP is highly regulated by Bcl-2 family proteins. It has been hypothesized that the equilibrium of anti- and pro-apoptotic Bcl-2 proteins determines the cell fate, a rheostatic mechanism illustrated by the observation that anti-apoptotic Bcl-2 proteins, via their BH3 domains, may sequester BH3-only pro-apoptotic proteins within the mitochondrial membrane to prevent their apoptotic effects [87]. Both Bcl-2 and Bax interact with ANT to modulate its function [88]. NO plays a role whereby it increases Bax expression and promotes apoptosis mediated by the opening of the PTP, a process that was antagonized by Bcl-2 protein [89]. Collectively, these observations suggest a role for NO whereby it induces apoptosis through mechanisms that govern mitochondrial PTP opening.

1.2.6.2 Nitric oxide modifies extrinsic apoptotic pathway mechanisms

The extrinsic apoptotic pathway is engaged upon binding of ligands to their specific death receptors, causing a recruitment of adapter proteins to the intracellular domain of the receptor, leading to the activation of caspase-8 and the resultant caspase cascade [90]. While NO did not activate these mechanisms alone, it was capable of inhibiting TNF-alpha-induced TRADD recruitment, caspase-8 activation, and the resultant apoptosis [91]. Therefore, while it doesn't appear that NO explicitly *activates* this system, this does demonstrate that the extrinsic apoptotic pathways can be *regulated* by NO.

1.2.6.3 Nitric oxide modifies caspase activation

The caspases are a family of proteases that are involved in the degradation of the cell during apoptosis [92]. They are generally divided into two categories: initiators and executioners. In response to apoptotic signals, initiator caspases are responsible for cleaving the executioner proenzymes into their active forms, which leads to a cascade of activation [92]. Initiator caspases respond to different stimuli, but culminate in the activation of the same

executioners. Active caspases participate in the destruction of the cell by inactivating proteins that normally inhibit apoptosis, disassembling cytoskeletal structures, and deregulating proteins by separating regulatory and catalytic domains [92].

The regulation of caspases by NO has not been adequately explained, as it has been found to either promote or inhibit apoptosis in different situations. Inhibitory actions of NO appear to center around the s-nitrosylation of a critical cysteine residue present in the caspase active sites, which reduces the caspase's activity and diminishes the subsequent activation cascade [93-96]. By contrast, NO donor drugs have been observed to induce apoptosis through activation of caspase-3, -6, -8 and -9 [97, 98]. In neonatal rat cardiomyocytes, several NO donors also induced apoptosis in association with caspase-3 activation [78], while in tubular epithelial cells, caspase-8 inhibition reduced NO-induced apoptosis [99]. Caspase-1 is activated in NO-induced thymocyte apoptosis [100]. These observations suggest that NO-mediated caspase regulation is not as simple as it would first appear, as it apparently has a dependence on cell type, NO concentration, and other factors to determine the eventual outcome.

1.2.6.4 Nitric oxide modifies cGMP signaling

cGMP is an important messenger molecule for many cellular pathways, as its principal targets include cGMP-dependent protein kinases, phosphodiesterases, and cGMP-regulated ion channels, where the regulation of each results in a large influence on downstream processes [101]. A large proportion of NO-induced cGMP-dependent effects are initiated by its binding to soluble guanylate cyclase (sGC) and the subsequent generation of cGMP [102].

The interaction of NO and the cGMP pathway with apoptotic mechanisms remains controversial, as it has been shown to demonstrate both pro- and anti-apoptotic effects. A role of cGMP in pro-apoptotic pathways, in some models, is evident by the observation of sGC

inhibition reducing apoptosis [103-105]. Protein kinase G (PKG) also appears to have a role in this mode of death, as its inhibition also reduces apoptosis levels [103, 105].

By contrast, NO prevented apoptosis in a manner that was dependent on cGMP formation [106-109]. cGMP has been tied to increased Bcl-2 expression [110], which interacts with other members of the Bcl-2 family of proteins to induce anti-apoptotic effects. NO-induced cGMP production led to inhibition of cytochrome c release from the mitochondria [111] and caspase activation [112]. cGMP also inhibited mitochondrial permeability transition pore opening [113]. An involvement of the Akt survival pathway has also been suggested to mediate the cGMP-dependent anti-apoptotic effects of NO [114, 115]. These results clearly demonstrate the complexity behind NO and cGMP in modulating cell survival.

1.2.7 Relationship of NO to the cardiovascular system

The complexities of NO that have been outlined here allow for NO to play an important role in the health and function of the heart and cardiovascular system. It is an endothelial-derived relaxing factor, capable of modulating vascular tone [116]. Through regulation of calcium movement, it is involved in modulating excitation-contraction (EC) coupling during systole, and myocyte relengthening during diastole [117]. These effects can influence the contractile response of the myocyte to stimulation. Furthermore, NOS isoforms are involved in neuronal regulation of the heart, where pre-synaptic NO aids in acetylcholine release [118] and post-synaptic NO amplifies the neurotransmitter's effect [119]. Disruption of NOS function or localization during some cardiac diseases can greatly affect any of these processes. For example, atherosclerosis and hypertension are associated with decreased NO production in the vascular endothelium, resulting in a diminished vasodilation capacity [120, 121]. By contrast, in response to myocardial infarction or other heart diseases, elevated cytokine levels cause increased NO production, contributing to cardiomyocyte apoptosis and heart failure [122-124]. In heart

transplants, NO synthesized by myocardium or immune cells induces tissue damage and apoptosis during rejection [125]. The importance in gaining a complete understanding of the underlying apoptotic mechanisms is realized as cardiomyocytes are believed to be terminally differentiated, and so any degree of myocyte loss has an impact on heart function or viability.

Specifically, abnormal nitration/nitrosylation of cardiac proteins is important in several pathways and may be a factor in cardiac dysfunction [126, 127]. A proteomic approach revealed that, in response to oxidative stress or aging, a significant amount of mitochondrial protein nitration was associated with altered protein functions in pathways such as energy production, antioxidant defence, and apoptosis [128, 129]. Complexes of the electron transport system are prone to tyrosine nitration, resulting in their inhibition and a breakdown of cellular ATP production [130]. Creatine kinase, involved in energy regulation and ATP trafficking, is also inhibited by nitration, which leads to decreased contractile force generation [131, 132]. Similarly, nitration of sarcoplasmic reticulum Ca^{2+}-ATPase [133] and alpha-actinin [134] contribute to depressed contractile ability, and may contribute to heart failure. In autoimmune myocarditis, although specific proteins have not entirely been identified, increased NOS2 expression and concomitant accumulation of nitrated proteins has been observed [135]. Similarly, non-specific protein nitration has been observed in heart failure [136] and ischemia-reperfusion injury [137]. Taken together, these observations demonstrate the critical importance of NO in cardiovascular regulation, and that cardiac protein nitration may be an underlying basis for cardiac dysfunction.

1.3 Tumor Suppressor p53

1.3.1 What is p53?

The protein p53 is a tumor suppressor which acts to inhibit the cell cycle, induce apoptosis, and regulate DNA repair [138-140]. These effects are brought about through a symphony of concerted actions, by-products of p53's multifunctional abilities to transcriptionally activate specific genes, repress other genes, and to influence its targets through transcription-independent processes. In addition, a number of proteins have been identified that play a part in modifying p53's activity, thus establishing a large regulatory network involved in carrying out these cellular outcomes.

The activity of p53 can be regulated by a number of modifications by a variety of enzymes, including phosphorylation, ubiquitination, acetylation, methylation, sumoylation, and neddylation. Multiple forms of regulation means that p53 can respond to several different stimuli. Phosphorylation interferes with the binding of p53 inhibitors (eg. Mdm2), resulting in a stabilized, active p53 [141]. Ubiquitination of p53 targets it for degradation at the proteasome [142]. Acetylation of p53 by its coactivator, p300, leads to increased sequence-specific DNA binding [143]. Lysine methylation of p53 results in heightened stability [144]. Sumoylation involves the addition of SUMO-1 (small ubiquitin-like modifier) molecules, and possibly acts to enhance p53 transcriptional activity [145]. Conversely, neddylation of p53 is the attachment of another ubiquitin-like protein, Nedd8, to lysine residues resulting in an inhibition of transcriptional activity [146]. Turnover of p53 protein is quite rapid, on the order of a few minutes, and it is likely a combination of increased transcription and post-translational stabilization which both contribute to increases in p53 protein [147, 148].

Trafficking of p53 to the nucleus is dependent on microtubules and the dynein motor protein complex [149-151]. It appears that the chaperone hsp90 complexes with p53, and

through association with other immunophilins, links p53 to dynactin of the motor complex [151, 152]. Once at the nuclear pore, the complexes enter the nucleus via an importin-dependent mechanism [152]. It has also been described that p53-binding protein 1 (53BP1) associates with both p53 and the 8 kDa light chain of dynein, the latter association which when interrupted results in reduced nuclear accumulation of p53 [150]. Hsp70 may play a role in trafficking p53 to the mitochondria [153], where it has been proposed to interact with mitochondrial membrane proteins to induce the formation of pores and leakage of pro-apoptotic factors [154].

1.3.2 Negative regulators of p53

The first regulator of p53 to be discovered was the negative regulator Mdm2 (murine double minute 2), which was found to physically associate with p53 and to inhibit its transactivation activity [155]. In addition to this inhibitory action, Mdm2 also possesses E3 ubiquitin ligase activity [156, 157], where it transfers an activated ubiquitin molecule to p53 at several C-terminal lysine residues, thus targeting it for cytosolic degradation by the proteasome [158]. These functions of Mdm2 allow it to participate in a negative feedback loop on p53, in that p53 initially transactivates Mdm2 expression [159], only to be deactivated by it shortly thereafter. To counter these inhibitory actions, Mdm2 can become phosphorylated at its p53-binding site, thereby reducing its affinity for p53 [160].

Mdm4, or MdmX (Mdm2-related protein) also inhibits p53-mediated transcription [161]. Like Mdm2, Mdm4 also appears to inhibit p53 transcriptional activity, although it is uncertain whether it contributes directly to p53 inhibition, or merely serves to stabilize the Mdm2-p53 interaction [162]. As Mdm4 does not have ubiquitin ligase activity, it may alternatively function to bind to p53 and protect it from Mdm2-mediated nuclear export and degradation [163, 164].

1.3.3 Positive regulators of p53

There are many proteins that participate in the positive regulation of p53. ATM (ataxia-telangiectasia mutated) protein kinase is a nuclear protein of the phosphatidylinositol-3 kinase-like protein family, and is activated in response to DNA damage [165]. It is one of the kinases capable of phosphorylating p53 at serine 15, resulting in activation and stabilization of p53 [166]. This post-translational modification results in a disruption of the p53-Mdm2/Mdm4 interaction, freeing p53 of that inhibitory constraint [141]. Furthermore, ATM has been shown to phosphorylate Mdm2 prior to p53 accumulation in response to DNA damage [167].

Chk2 is another serine/threonine kinase that is involved in radiation-induced apoptosis. It has been proposed to phosphorylate p53 in response to DNA damage at serine 20, which is nearby to the Mdm2 binding site [168]. Phosphorylation here also interferes with the p53-Mdm2 interaction, thereby leading to stabilization of p53 in its active form [168].

Casein kinase (CKII) also phosphorylates p53 in response to DNA damage. It phosphorylates p53 at serine 389, yet interestingly, does so in response to UV radiation but not gamma radiation [169]. This implies that CKII is activated in response to UV, but a separate pathway is at work to govern the cellular response to gamma radiation. Mutating the serine to an alanine residue resulted in partially decreased DNA binding [170], and decreased p53 transcriptional activity and apoptosis following UV, but not gamma irradiation [171].

p19Arf (p14Arf in human) regulates p53 through binding to active p53-DNA complexes, leading to their stabilization [172]. In addition, p19Arf interacts with Mdm2 via its N-terminal domain [173]. This results in the retention of Mdm2 within the nucleolus away from p53 [174], as well a blockage of its ubiquitin ligase activity [175]. Both actions result in an attenuation of Mdm2's inhibitory effects on p53.

1.3.4 p53 causes apoptosis via transcriptional regulation

One of the main functions of p53 is transcriptional activation of apoptotic control genes [139]. In fact, many mutant p53 isoforms found in tumors have an impaired ability to carry out this function, leading to their inability to execute the apoptotic program [176]. This derives from its binding to specific DNA sequences via its DNA-binding domain [177]. Mutations in this domain prevent proper structural conformation and subsequent sequence recognition. The significance of p53's integrity to normal apoptotic function was confirmed by the discovery of small peptides and compounds which modify the mutated form into apparent wild-type conformation and rescue its ability to induce apoptosis [178].

A number of genes, in both the intrinsic and extrinsic apoptotic pathways, have been identified as being downstream targets of p53 [139]. The intrinsic pathway is thought to be the main mechanism behind p53-mediated apoptosis, with the extrinsic pathway serving to enhance the response [179].

In the intrinsic pathway, the main p53-transcriptionally-controlled genes belong to the Bcl-2 family. Expression of the proapoptotic protein Bax (Bcl-2-associated X) is increased in p53-dependent apoptosis [180], and contains a p53 binding site in its promoter for direct transcriptional activation by p53 [181]. A number of Bcl-2 homology 3 (BH3)-domain proteins also contain p53 binding sites within their promoters and are transcriptionally controlled by p53. Significantly, these include Noxa [182], PUMA (p53 upregulated modulator of apoptosis) [183], and Bid (BH3 interacting domain death agonist) [184]. Noxa localizes to the mitochondria, dependent on its BH3 domain, where it associates with anti-apoptotic Bcl-2, Bcl-xL, and Mcl-1 to sequester them from bound pro-apoptotic proteins and promote mitochondrial permeability transition, cytochrome c release, and caspase activation[182]. PUMA also localizes to the mitochondria and promotes apoptosis through association and sequestration of other BH3-domain-containing proteins, especially with Bcl-2 [183]. Proapoptotic Bid protein becomes

active following cleavage by active caspase 8 and post-translational myristoylation, at which point it inserts into the outer mitochondrial membrane and activates Bax and Bak via their BH3 domains to initiate the mitochondrial death response, thus serving as a linker of the intrinsic and extrinsic pathways [184].

The extrinsic pathway also contains gene targets that are susceptible to activation by p53. The gene sequence for Fas/CD95 contains a p53-binding site and has been shown to be responsive to p53 [185]. Activation of the Fas protein, a membrane-spanning death receptor, by circulating Fas ligand initiates the formation of the death-inducing signaling complex (DISC), which ultimately recruits and activates caspase 8. Another transcriptionally regulated gene codes for KILLER/DR5, a death receptor with specificity for tumor necrosis factor-related apoptosis-inducing ligand (TRAIL), which also induces apoptosis [186].

In addition to affecting gene regulation of proteins within the intrinsic or extrinsic apoptotic pathways, p53 can also activate genes encoding proteins involved in apoptosis in other ways. Of note is the gene for Apaf-1 (apoptotic protease-activating factor 1), which, once bound to cytochrome c in the cytosol, mediates caspase-9 autocatalytic activation and propagation of the caspase cascade [187]. As well, caspase-6 is also a transactivation target of p53, the furthest-known downstream point of genetic regulation by p53, which may serve to lower the threshold required to induce death [188]. PERP (p53 apoptosis effector related to Pmp22) is found on the plasma membrane, and its expression, regulated by p53, leads to fibroblast cell death [189]. PIDD (p53-induced protein with death domain) is another protein under transcriptional control by p53 [190]. This protein, along with RAIDD, participates in a protein complex termed the PIDDosome, resulting in activation of caspase-2 [191]. It is believed that p53DINP1 (p53-dependent damage-inducible nuclear protein 1) is a part of a protein complex that is responsible for p53 Ser46 phosphorylation and its activation, and so is involved in a regulatory positive feedback loop with p53 [192]. The protein p53AIP1 (p53-regulated apoptosis-inducing protein

1) is suggested to play a part in disruption of mitochondrial transmembrane potential leading to apoptosis as a result of its p53-dependent transcription [193]. The gene coding for ferredoxin reductase was observed in colon cancer cells to be transcribed in a p53-dependent manner, with the protein localizing to mitochondria and inhibiting oncotic growth, implying a role for p53 in oxidative stress and redox regulation [194]. Furthermore, deficient ferredoxin reductase resulted in attenuated apoptosis [194]. Finally, p53 increases the expression of PTEN (phosphatase and tensin homolog) [195]. PTEN functions to inhibit the PI_3 kinase pathway by dephosphorylating phosphoinositides, thus reducing the antiapoptotic ability of this pathway [196].

Besides activating transcription of its genetic targets, p53 also functions to repress a number of genes as well. Histone deacetylases also physically associate with p53, mediated by mSin3a [197], and binds within certain promoter sequences to block transcription by modifying the histones, creating a configuration of chromatin where transcription is not favoured [198]. Survivin belongs to the IAP family (inhibitor of apoptosis), and its expression is repressed by p53 [199, 200], possibly through a similar mechanism, or alternately/additionally by blocking transcription factor E2F-mediated gene activation [199]. Histone deacetylation and p53 activation also appear to be involved in c-myc transcriptional repression, leading to cell cycle arrest [201]. There is a hypothesis that p53 is involved in a negative feedback loop in response to nitric oxide, whereby high NO leads to DNA damage and an increase in p53 expression, followed by p53 repressing expression of the NOS2 gene and production of NO [202].

Taken together, p53 is a major regulator of genes involved in cellular health and survival, with it being capable of moderating the genetic responses at a number of different positions in the apoptosis pathways.

1.3.5 p53 mediates apoptosis through transcription-independent events

Beyond all of these transcription-dependent events that p53 mediates, there are also an increasing number of transcription-independent mechanisms contributing to p53-mediated cell death. While the transcriptional effects of p53 take place in the nucleus, p53 found in the mitochondrial and cytosolic compartments are nonetheless active participants in propagating the death signal.

p53 is an activator of the intrinsic mitochondrial apoptotic pathway, with multiple points of impact within that mechanism. This hypothesis was first put forward with the observation that p53 was observed to translocate to the mitochondria during p53-dependent apoptosis [203, 204]. It was observed to rapidly accumulate in the mitochondrial fraction within 1 hour of activation, and this preceded mitochondrial membrane depolarization, cytochrome c release, and caspase 3 activation [203]. Further support of a transcription-independent apoptosis pathway came when the targeting of p53 to the mitochondria, which bypasses nuclear import and p53-dependent gene activation, was found to be sufficient to induce apoptosis [203, 205, 206]. A polymorphic variant of p53, with a proline at codon 72, was found to have a diminished ability to relocate to mitochondria, and concomitantly, this variant also showed reduced apoptotic abilities [207]. This effect can be compared to another p53 polymorphism, with arginine at codon 72, where mitochondrial translocation occurs unhampered, resulting in cytochrome c release and apoptosis [207]. Furthermore, by targeting both variants to the mitochondria, through the use of a mitochondrial leader sequence, differences in apoptosis were equalized, thus showing convincingly the importance of this particular amino acid location in proper p53 function [207].

p53's non-transcriptional mechanisms revolve around interactions with Bcl-2 family members. Members of this family can be classified as being either antiapoptotic proteins (eg. Bcl-2, Bcl-xL) or proapoptotic proteins, of which they can be further separated into multi-

domain (BH1,2,3,4) proteins (eg. Bax, Bak) or BH3-only proteins (eg. Bad, Noxa, PUMA) [208]. It is hypothesized that the equilibrium of anti- and pro-apoptotic proteins determines the cell fate, a rheostatic mechanism illustrated by the observation that antiapoptotic Bcl-2 proteins, via their BH3 domains, may sequester proapoptotic BH3-only proteins within the mitochondrial membrane to prevent their effects [87]. Generally, the BH3 proteins activate Bax or Bak to induce mitochondrial permeabilization, whereas Bcl-2 and Bcl-xL bind to the BH3 proteins to prevent that action [209]. In this complex regulatory network, Noxa interacts with Bcl-xL and Mcl-1 [182], suggesting that Noxa may also tie up these proteins away from their pro-apoptotic partners to promote apoptosis. Bcl-xL can also inhibit Bad, similarly to Bak [210].

p53 can form inhibitory complexes with some of these anti-apoptotic proteins, via their BH3 domains, thus sequestering them away from their pro-apoptotic binding partners and acting as a "derepressor" of their pro-apoptotic functions [205]. As this binding also occurs at p53's DNA binding domain, this interaction exemplifies how a missense mutation in this particular region of p53 can affect both transcription-dependent and –independent mechanisms. Once expressed (transcriptionally activated by p53), pro-apoptotic PUMA disrupts the association of p53 with Bcl-xL by binding to Bcl-xL itself, which frees p53 to exert its other transcription-independent activities [211]. Under normal conditions, most p53 was found to be trypsin digestion-sensitive, indicative of an association with the outer mitochondrial membrane with Bcl-2 or Bcl-xL, while a small amount was found within the matrix itself, perhaps in a complex with mitochondrial import protein mt hsp70 protein [204]. Also, p53 directly interacts with and activates the pro-apoptotic Bak by displacing its anti-apoptotic partner Mcl-1, resulting in Bak's oligomerization within the mitochondrial membrane, leading to membrane permeabilization and cytochrome c release [212]. Bax is bound and activated by p53, causing its mitochondrial membrane integration [213]. Upon activation, Bax changes from being monomeric and cytosolic or having a loose association with the mitochondria, to being found predominantly

inserted into the mitochondrial membrane in an oligomeric form, a process inhibited by Bax's association with Bcl-2 [214]. This oligomeric Bax channel then mediates release of cytochrome c and other apoptogenic factors from within the mitochondria [215, 216]. Alternately, some studies have implicated an interaction for Bax with the transition pore, where Bax induced VDAC opening in artificial liposomes [217, 218], and inhibitors of mitochondrial permeability transition were sufficient to inhibit this opening [219].

These examples demonstrate many different ways by which p53 can regulate apoptosis by transcription-independent mechanisms. When taken with the multitude of transcription-dependent effects, it is clear that p53 is a critical component of the cell's death pathways.

1.3.6 p53 causes cell cycle arrest

The apoptotic response mediated by p53 runs in parallel to the cell cycle arrest response, and each process can slow or block the other. Excessive amounts of cell cycle inhibitors can prevent the apoptotic machinery from functioning properly, and likewise, high levels of apoptotic products can interfere with the cell cycle regulation and lead to apoptosis.

Cell cycle inhibitors p21 and 14-3-3σ are two of the major mediators of cell cycle arrest whose actions must importantly be prevented for the apoptotic program to take priority [139]. p21(Waf1/Cip1) is an inhibitor of cyclin-dependent kinases, capable of preventing phosphorylation of Rb and blocking the cell's transition from G1 to S phase [220]. It is transcriptionally activated by p53 [221] and is regarded as the main mediator of p53's cell cycle control [222]. p21 also binds to proliferating-cell nuclear antigen (PCNA), which inhibits DNA polymerase [223]. p21 can also cause G2 arrest by inhibiting Cdc2 through a number of proposed mechanisms [224].

14-3-3 proteins are chaperones that are mainly cytosolic, but can interact with phosphoserine residues on other proteins to carry them into the nucleus, or to sequester them in

the cytosol [225]. The expression of the 14-3-3σ isoform is upregulated by p53 in response to gamma radiation and DNA damage, resulting in an arrest at the G2/M checkpoint [226]. The increase in 14-3-3σ following DNA damage results in its binding to the Cdc2-cyclin B1 complex and retaining it within the cytosol, thus preventing its activation and the initiation of mitosis, resulting in arrest in G2[224].

1.3.7 p53 regulates DNA repair

In addition to regulating apoptosis or halting the cell cycle, p53 also participates in the regulation of DNA repair [227]. For its roles in DNA repair and eliminating the cell if the damage is too great to overcome, it has earned the title of "guardian of the genome" [228]. It is quickly activated in response to many DNA damaging agents [138]. The transcription of DDB2 and XPC, two factors involved in the removal of cyclobutane pyrimidine dimers and pyrimidine 6-4 pyrimidine photoproducts following UV or oxidative DNA damage, are regulated by p53 [227]. Also, p53 associates with XPB and XPD proteins, which are also involved in nucleotide excision repair [229]. It can bind directly to the DNA in some types of damage to recruit the cell's repair machinery to the site [140], including p300 which acetylates histones and causes chromatin relaxation [230]. Similarly, mismatch repair proteins [227] and base excision repair proteins [231] activate p53. Homologous recombination is inhibited by p53 binding to Rad51 [232], the binding of which also stimulates an intrinsic 3' to 5' exonuclease activity of p53, allowing it to directly function in DNA proofreading and base excision repair [233]. If DNA strand breaks are left unrepaired, p53-dependent apoptosis is often initiated [227]. As is evident, p53 definitely earns its reputation for its contributions to maintaining the integrity of the genome.

1.4 Nitric oxide induces p53-dependent mechanisms

NO generation was first shown to cause p53 accumulation in macrophages and pancreatic cells, and was prevented by an NOS2 inhibitor that stopped NO production and apoptosis [234]. It was also shown that p53 represses the expression of NOS2, providing a mechanism for a negative feedback loop acting to reduce NO-induced damage [235]. Concomitantly, p53 knockout mice were found to have greatly increased NOS2 and NO synthesis under basal conditions [236]. Introduction of antisense p53 RNA resulted in a down-regulation of p53 following NO treatment or NOS2 induction, which was associated with decreased DNA fragmentation, further indicating the importance of p53 in NO-induced apoptosis [237]. Seemingly paradoxically, cytokines or low concentrations of NO administered to macrophages prior to a larger lethal NO dose imparted a modest resistance to cell death and blocked p53 accumulation [238].

A number of effects of NO as it relates to p53 expression have been described. Increased p53 levels are mainly mediated by a decrease in p53 protein turnover rate, caused by stabilization of the protein and decreased degradation [239]. A significant contributor to this effect is how NO causes a decrease of Mdm2 protein [239], and also modifies a critical cysteine residue of Mdm2 that disrupts p53 binding [240]. As Mdm2 targets p53 for cytosolic degradation by the proteasome, these actions help enable p53 to accumulate. Similarly, SIN-1 caused p38 MAP kinase phosphorylation, which upregulated p19ARF and its association with Mdm2, leading to the separation of Mdm2 from p53 [241]. In some models, p38 also phosphorylates serine 15 of p53 to cause its activation, a process dependent on PI_3K [242, 243]. Inhibition of PI_3K switched the mode of death from apoptosis to necrosis, implicating PI_3K signaling in NO-dependent apoptosis [243]. Impaired cytoplasmic shuttling, leading to p53 stabilization, is also a result of NO-induced p53 post-translational modifications [244, 245]. Interestingly, these changes include a distinct p53 phosphorylation pattern that is different from

those elicited by UV light, gamma irradiation, or adriamycin, suggesting an overlap and convergence of kinase signaling pathways on p53 [246]. An important note is that high concentrations of NO resulted in impaired DNA binding and function of p53 caused by nitration of key residues [247, 248].

Cellular effects caused by NO-mediated p53 induction have been observed in numerous pathways. In particular, the mitochondrial apoptotic pathways have been implicated. Down-regulation of Bcl-xL was specifically observed, prior to cytochrome c release and caspase activation [249]. As Bcl-xL exerts anti-apoptotic effects by binding to and sequestering pro-apoptotic BH3-only proteins, its down-regulation allows those proteins to exert their apoptotic functions. Similarly, pro-apoptotic BH3 proteins PUMA and Noxa are also up-regulated by p53 in response to NO [250]. NO-induced p53 accumulation and caspase activation are ATP-dependent processes, as the mode of death of ATP-starved cells changed from apoptosis to necrosis [249]. Similarly, an effect on cell cycle control has been described, whereby NO up-regulates p21 expression through p53 activation, resulting in cell cycle arrest [251, 252]. p21 also feeds back to enhance p53 accumulation by activating p19ARF, causing deactivation of Mdm2 [253].

These examples all serve to demonstrate the complexity of effects induced by NO-induced p53 activation. Many of these mechanisms occur concurrently and are in equilibrium with each other, making it complicated to define specific actions. In addition to the effects listed here, the functions of p53, in all likelihood, include many of those described previously but have not yet been studied in terms of a response to NO.

Tables

Table 1: Nitric oxide and relevant derivatives

NAME	CHEMICAL FORMULA
Nitric oxide	NO
Nitroxyl	NO^-
Nitrite	NO_2^-
Nitrate	NO_3^-
Nitrosonium	NO^+
Nitrous anhydride	N_2O_3
Peroxynitrite	$ONOO^-$
Nitrogen dioxide	NO_2
s-Nitrosothiol (in general)	R-S-NO (R-S = protein thiol)

2.0 AIM, HYPOTHESES, AND RATIONALE

The specific aim of this study is to gain a more thorough understanding of the complexities of nitric oxide signaling mechanisms and how it participates in the cell death of cardiomyocytes.

The hypotheses for this study and their rationales are as follows:

1. I hypothesize that NO will induce cardiomyocyte cell death with associated DNA damage, occurring in a p53-dependent and a mitochondria-dependent manner. In situations of high NO concentrations, NO has been shown to induce DNA damage and cause death of the cell. As p53 is highly involved in the maintenance of an intact genome, through regulation of cell death machinery or DNA repair mechanisms, it may be involved in mediating the cell death response to NO. Also, as the mitochondria are involved in apoptotic signalling, NO may act through this channel to bring about cell death, perhaps in an interaction with p53.

2. I hypothesize that NO-induced cell death will occur through the formation of the reactive nitrogen species, peroxynitrite, and will be reduced by isomerization of peroxynitrite to nitrate. Peroxynitrite is far more reactive than NO itself. Therefore, instead of NO, peroxynitrite may be the species that is responsible for causing cell death. As nitrate does not have nearly as highly damaging effects as peroxynitrite, the conversion of peroxynitrite to nitrate should reduce the damaging effects of NO treatment.

3. I hypothesize that protein tyrosine nitration, specifically associated with the mitochondria, is a component of NO- and peroxynitrite-induced cell death. Furthermore,

I hypothesize that conversion of peroxynitrite to nitrate, by the isomerase FeTPPS, will reduce the amount of protein tyrosine nitration and cell death. The nitrosylation/nitration of proteins has been proposed to be a general method of regulation of proteins, akin to phosphorylation. As such, modifications of key components of the cell death pathways may be important mechanisms. Also, as the mitochondria play a significant role in mediating certain forms of apoptosis, modification of mitochondrial proteins may be important to NO-induced cell death. If protein tyrosine nitration is due to peroxynitrite formation, conversion of peroxynitrite to nitrate should reduce the amount of peroxynitrite, tyrosine nitration, and concomitantly, the amount of cell death.

3.0 EXPERIMENTAL MATERIALS AND METHODS

3.1 Materials

Unless otherwise stated, all chemicals were purchased from Sigma Chemical Co. (St. Louis, MO, USA). Culture media, fetal calf serum, antibiotic-antimycotic were obtained from Gibco (Burlington, ON, Canada). The MTT assay kit was obtained from Promega (Madison, WI, USA). Pifithrin (506134) was purchased from VWR (Mississauga, ON, Canada). Anti-mouse HRP and anti-rabbit HRP antibodies were purchased from New England Biolabs (Pickering, ON, Canada). FeTPPS was purchased from Calbiochem (San Diego, CA, USA). Anti-p53 antibodies (WBB08) were purchased from Calbiochem (San Diego, CA, USA). Anti-cytochrome c antibodies (65981A) were purchased from BD Pharmingen (San Jose, CA, USA). Anti-nitrotyrosine antibodies (06-284) were from Upstate (Temecula, CA, USA). Chemiluminescent reagents were purchased from Amersham Biosciences (Piscataway, NJ, USA). DePsipher^{TM} stain was purchased from Trevigen Inc. (Gaithersburg, MD, USA). Chemiluminescent film was from Kodak (Rochester, NY, USA).

3.2 Embryonic chick cardiomyocyte culture

Embryonic chick ventricular cardiomyocytes were cultured using previously described methods [254]. Brown hatching eggs were obtained from Coastline Chicks (Abbotsford, BC, Canada) and kept in an automatic egg incubator at 37°C for 7 days. Following this incubation time, chick embryos were removed and their hearts excised in a sterile tissue culture hood. The atria were separated from the ventricles, and ventricles minced into roughly 1 mm^3 pieces. The minced tissue was then suspended in disaggregation medium and mixed for 7 minutes in a 37°C water bath. Disaggregation medium was composed of 0.005% trypsin, 0.1% bovine serum albumin, and DNAse ($1.1x10^5$ Dornase units) in DMS8 salt solution (116 mM NaCl, 5.4 mM

KCl, 0.4 mM NaH_2PO_4-H_2O, 0.75 mM Na_2PO_4-$7H_2O$, 5.5 mM glucose in water). Following the first digestion step, the medium, which contained red blood cells and cellular debris, was discarded and replaced with fresh medium. In the 4 subsequent digestion steps, replacement with fresh disaggregation medium was preceded by removal of the current aliquot of medium from the digestate and its addition to 818A medium to stop the digestion process. 818A medium was composed of 73% DBSK (116 mM NaCl, 0.8 mM $MgSO_4$, 0.9 mM NaH_2PO_4, 5.5 mM dextrose, 1.8 mM $CaCl_2$, 26 mM $NaHCO_3$), 20% medium 199, 6% fetal calf serum, and 1% antibiotic-antimycotic (10,000 mg/ml streptomycin sulfate, 10,000 U/ml penicillin G sodium, and 25 µg/ml amphotericin B). When the digestions were complete, the cells were pelleted by centrifugation at 1000 x g for 3 minutes. The supernatant was discarded and the pellets were resuspended in 818A medium. The cells were then counted on a haemocytometer and plated into culture dishes. Cells were plated at approximately 3.0 x 10^6 cells per 65 mm culture dish, or 0.5 x 10^6 cells per 35 mm culture dish with coverslip for microscopy. MTT wells were plated at a density of 30,000 cells/50 ul. The cells were then maintained at 37°C and 5% CO_2 for 72 hours prior to experimentation. This protocol was approved by the University Committee on Use of Animals for Research

3.3 MTT Assay

The MTT assay, an index of cell viability, is based on the ability of viable cells to reduce MTT (3-(4,5-dimethylthiazol-2-yl)-2,5-diphenyl tetrazolium bromide) from a water-soluble yellow dye to a dark blue insoluble formazan product [167]. Cardiomyocytes, seeded in multiwell microtitre plates and incubated at 37°C for 72 h, were administered treatment and returned to the incubator for a further 24 h. MTT dye was added to each well for the final 4 h of the experiment. Solubilization solution was added to stop the reactions, and complete solubilization was allowed to occur overnight in a humidified chamber at 25°C. As the

absorbance curve of the MTT dye exhibits a linear portion ranging from 570 nm to 655 nm, the absorbance was determined at 570 nm on a multiwell plate reader (Dynatech MR5000, Chantilly, Virginia, USA) using BioLinx 2.2 data capture software (Dynatech Laboratories Inc, Chantilly, Virginia, USA) [255]. Background absorbance of medium in the absence of cells was subtracted. All samples were assayed in duplicate and the mean for each experiment was calculated.

3.4 Western Blots

Following the treatment course, medium was removed from the culture dishes and briefly centrifuged to pellet any cellular debris or detached cells. For whole cell lysates, RIPA buffer (150 mM NaCl, 1% Triton X-100, 0.5% sodium deoxycholate, 0.1% SDS, 50 mM Tris, pH 8) was added to the dishes and the cells were scraped into solution. The lysate was then used to resuspend the pellet, and then transferred to Eppendorf tubes and passed through a 26G syringe 10 times. Aliquots were removed for protein concentration determination, utilizing BioRad Protein Assay (BioRad, Hercules, California, USA), prior to the addition of 3X gel loading buffer (0.5M Tris-HCl pH6.8, 15% β-mercaptoethanol, 30% glycerol, 6% (w/v) SDS, 0.05 bromophenol blue in distilled water). Samples were then boiled for 5 minutes and stored at 4°C.

For cell fractionation experiments, cells were harvested in hypotonic buffer (10 mM Tris-HCl pH 7.4, 25 mM NaF, 2 mM Na_3VO_4, 1 mM $ZnCl_2$, 10 mM β-glycerol-phosphate, 10 mM tetrasodium pyrophosphate), and passaged through a 26G syringe 10 times. For mitochondrial/cytosolic separations, samples were centrifuged at 600 x g for 10 minutes at 4°C to remove cell debris and nuclei. The supernatant was kept and further centrifuged at 15000 x g for 5 minutes at 4°C to separate the mitochondria (pellet) from the cytosol (supernatant). The mitochondrial pellet was resuspended in RIPA buffer. For nuclear/cytosolic separations, samples were centrifuged at 600 x g for 10 minutes at 4°C to separate nuclei (pellet) from

cytosol (supernatant). The nuclear pellet was then resuspended in RIPA buffer. Aliquots of each sample were removed for protein concentration determination prior to the addition of 3X gel loading buffer and boiling.

SDS-polyacrylamide gel electrophoresis (SDS-PAGE) was used to separate the proteins. Appropriate percentage lower, resolving gels and upper, stacking gels were cast using mini Protean II gel assemblies (BioRad). Equal amounts of protein were added to each well, and the gel was allowed to run. Initially, a voltage of 100 mV was applied while the gels entered the stacking gel, following which the voltage was increased to 200 mV once the proteins had entered the resolving gel. The gel was run until sufficient separation of molecular weight markers (BioRad Precision Plus) was observed. The gels were then equilibrated in blotting buffer (150 mM Tris pH 8.3, 200 mM glycine, 20% methanol) for 30 minutes prior to transfer to nitrocellulose membrane (BioRad). Transfer occurred overnight at 55 mV and 200 mA at 4°C. Following transfer, the membranes were blocked in 5% milk in 0.1% TBST for 1 hour. The membranes were then washed 3 times in 0.1% TBST prior to the addition of primary antibodies, which were then allowed to react for 1-2 hours. Membranes were washed again, 3 times, following this and prior to the addition of secondary antibodies, which were allowed to react for 1 hour. Antibodies were diluted to a concentration of 1:1000, according to manufacturer instructions. After 3 final washes, the proteins were visualized on Kodak X-Omat photographic paper using a chemiluminescent detection kit. Western blots were scanned to computer using Hewlett Packard Precisionscan Pro 3.1 software, and subjected to densitometry using Scion Image 4.0.2.

3.5 Comet Assay

Comet assays were used to evaluate the extent of DNA damage [256]. Blank microscope slides were coated with agarose 24 h before experimentation. Molten 1% agarose (500 mg in 50

ml PBS) was added drop-wise to the top of the slides and allowed to solidify overnight at 25° C. Cultured cardiomyocytes were drained of medium and incubated for 10 minutes with 0.005% trypsin in PBS at 37° C. Cells were harvested by gently scraping and combining with fresh medium, following which they were pelleted by brief centrifugation and resuspended in 400 µl of PBS. The cell suspension was combined with molten 1% low melting point agarose (500 mg in 50 ml distilled water), which had cooled to approximately 37° C, in a ratio of 10 µl cell suspension (~10,000 cells) to 75 µl agarose, and added drop-wise on top of the base agarose layer on the slides. After 10 min at 4° C to allow for solidification, the slides were immersed in lysing solution (2.5 M NaCl, 100 mM EDTA, 10 mM Tris, 1% Triton X-100, 10% DMSO, pH 10) and kept at 4° C for 2 h. Following lysis, the slides were gently placed side-by-side in a horizontal electrophoresis tank (BioRad) for 20 minutes in alkaline electrophoresis buffer (0.3 N NaOH, 1 mM EDTA, pH 13). Electrophoresis was then begun at 24V, 300 mA for 30 minutes. Following this, the slides were carefully removed from the buffer and drained on paper towels. They were then covered drop-wise with neutralization buffer (0.4 M Tris, pH 7.5), left to sit for 5 min, and then drained. This was repeated twice. Ethidium bromide (80 ul, 2 ug/ml) was used to stain the slides for 5 min. Slides were destained in distilled water for 30 min prior to covering with a glass coverslip. Slides were viewed through a Zeiss IM35 inverted epifluorescent microscope. Representative cells were photographed and scanned into a computer to allow for detailed measurement and analysis of the comets using CometScore software (TriTek Corporation, Virginia, USA). Comet tail length was measured in pixels from the trailing edge of the cell to the end of the tail, and the amount of DNA at each pixel was assumed proportional to the pixel intensity.

3.6 Microscopy - DePsipher™ Staining

Cardiomyocytes, cultured and treated directly on to glass coverslips, were visualized using a DePsipher™ (Trevigen) staining kit to examine mitochondrial membrane potential, according to the manufacturer's protocols. Coverslips were transferred to small weigh boats and DePsipher™ solution (1 ug/ml 5,5',6,6'-tetrachloro-1,1',3,3'-tetraethylbenzimidazolylcarbocyanine iodide), prepared in prewarmed 1X reaction buffer, was pipetted on to each coverslip. The coverslips were incubated for 15 min at 37°C in a 5% CO_2 incubator prior to being washed 3 times with prewarmed 1X reaction buffer supplemented with 2% stabilizer solution. The coverslips were air-dried, set on microscope slides, and viewed on a Zeiss IM35 inverted epifluorescent microscope. Cells with healthy mitochondrial potentials display red aggregates of dye, while disrupted potentials are characterized by the green monomeric form of the dye. Representative photographs were taken and scanned into a computer.

3.7 Microscopy – Wright Giemsa Staining

Cardiomyocytes were plated and grown on cover slips. To examine basic cell morphology, a modified Wright Giemsa staining kit, Diff-Quik, (Harleco, Kansas City, USA) was used to visualize the cells. After treatment, coverslips were removed from the culture dishes, dipped for 15 seconds in 10% methanol fixative, followed sequentially by 15 seconds in eosin and methylene blue stains, and a final wash with distilled water. After air-drying, the coverslips were mounted on glass slides and viewed under white light on a Zeiss IM35 inverted microscope.

3.8 Microscopy – Immunocytochemistry

Immunocytochemical techniques were followed to visualize the cellular distribution of p53, as described [257]. Cells, grown on coverslips, were fixed with 3.7% paraformaldehyde and permeabilized with 1% Triton X-100. They were then washed with stabilization buffer ((50 mM imidazol, 50 mM KCl, 50 μM $MgCl_2 \cdot H_2O$, 0.5 mM EGTA, 100 μM EDTA, 37% w/v glycerol, 0.007% v/v mercaptoethanol)) followed by 1% glutaraldehyde in stabilization buffer. Cells were washed in 1 mg/ml sodium borohydride in PBS, rinsed with PBS, and then incubated with anti-p53 antibodies in PBS for 1h, followed by anti-rabbit-FITC antibodies for 1h. Coverslips were then rinsed with PBS, mounted on slides, and viewed under fluorescent light.

3.9 Griess Assay

The Griess assay was used to quantitate the amount of nitrite in solution, as an indicator of NO released from the indicated treatments. Cell free culture medium was incubated for 24 h at 37°C and 5% CO2, following treatments. Aliquots (100 μl) of samples or NO2 standards were combined with 50 μl 1% sulphanilamide and 50 μl 0.1% N'N-naphthylethylenediamine in duplicate wells of a 96-well plate. The absorbance was read at 570 nm after 10 minutes, and concentrations of nitrite determined by comparison to the NO2 standard curve.

3.10 Data Analysis

Data is presented as mean ± SEM, unless otherwise stated. Hypothesis testing was by analysis of variance (ANOVA). The null hypothesis was rejected if the probability of a Type I error was less than 5% ($p<0.05$).

4.0 RESULTS

4.1 GSNO releases NO

The Griess reaction was used to initially verify that GSNO releases NO into solution in our model system. Indeed, GSNO produced an increase of the NO metabolite, nitrite (NO_2^-), in the medium (Figure 1). Following 24 h in cell-free medium, 0.1 mM GSNO yielded 3.4±1.8 μM nitrite, while 1.0 mM GSNO resulted in 31.0±9.3 μM nitrite. Controls contained 13.8±14.8 μM nitrite.

4.2 GSNO induces cell death

GSNO-induced cell death was examined by MTT assay. GSNO induced a significant concentration-dependent reduction in MTT absorbance (Figure 2 inset). As evident by the significant linear relationship between MTT absorbance and cell number in these cells [254], GSNO produced a statistically significant ($p<0.05$) concentration-dependent increase in cell death (Figure 2), with approximately 100% cell death after treatment with 10 mM for 24 h. Statistically significant ($p<0.01$) changes in cell death were found specifically at concentrations of 1.0 and 10 mM GSNO.

4.3 GSNO causes morphological changes

Cell morphology was assessed by the use of a modified Wright Giemsa stain. Control cells appeared healthy, showing a standard triangular shape characteristic of cardiomyocytes, with large round nuclei and compact nucleoli (Figure 3A). Following 24 h treatment of 0.1 mM GSNO, it was evident that the cells were becoming damaged, as the nuclei showed signs of disruption, granular bodies formed in the cytosol, and the cell began to lose its shape (Figure 3B). After 1.0 mM GSNO, the nuclei showed extensive damage and degradation (Figure 3C).

4.4 GSNO causes an increase in p53 expression

To determine whether GSNO would increase cellular p53 protein expression, cells were treated with GSNO for 1 hr. Whole cell lysates showed an increase in p53 by 1.3±0.5 fold compared to control after 0.001 mM, 1.6±0.2 fold after 0.01 mM, 1.3±0.2 fold after 0.1 mM ($p<0.01$), 1.0±0.2 fold after 1.0 mM, and 1.1±0.6 fold after 10 mM (Figure 4).

The time course of the effect of GSNO on p53 expression showed an apparent maximal increase within 4 h and a return to baseline levels thereafter (Figure 5). GSNO concentration of 0.1 mM produced an increase of 1.6 fold at 4 h following treatment. GSNO at 1.0 mM also caused an average increase at 4 h of 1.6±0.04 ($p<0.01$). After 24 h 1.0 mM GSNO, a minor but highly statistically significant ($p<0.01$) increase of p53 expression was still present. As 0.01 mM GSNO was associated with a 1.6±0.2 ($p<0.05$) fold increase over baseline after only 1 h, lower concentrations of GSNO appear to induce increased p53 expression more rapidly than higher concentrations.

4.5 GSNO does not produce p53 translocation from cytosol to mitochondria

The potential translocation of p53 from the cytosol to the mitochondria was examined by Western blotting. The cytosol fractions of p53 were increased following 1 h and 4 h treatments of 0.1 mM GSNO, with a 1.8±0.5 fold increase at 1 h and 1.8±0.6 fold increase at 4 h compared to control (Figure 6). In comparison, the mitochondrial fraction had very low levels of p53 and there was no change induced by NO. Instead, there was a small non-significant decrease of 0.8±0.2 fold after 1 h and 0.8±0.3 fold after 4 h. Thus, there was no evidence that GSNO caused p53 to translocate to the mitochondria.

4.6 GSNO does not cause major cytochrome c release from mitochondria

Cytochrome c release from mitochondria was evaluated as a marker of mitochondria-dependent apoptosis. Palmitate induced the release of cytochrome c from the mitochondria into the cytosol, as previously observed [258], with an approximately 2.6-fold increase in the cytosol and a 0.5-fold decrease in the mitochondria. By comparison, 1.0 mM GSNO caused a small 1.4-fold increase of cytochrome c in cytosol and 0.8-fold decrease in mitochondria (Figure 7).

4.7 GSNO does not cause a change in mitochondrial potential

Reduction of mitochondrial membrane potential ($\Delta\Psi_m$) is associated with loss of mitochondrial function and apoptosis [259, 260]. Fluorescent microscopic examination of the amount of red and green fluorescence of DePsipher dye assesses the overall state of mitochondrial $\Delta\Psi_m$ in a population of cells [261]. Where the $\Delta\Psi_m$ is reduced, the dye remains in its monomeric form and fluoresces green, whereas normal $\Delta\Psi_m$ facilitates the aggregation and accumulation of the dye within the mitochondria where it fluoresces red/orange [262]. GSNO, 1 mM, did not induce a significant change of red/orange and green fluorescence, indicating that NO-induced cell death does not occur via a mechanism involving $\Delta\Psi_m$ disruption (Figure 8). Comparatively, treatment with ceramide as a positive control [263] resulted in a complete absence of red/orange polymer, indicating loss of $\Delta\Psi_m$.

4.8 Cyclosporin A does not reduce GSNO-induced cell death

Cyclosporin A inhibits mitochondrial permeability transition pore (PTP) opening by binding to the cyclophilin component of the pore [260]. Cells were co-treated with cyclosporin A and a range of concentrations of GSNO, from 0.001 mM to 1.0 mM, to evaluate the involvement of the PTP in NO-induced death. Cyclosporin A, at concentrations that have been

established to inhibit mitochondria-dependent apoptosis in these cells [258], had no significant effect on the amount of cell death (Figure 9). This suggests that the PTP is not involved in this mode of death, and further supports no mitochondrial involvement in NO-induced cell death.

4.9 GSNO causes nuclear p53 accumulation

The translocation of p53 from the cytosol into the nucleus was evaluated in response to GSNO. Expression of p53 in the nucleus increased dramatically in response to 1.0 mM GSNO concentration, by a factor of approximately 2.9-fold (Figure 10A, B). Furthermore, immunocytochemistry with p53-specific antibodies demonstrated an increased amount of p53, mainly localized centrally within the cell, which may correlate with the nuclear compartment (Figure 10C, D).

4.10 p53 inhibition does not reduce GSNO-induced cell death

To determine whether p53 was operative in NO-induced cell death, we used the p53 inhibitor pifithrin [264]. The concentration of pifithrin was selected for its ability to reduce cell death in cardiomyocytes [265], as well as neural [266] and hepatic cells [267] and also because lower concentrations are less effective and higher ones possess cytotoxicity [265]. Pifithrin treatment did not significantly alter the cell death induced by GSNO at concentrations of 0.1 mM and 1.0 mM (Figure 11A), suggesting that NO-induced cell death is independent of p53's transactivation ability.

Microscopic examination of the cells also demonstrated that 1.0 mM GSNO induced a loss of cellular and nuclear integrity, which was not prevented by co-treatment with pifithrin (Figure 11B). By contrast, adriamycin, which is known to induce cell death through a p53-dependent pathway [265], caused a dramatic change in cellular morphology which was prevented by co-treatment with pifithrin (Figure 12A).

4.11 Pifithrin does not reduce GSNO-induced DNA fragmentation

The comet assay was employed to quantitatively analyze the amount of DNA fragmentation. In this assay, damaged DNA can be differentiated from genomic DNA by microscopic visualization following electrophoresis and ethidium bromide staining. We found that 0.01 mM and 1.0 mM GSNO for 24 h, respectively, caused 23.2±3.6% and 31.7±4.1% of total DNA to appear in the comet tails, representing 2.1±0.3 and 2.6±0.5 fold changes compared to control (Figure 13). These results were each significantly different from control ($p<0.01$). Control cells had 10.8±2.1% DNA fragmentation, consistent with the amount of cell death that has previously been demonstrated with a variety of methodologies by this stage of cell culture [177, 254, 268]. In combination with 0.01 mM and 1.0 mM GSNO, pifithrin respectively showed 22.5±3.0% and 28.7±3.4% total DNA in the comet tails, representing 1.9±0.3 and 2.3±0.2 fold more DNA in the tail. Compared to cells that received NO but not pifithrin treatments, these results were not statistically different. However, they remained significantly ($p<0.01$) different from cells treated with only pifithrin. Based on these results, GSNO causes a concentration-dependent increase in DNA damage that is unaffected by this inhibitor of p53.

By contrast, adriamycin induced an increase in DNA fragmentation that was observable by comet assay, from 10.8±2.1% to 30.6±11.7% of total DNA in the tail, which was clearly reduced by pifithrin treatment down to 12.5±3.0% (Figure 12B,C).

4.12 SIN-1 causes nitrite accumulation in solution

The Griess reaction was also used to evaluate NO release from SIN-1, and to quantitate the amount of nitrite in solution. After a 24 h incubation in cell-free medium, 0.5 mM SIN-1 yielded 177.7±21.6 μM nitrite, representing an approximately 13-fold increase above the 13.8±14.8 μM found in the control (Figure 14).

4.13 SIN-1 induces cell death

SIN-1 induced a significant ($p<0.001$) concentration-dependent reduction in cardiomyocyte viability, as assessed by the MTT assay (Figure 15). Nearly 100% of cells were killed with 1.0 mM SIN-1 for 24 h, and 0.5 mM resulted in 55.2±5.2% cell death, which approximates the EC50 for these cells. This is comparable to previous work in adult rat ventricular cells that determined that the EC50 in that system to be 0.25 mM [269]. For this reason, we utilized the concentration of 0.5 mM to examine the cellular response in further experiments.

4.14 SIN-1-induced cell death is increased by H_2O_2

We have previously shown that H_2O_2 enhances cell death in response to the NO donor sodium nitroprusside [254]. In order to determine whether the generation of oxidative free radicals by H_2O_2 would also accentuate SIN-1-induced cell death, we co-treated cells with SIN-1 and H_2O_2 (Figure 16). The combination of 100 μM H_2O_2 plus 0.5 mM SIN-1 significantly ($p<0.01$) increased the amount of cell death caused by SIN-1 alone from 50.8±6.8%, to 96.6±1.8%. The lower concentration of 10 μM H_2O_2 in combination with SIN-1 increased the cell death to 56.3±10.9%, although this was not a statistically significantly increase. H_2O_2 alone at the low concentration of 10 μM induced 11.1±6.0% cell death, while 100 μM caused 77.0±7.6% cell death.

The Griess reaction was used to evaluate nitrite levels following treatment with the combination of SIN-1 and H_2O_2, to examine whether the increase in cell death following the SIN-1/H_2O_2 combination was due to heightened NO levels (Figure 18). Co-treatment of 0.5 mM SIN-1 with 100 μM H_2O_2 did not significantly alter NO concentrations in the medium, as it

produced 179.8±17.8 μM nitrite, compared to treatment of 0.5 mM SIN-1 alone, which produced 177.8±17.8 μM nitrite.

4.15 FeTPPS reduces cell death caused by SIN-1 and SIN-1 / H_2O_2

To determine whether reduction in peroxynitrite would modify cell death, FeTPPS, a peroxynitrite isomerase that converts peroxynitrite into the less toxic nitrate, was utilized [270]. The co-treatment of FeTPPS with SIN-1 showed a concentration-dependent reduction of the amount of cell death induced by SIN-1 alone (Figure 17). A maximal reduction was observed with FeTPPS at 50 μM, where it caused a significant ($p<0.05$) reduction of 1.0 mM SIN-1-induced cell death, from 89.7±4.2% cell death down to 71.1±6.1%.

The observed increase in cell death of 0.5 mM SIN-1 in combination with 100 μM H_2O_2 also decreased with the addition of FeTPPS (Figure 19). Both 50 μM and 20 μM FeTPPS caused significant reductions of cell death induced by this combination. The concentration of 20 μM FeTPPS significantly ($p<0.05$) reduced the cell death from 96.6±1.8% to 81.2±6.8%. With an even greater change, the concentration of 50 μM FeTPPS significantly ($p<0.01$) reduced the amount of cell death from 96.6±1.8% to 60.9±7.3%. Varying FeTPPS concentrations also tended to reduce cell death induced by the combination of 0.5 mM SIN-1 and 10 μM H_2O_2, but this was not statistically significant.

FeTPPS alone did not alter nitrite concentration (control, 13.8±14.8 μM nitrite vs. 50 μM FeTPPS, 8.7±0.5 μM nitrite). Furthermore, FeTPPS did not reduce SIN-1-induced nitrite levels (167.4±18.4 μM), nor did it reduce nitrite from the combination of SIN-1 and H_2O_2 (164.1±16.9 μM).

4.16 FeTPPS reduces cell death induced by the combination of GSNO and H_2O_2

The amount of cell death induced by the combination of 100 μM H_2O_2 with GSNO was dramatically reduced by FeTPPS (Figure 20). GSNO at 0.1 mM in combination with 100 μM H_2O_2 caused 57.1±15.3% cell death, which was significantly ($p<0.05$) reduced to 23.2±5.3% by 20 μM FeTPPS, and to 22.1±5.7% by 50 μM FeTPPS ($p<0.05$). The higher concentration of 1.0 mM GSNO in combination with 100 μM H_2O_2 caused 99.2±0.7% cell death. This amount of cell death was significantly ($p<0.01$) reduced by 10 μM FeTPPS to 66.6±7.5%. FeTPPS at the concentration of 20 μM reduced it further to 53.7±4.6% ($p<0.01$), and 50 μM reduced it to 56.4±6.8% ($p<0.01$).

When tested with GSNO alone, FeTPPS did not reduce cell death. The concentration of 0.1 mM GSNO induced 6.1±3.7% cell death and 1.0 mM GSNO caused 46.3±12.9% cell death. FeTPPS did not significantly change either of these results.

Nitrite levels following GSNO, H_2O_2, and FeTPPS combinations were also measured (Figure 18). GSNO alone produced 47.8±6.7 μM nitrite, while the inclusion of H_2O_2 produced an insignificant change to 55.2±3.4 μM. Whereas FeTPPS dramatically reduced the amount of cell death following GSNO or GSNO/H_2O_2 treatments, it had no significant effect on the nitrite levels, with 59.7±7.8 μM when included with GSNO alone, and 73.5±7.0 μM with GSNO/H_2O_2.

4.17 FeTPPS reduces H_2O_2-induced cell death

FeTPPS also reduces H_2O_2-induced cell death (Figure 21). Alone, 100 μM H_2O_2 caused 74.3±6.9% cell death, but in combination with 10 μM FeTPPS, that amount decreased to 63.6±6.2%. A significant ($p<0.05$) reduction was observed with 20 μM FeTPPS, with a reduction down to 53.5±6.6%. The highest concentration of FeTPPS, 50 μM, reduced the cell death to 56.8±5.6%. The amount of cell death induced by 10 μM H_2O_2, 9.0±4.0%, was not significantly altered by any concentration of FeTPPS tested.

4.18 Pifithrin does not reduce SIN-1-induced cell death

The effects of p53 inhibition by pifithrin on SIN-1-induced cell death were evaluated (Figure 22). No concentration of pifithrin was able to significantly modify the 7.5±8.5% cell death induced by 0.1 mM SIN-1. Also, 1.0 mM SIN-1 caused 100% cell death, which did not change with any concentration of pifithrin.

4.19 Cyclosporin A does not reduce SIN-1-induced cell death

The effect of the mitochondrial PTP blocker cyclosporin A on SIN-1-induced cell death was also assessed (Figure 23). Similar to the results obtained with cyclosporin A in combination with GSNO, our data indicates that cyclosporin A, at concentrations that were previously established to reduce cell death in these cells by palmitate (which acts through a mitochondrial pathway) [258], had no significant effect on the amount of cell death induced by SIN-1 over a wide concentration range from 0.001 to 1.0 mM.

4.20 SIN-1 causes a reduction of mitochondrial transmembrane potential

Changes in $\Delta\Psi_m$ was evaluated by DePsipher dye to determine if SIN-1 causes cell death via a mechanism that involves a reduction of the $\Delta\Psi_m$ (Figure 24). Untreated control cells were found to possess high quantities of the orange aggregated dye, indicative of healthy, intact mitochondrial transmembrane potential. Cells treated with 100 μM ceramide were used as a positive control, as it has previously been demonstrated to produce a loss of $\Delta\Psi_m$ [263]. Treatment with 0.5 mM SIN-1 for 24 h caused a dramatic decrease in abundance of the orange aggregates, as well as a concomitant increase in the green dye monomers, representative of reduced $\Delta\Psi_m$. By contrast, co-treatment of SIN-1 with 50 μM FeTPPS reduced the amount of

green staining and partially restored the abundance of orange aggregates back towards control levels.

4.21 Protein tyrosine nitration

The amount of whole cell protein nitration was examined by Western blotting using anti-nitrotyrosine antibodies (Figure 25). Control samples demonstrated minimal amounts of nitrotyrosine. However, 0.5 mM SIN-1 for 24 h showed a dramatically increased nitrotyrosine signal. Also, 10 μM H_2O_2 alone showed no bands, and in combination with SIN-1, did not produce a major increase in the amount of nitrotyrosine formed by SIN-1 alone. FeTPPS was associated with minimal nitrotyrosine banding, and it greatly diminished the intensity of both the SIN-1 and SIN-1 plus H_2O_2 nitrotyrosine signals.

Furthermore, the specific compartmentalization of protein tyrosine nitration was examined by mitochondrial and cytosolic fractionation of cell lysates (Figure 26). Cardiomyocytes were treated with SIN-1, 0.5 mM for 24 h and mitochondrial and cytosolic subcellular fractions were separated using methodology that we have shown isolates a relatively pure mitochondrial preparation based on the presence of mitochondrial markers and the absence of cytosolic ones [268]. Treatment with 0.5 mM SIN-1 for 24 h showed increased nitrotyrosine content in both the cytosol and mitochondrial fractions, relative to the minimal amount of banding in the control. It is noteworthy that the mitochondrial fraction primarily showed a strong nitrotyrosine signal near the protein molecular weight of 75 kDa. Treatment with FeTPPS had minimal effect on decreasing the SIN-1 signal in the cytosol but had more of an effect to reduce nitrotyrosine signal when SIN-1 was combined with H_2O_2. In both fractions, FeTPPS reduced the nitrotyrosine signals following SIN-1 plus H_2O_2 treatment.

Protein tyrosine nitration was also assessed by immunocytochemistry (Figure 27). Control cells demonstrated a basal amount of green nitrotyrosine fluorescence. Cardiomyocytes

treated with 0.5 mM SIN-1 for 24 h displayed a diffuse green staining pattern that covered the entire cells. This staining pattern may be indicative of membrane-associated nitration, as it appeared to preclude any significant amount of intracellular staining or viewable morphological characteristics, as noted by the absence of the normally distinguishable nucleus. On the other hand, 24 h 1.0 mM GSNO treatment resulted in an increased amount of intense green staining, indicative of augmented nitrotyrosine formation, while still being able to distinguish the nucleus and a slightly shrunken morphology, as observed with the modified Wright Giemsa stain (Figure 3). Incubation with 50 μM FeTPPS reduced the basal control levels of nitrotyrosine to a minimal amount. FeTPPS also reduced nitrotyrosine staining in SIN-1 and GSNO treatments. In the SIN-1 plus FeTPPS cells, the diffuse green pattern was greatly diminished, and the nucleus and other, apparently intracellular, nitrotyrosine residues were visible. However, there still appeared to be increased nitrotyrosine staining, compared to the control. The GSNO plus FeTPPS resulted in a lessening of the amount of green fluorescence induced by GSNO itself, but there was not a total elimination of staining.

Figures

Figure 1: S-nitrosoglutathione releases nitric oxide in solution

Nitrite in solution was used as an indicator of the presence of nitric oxide (NO) released from the donor S-nitrosoglutathione (GSNO). Cell free culture medium was incubated for 24 h at 37°C and 5% CO_2 in the presence or absence of 0.1 mM and 1.0 mM GSNO. A standard curve of nitrite concentrations was prepared from 1.0 mM sodium nitrite, $NaNO_2$. Aliquots of samples and standards (100 µl) were taken and combined with 50 µl 1% sulphanilamide and 50 µl 0.1% N'N-naphthylethylenediamine (Griess reaction) in duplicate wells of a 96-well plate. The absorbance was read at 570 nm after 10 minutes. Results are presented as the mean concentration [uM] of nitrite, NO_2^-, in solution ± SEM for each concentration of GSNO. 1.0 mM GSNO (N=8), 0.1 mM GSNO (N=6) and control (N=8).

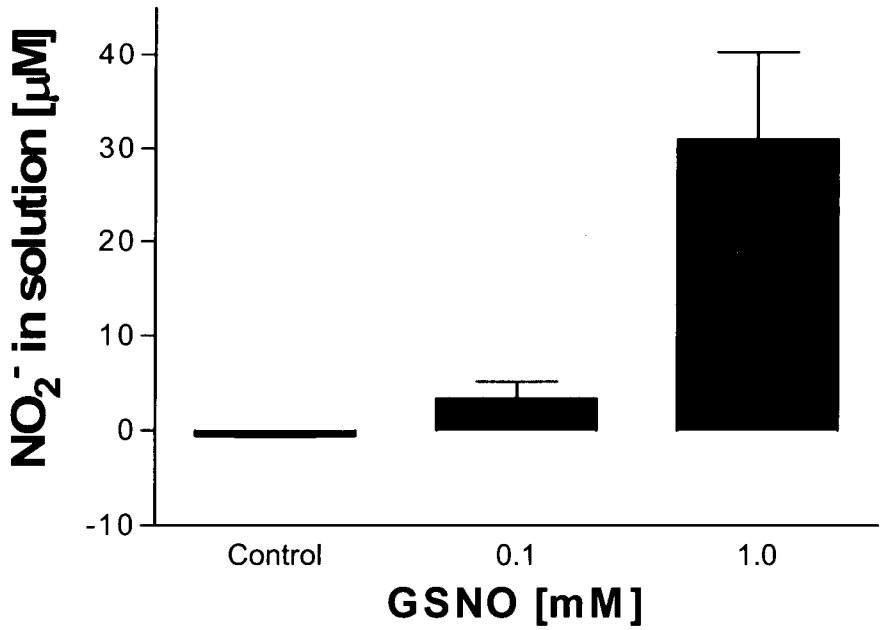

Figure 2: S-nitrosoglutathione induces cell death

Cardiomyocytes were maintained in culture for 72 h in 96-well plates. The amount of cell death following S-nitrosoglutathione (GSNO) treatment was examined by MTT assay. GSNO was added in duplicate at concentrations of 0.001 mM (N=9), 0.01 mM (N=10), 0.1 mM (N=11), 1.0 mM (N=11), and 10 mM (N=9) for 24 h. MTT dye (10 µl) was added to each well for the final 4 h of the experiment. The experiment was stopped with the addition of 100 µl solubilization solution to each well and left to solubilize for 24 h. Absorbance was then measured at 570 nm. Results are presented as mean percent change of cell death relative to control ± SEM (**p<0.01). Inset: Mean corrected absorbance values ± SEM are shown (**p<0.01).

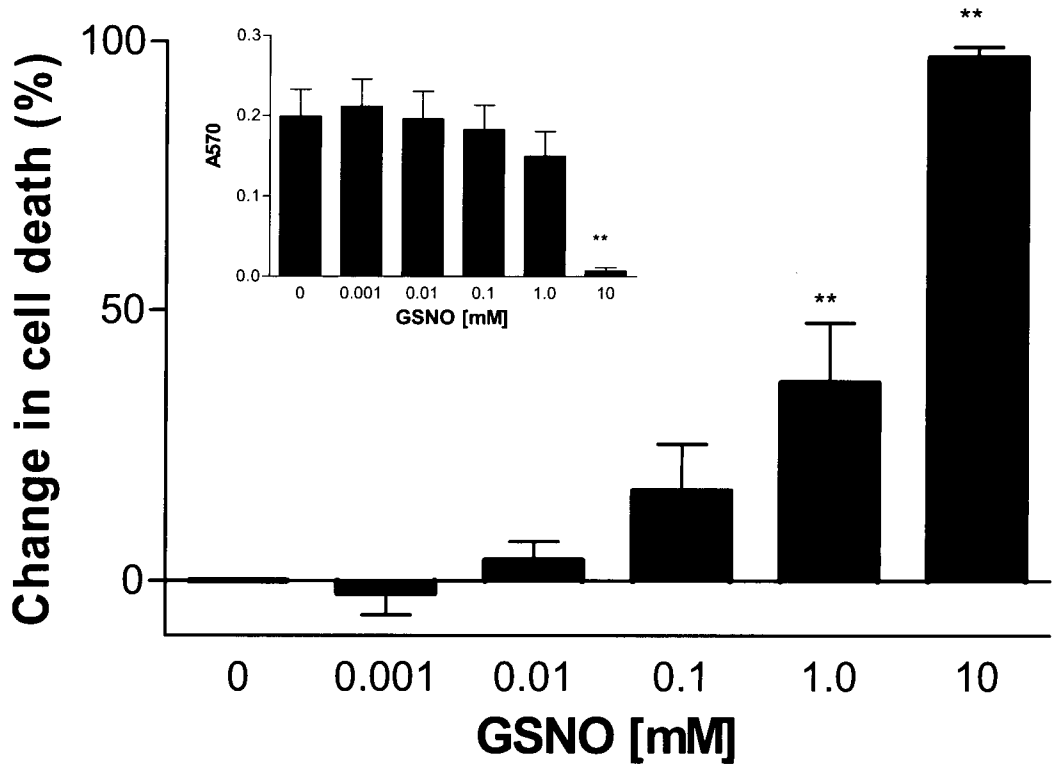

Figure 3: S-nitrosoglutathione causes changes in cellular morphology
Cardiomyocytes were cultured directly on to glass coverslips and maintained for 72 h. Cells were treated with 0.1 mM S-nitrosoglutathione (GSNO) (panel B), 1.0 mM GSNO (panel C), or diluent (panel A) for 24 h, prior to staining by a modified Wright Giemsa method. Coverslips were dipped for 15 seconds each sequentially in 10% methanol, eosin, and methylene blue solutions. Representative photomicrographs are shown.

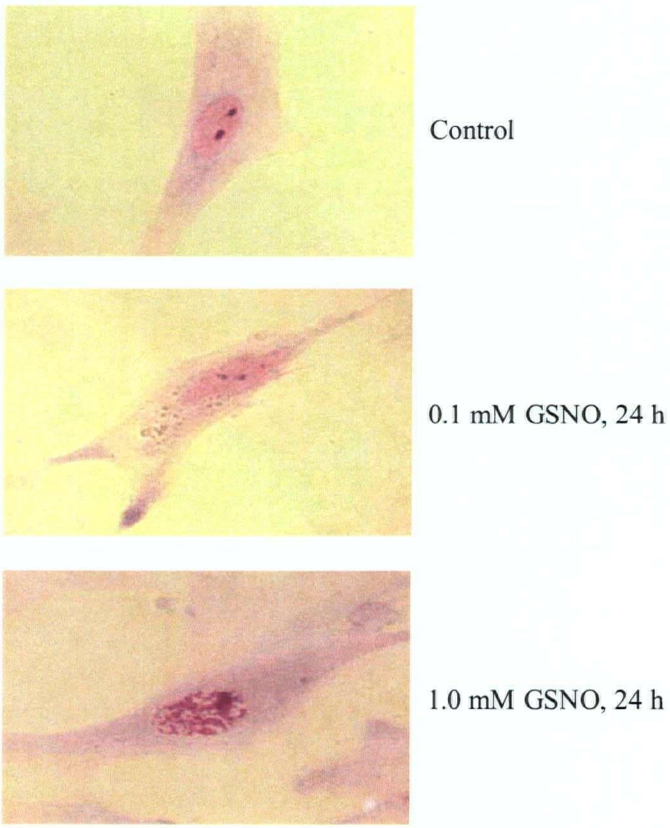

Figure 4: S-nitrosoglutathione causes an increase in p53 expression
Cardiomyocytes in culture for 72 h were treated with S-nitrosoglutathione (GSNO) or diluent for 1 h (N=3), and then harvested in RIPA buffer. Equal amounts of protein, assessed by the Bradford assay, were loaded on to 12% SDS-PAGE gels, transferred to nitrocellulose membranes, probed with p53-specific antibodies and HRP-conjugated secondary antibodies, visualized on photographic film by chemiluminescence exposure, and subjected to densitometric analysis. Panel A is a representative Western blot. Panel B shows graphical results presented as mean fold change ± SEM compared to control (**$p<0.01$).

A

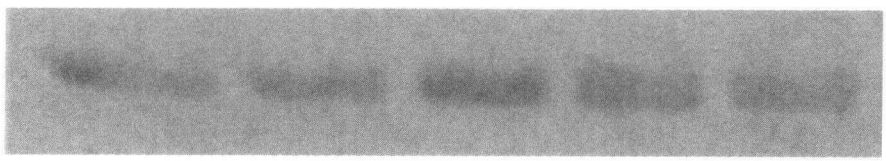

B

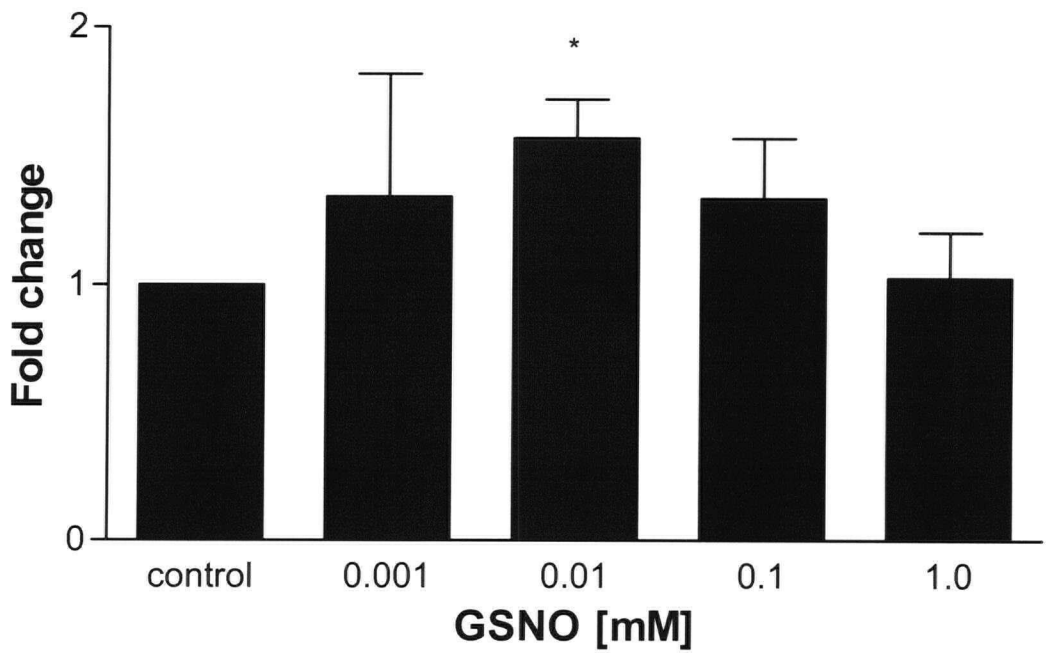

Figure 5: S-nitrosoglutathione causes a time-dependent increase in p53 expression
Cardiomyocytes in culture for 72 h were treated with S-nitrosoglutathione (GSNO) or diluent for the indicated times. Cells were harvested in RIPA buffer and equal amounts of protein, assessed by the Bradford assay, were loaded on to a 12% SDS-PAGE gel, examined by Western blotting and subjected to densitometric analysis. Results are presented as mean fold change ± SEM compared to control (*$p<0.05$, **$p<0.01$). Panel A: control (N=3) vs. 0.001 mM GSNO, 1 h (N=3). Panel B: control (N=3) vs. 0.01 mM GSNO, 1 h (N=3). Panel C: control (N=3) vs. 0.1 mM GSNO 1 h (N=3), 2 h (N=1), 4 h (N=1), 24 h (N=2). Panel D: control (N=3) vs. 1.0 mM GSNO 1 h (N=3), 2 h (N=2), 4 h (N=2), 24 h (N=2).

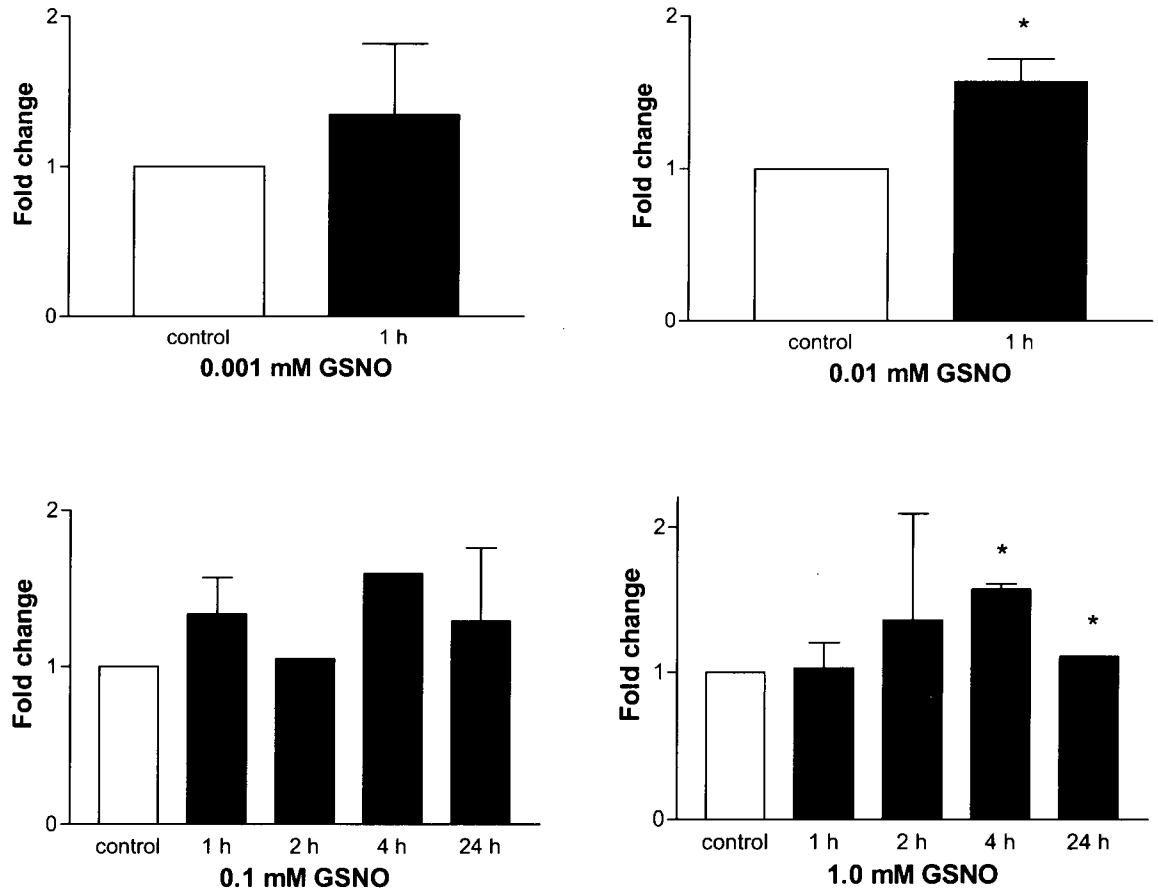

Figure 6: S-nitrosoglutathione causes no p53 translocation from cytosol to mitochondria
Cardiomyocytes were maintained in culture for 72 h. Cells were treated with 0.1 mM S-nitrosoglutathione (GSNO) or diluent for the indicated times (N=3). Mitochondrial and cytosolic fractions were obtained by differential centrifugation. Equal amounts of protein from each fraction, assessed by the Bradford assay, were loaded on to a 12% SDS-PAGE gel, examined by Western blotting with anti-p53 antibodies and subjected to densitometric analysis. Panel A shows a representative Western blot. Panel B shows results presented as mean fold change ± SEM.

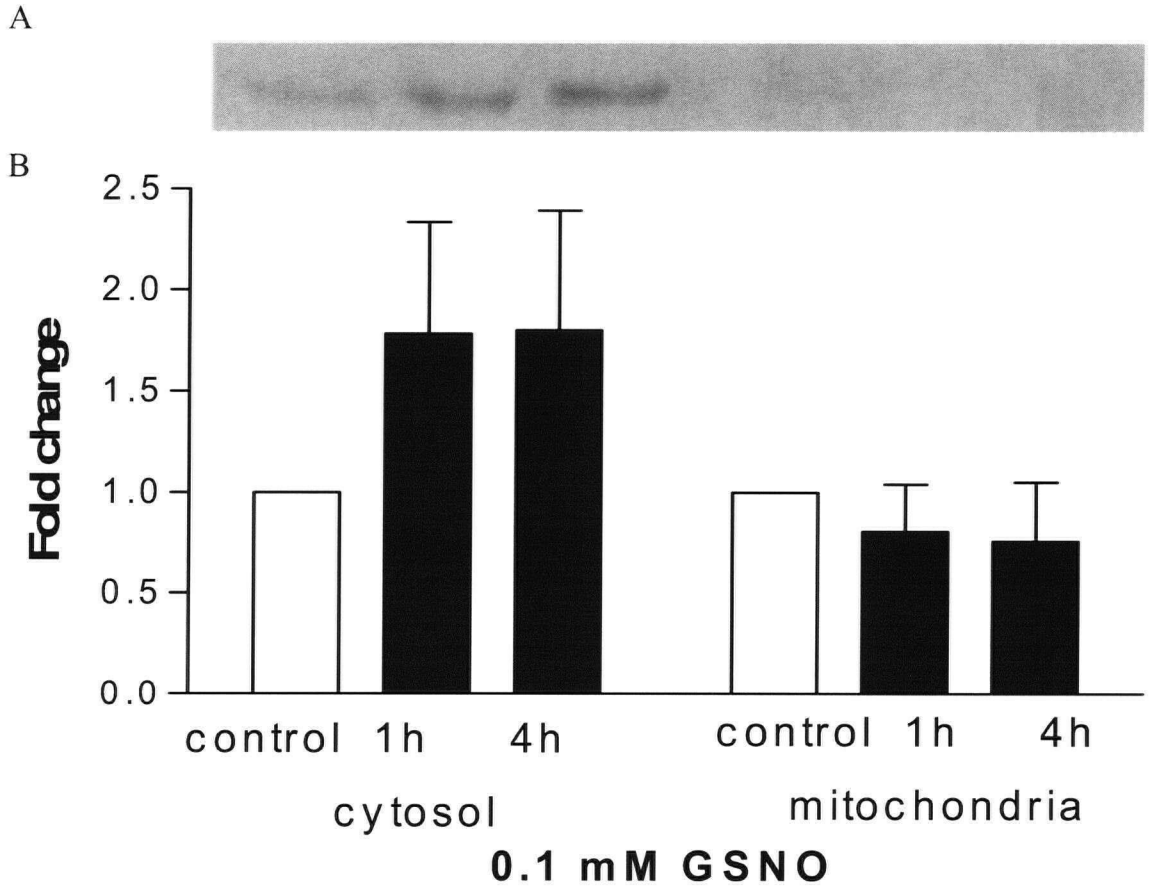

Figure 7: S-nitrosoglutathione causes no cytochrome c translocation from mitochondria to cytosol

Cardiomyocytes were maintained in culture for 72 h. Cells were treated with either 500 μM palmitate or 1 mM S-nitrosoglutathione (GSNO) for 24 h (N=1). Mitochondrial and cytosolic fractions were obtained by differential centrifugation. Equal amounts of protein from each fraction, assessed by the Bradford assay, were loaded on to a 12% SDS-PAGE gel, examined by Western blotting with anti-cytochrome c antibodies and subjected to densitometric analysis. Panel A shows a representative Western blot. Panel B shows results presented as mean fold change relative to control.

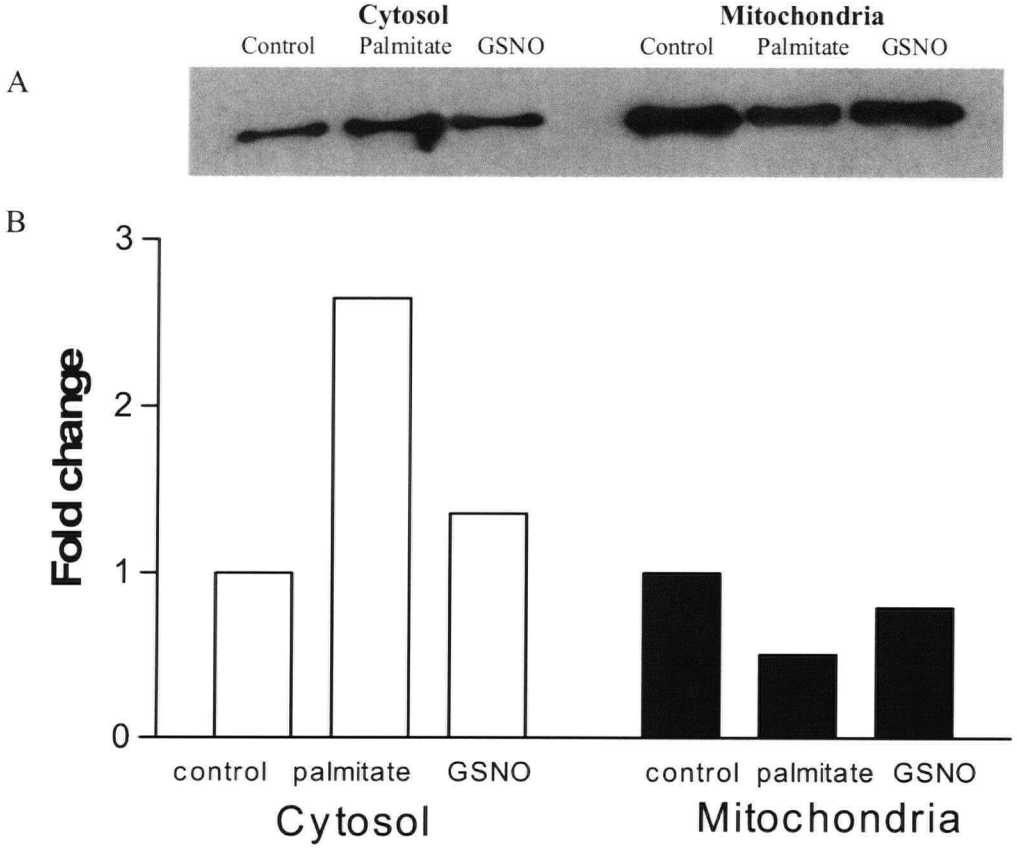

Figure 8: S-nitrosoglutathione does not alter mitochondrial membrane potential
Cardiomyocytes were plated directly on to glass coverslips and maintained in culture for 72 h. Cells were treated with 1 mM S-nitrosoglutathione (GSNO) for 24 h, or 100 μM ceramide for 24 h as a positive control. Coverslips were stained with DePsipher™ to visualize mitochondrial membrane potential. Red/orange aggregates indicate healthy mitochondria; green monomers indicate reduced mitochondrial membrane potential. Representative cells are shown (N=3, except N=2 for GSNO).

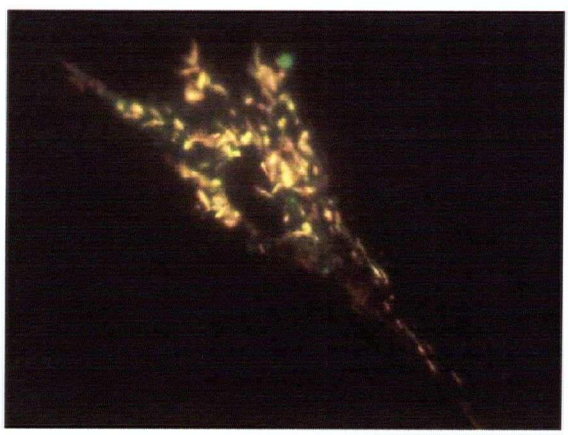

Control

Ceramide

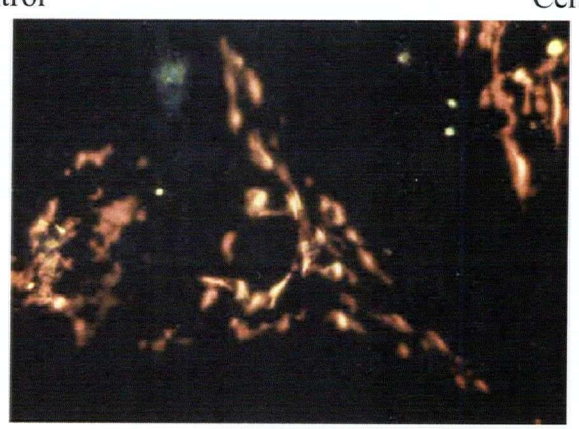

GSNO

Figure 9: Cyclosporin A does not affect S-nitrosoglutathione-induced cell death
Cardiomyocytes were maintained in culture for 72 h in 96-well plates. The amount of cell death following S-nitrosoglutathione (GSNO), at the indicated concentrations, combined with cyclosporin A 0.1 μM (lined), 1.0 μM (solid), or diluent (clear) was examined by MTT assay (N=5). GSNO and cyclosporin A were added for 24 h, and each well was conducted in duplicate. MTT dye (10 μl) was added to each well for the final 4 h of the experiment. The experiment was stopped with the addition of 100 μl solubilization solution to each well and left to solubilize for 24 h. Absorbance was then measured at 570 nm. Results are presented as mean percent change of cell death relative to control ± SEM.

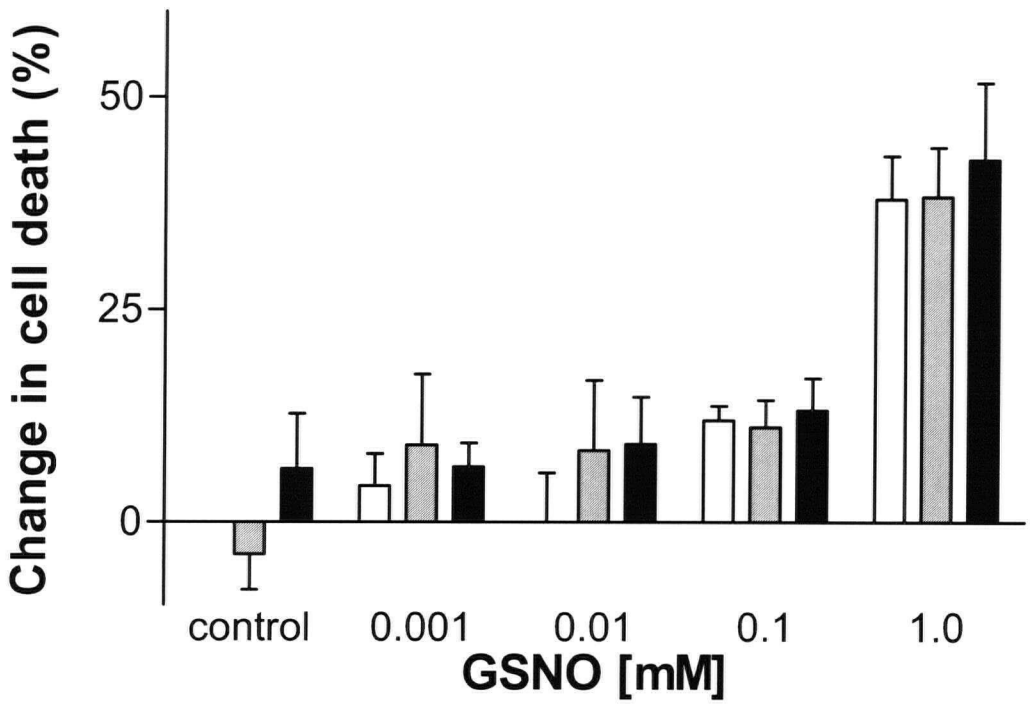

Figure 10: S-nitrosoglutathione causes nuclear p53 accumulation

Panels A and B: Cardiomyocytes were maintained in culture for 72 h. Cells were treated with diluent or S-nitrosoglutathione (GSNO) at the indicated concentrations for 24 h (N=1). Nuclear and cytosolic fractions were obtained by differential centrifugation. Equal amounts of protein from each fraction, assessed by the Bradford assay, were loaded on to a 12% SDS-PAGE gel, examined by Western blotting, and subjected to densitometric analysis. Panel A shows a representative Western blot. Panel B shows results presented as fold change relative to control. Panels C and D: Cardiomyocytes, cultured directly on to glass coverslips, were treated with 1.0 mM GSNO or diluent for 24 h, and subjected to immunocytochemistry using anti-p53 antibodies and FITC-conjugated secondary antibodies before viewing through an epifluorescent microscope. Panel C shows a representative control cell. Panel D shows a representative cell following treatment with 1.0 mM GSNO for 24 h.

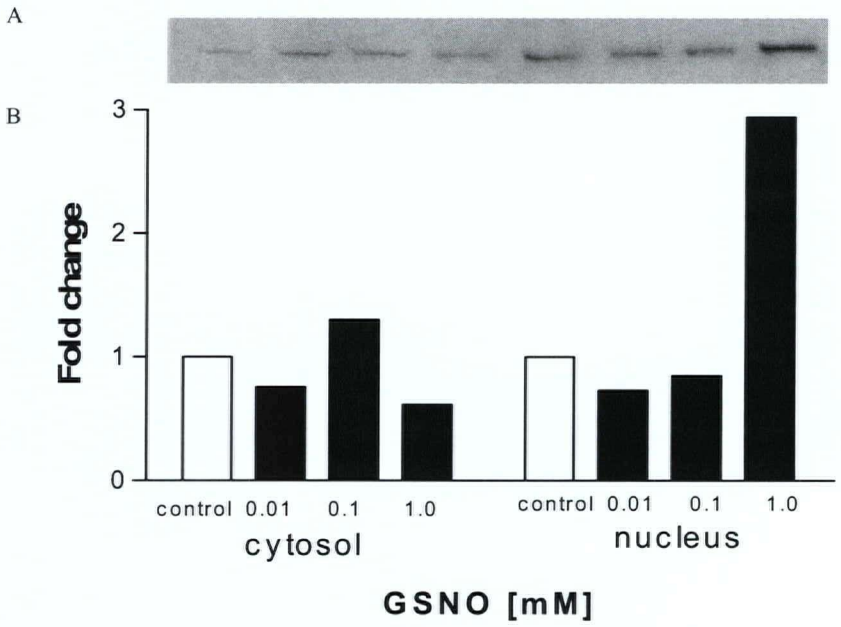

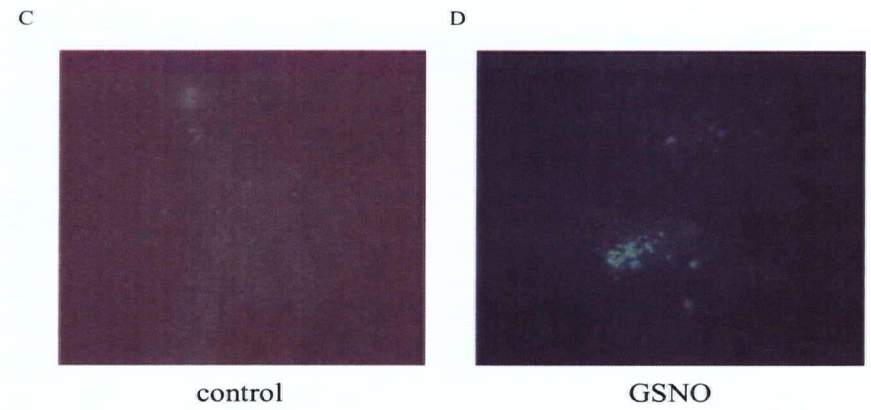

Figure 11: Pifithrin does not reduce S-nitrosoglutathione-induced cell death
Cardiomyocytes were maintained in culture for 72 h in 96-well plates. Panel A: The amount of cell death following S-nitrosoglutathione (GSNO) at the indicated concentrations and pifithrin treatment (N=9 for all treatments, except 0.1 μM pifithrin, N=8) was examined by MTT assay. Each well on the plate was conducted in duplicate. MTT dye (10 μl) was added to each well for the final 4 h of the experiment. The experiment was stopped with the addition of 100 μl solubilization solution to each well and left to solubilize for 24 h. Absorbance was then measured at 570 nm. Results are presented as mean percent change in cell death relative to control ± SEM. Panel B: Cells were treated with 1.0 mM GSNO or GSNO plus 10 μM pifithrin, and visualized by modified Wright-Giemsa staining. Representative cells are shown.

A

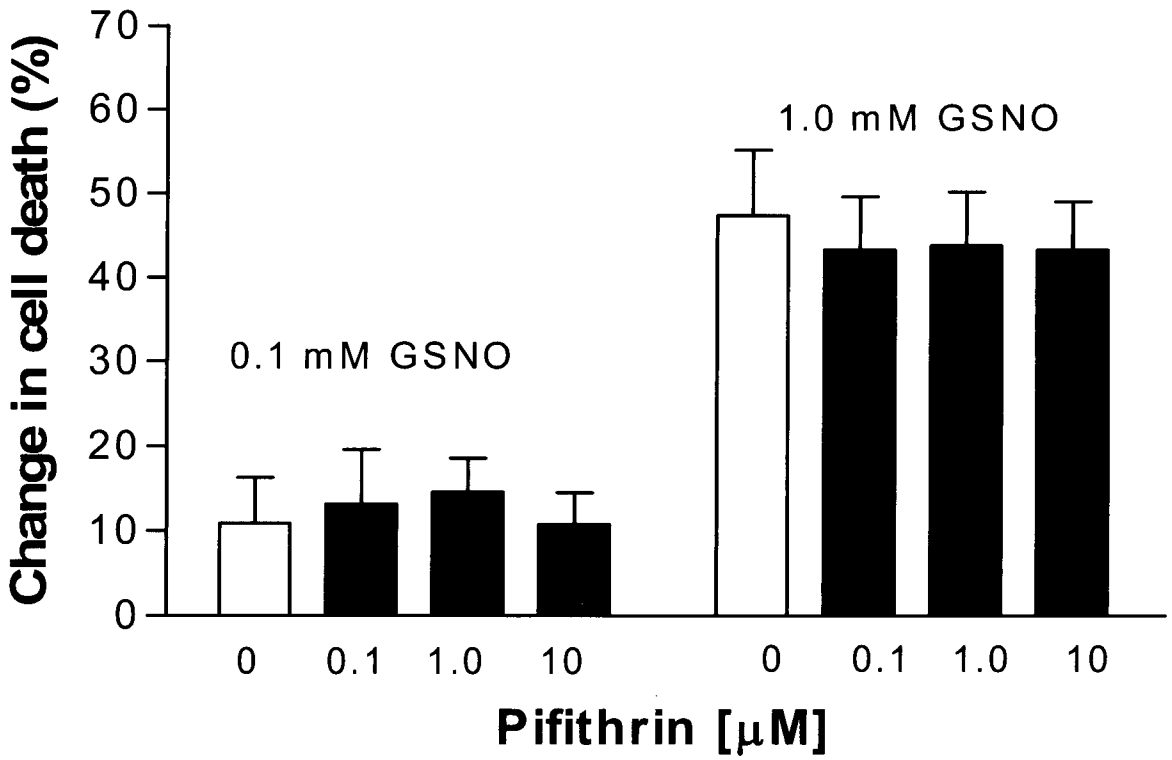

B

GSNO

GSNO + pifithrin

Figure 12: Pifithrin reduces adriamycin-induced p53-dependent DNA and cellular damage
Cardiomyocytes were maintained in culture for 72 h. Panel A: Cells were treated with 5 μM adriamycin or adriamycin plus 10 μM pifithrin for 24 h, and visualized by modified Wright-Giemsa staining. Representative cells are shown. Panel B: Cells treated with 5 μM adriamycin, 10 μM pifithrin, or a combination of both for 24 h. The amount of DNA fragmentation was analyzed by comet assay. Cells were treated with 5 μM adriamycin, 10 μM pifithrin, or a combination of both for 24 h (N=3). Cells were embedded in agarose, permeabilized, subjected to electrophoresis and stained with ethidium bromide. Representative cells of the indicated treatments are shown. Panel C: Comet assay results are presented as % total DNA in the comet tail ± SEM for the indicated treatments compared to controls.

A

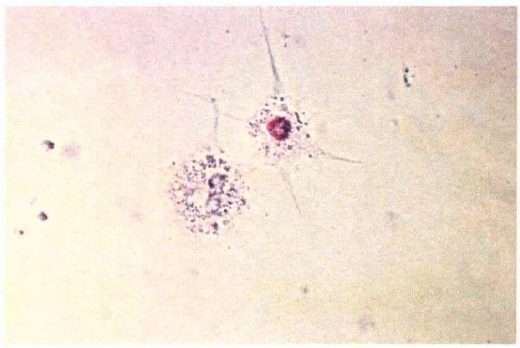

adriamycin

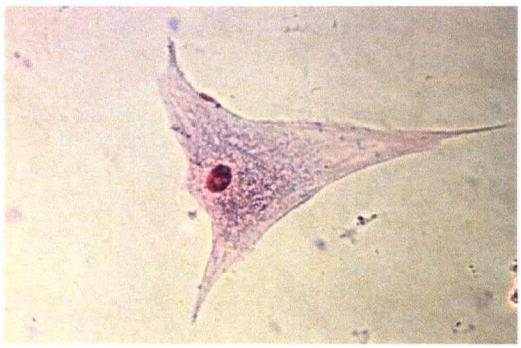

adriamycin + pifithrin

B

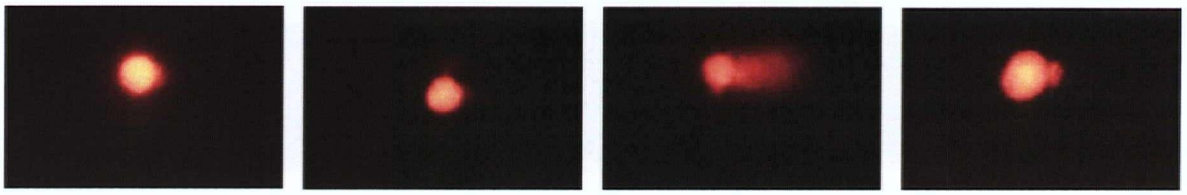

control | pifithrin | adriamycin | adriamycin + pifithrin

C

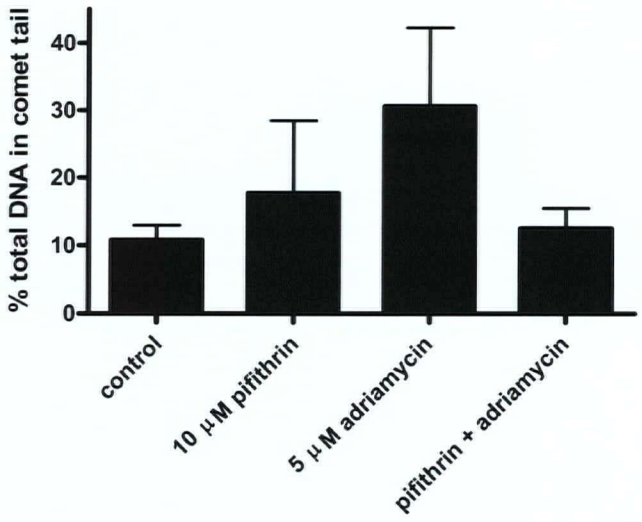

Figure 13: S-nitrosoglutathione causes DNA fragmentation that is not modified by pifithrin
Cardiomyocytes were maintained in culture for 72 h. The amount of DNA fragmentation was analyzed by comet assay. Cells were treated with 0.01 mM (N=6) and 1.0 mM (N=6) S-nitrosoglutathione (GSNO), or 10 μM pifithrin alone (N=5) or in combination with 0.01 mM (N=6) and 1.0 mM GSNO (N=6) for 24 h. Cells were embedded in agarose, permeabilized, subjected to electrophoresis and stained with ethidium bromide. Panel A shows representative cells of the indicated treatments. Panel B depicts the results presented as mean fold change in % DNA in comet tail, relative to control for the indicated treatments. Panel B Inset: Results are presented as % total DNA in the comet tail for the indicated treatments compared to control. Significant differences between NO and control/pifithrin are denoted (*$p<0.05$, **$p<0.01$). There is no statistically significant difference between NO and NO/pifithrin treatments.

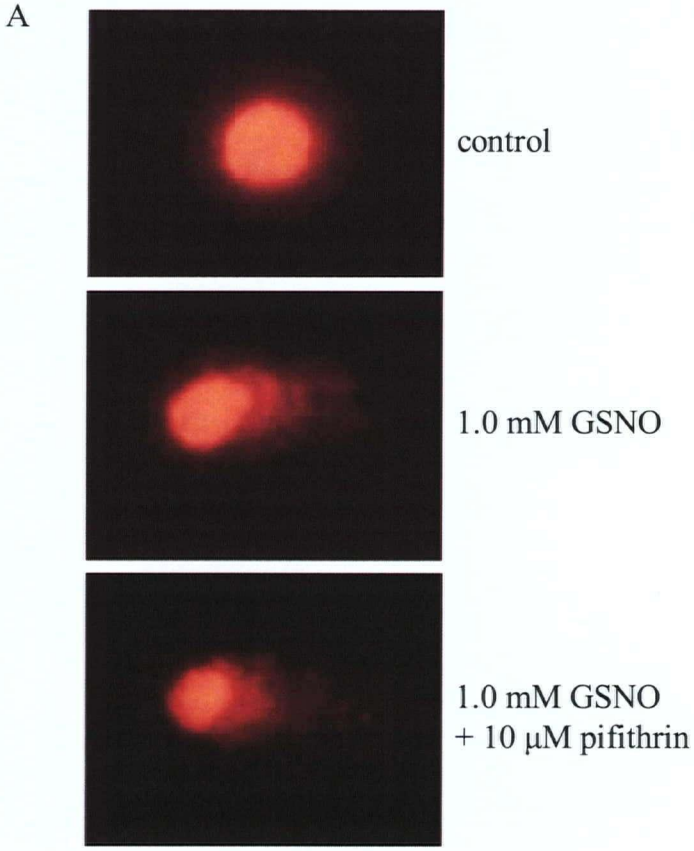

B

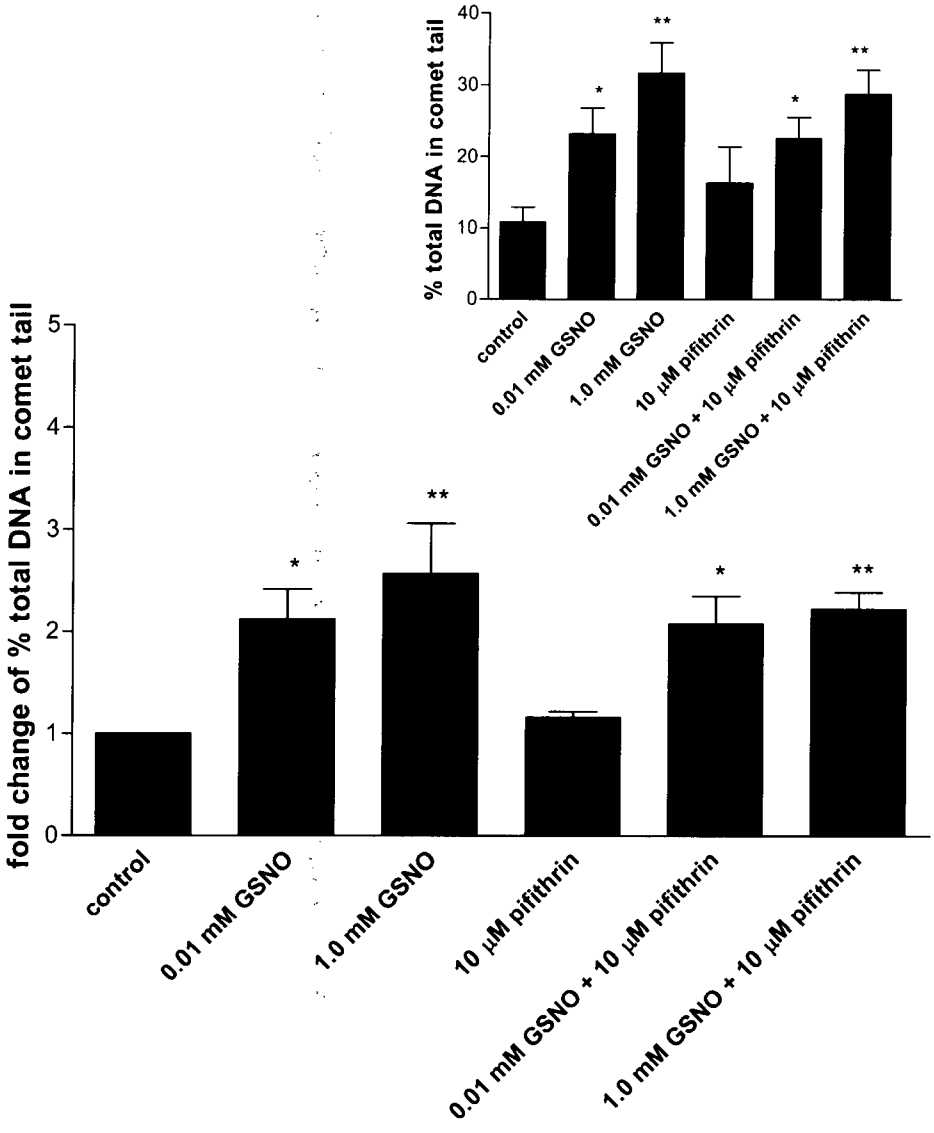
% total DNA in comet tail
0
10
20
30
40
control
0.01 mM GSNO
1.0 mM GSNO
10 μM pifithrin
0.01 mM GSNO + 10 μM pifithrin
1.0 mM GSNO + 10 μM pifithrin
fold change of % total DNA in comet tail
0
1
2
3
4
5
control
0.01 mM GSNO
1.0 mM GSNO
10 μM pifithrin
0.01 mM GSNO + 10 μM pifithrin
1.0 mM GSNO + 10 μM pifithrin

Figure 14: 3-morpholinosydnonime releases nitric oxide in solution

Nitrite in solution was used as an indicator of the presence of nitric oxide (NO) released from the donor 3-morpholinosydnonime (SIN-1). Cell free culture medium was incubated for 24 h in an incubator set to 37°C and 5% CO_2 in the presence or absence of 0.5 mM SIN-1. A standard curve of nitrite concentrations was prepared from 1.0 mM sodium nitrite, $NaNO_2$. Aliquots of samples and standards (100 µl) were taken and combined with 50 µl 1% sulphanilamide and 50 µl 0.1% N'N-naphthylethylenediamine (Griess reaction) in duplicate wells of a 96-well plate. The absorbance was read at 570 nm after 10 minutes. Results are presented as concentration [uM] of nitrite, NO_2^-, in solution ± SEM. Results for 1.0 mM S-nitrosoglutathione (GSNO) are shown for comparison.

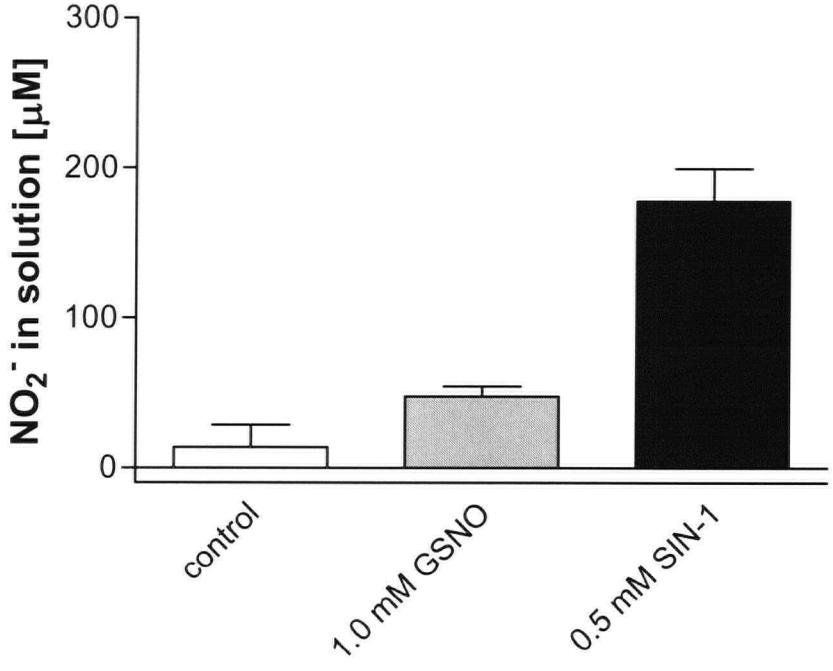

Figure 15: 3-morpholinosydnonime induces cell death

Cardiomyocytes were maintained in culture for 72 h in 96-well plates. The amount of cell death following 3-morpholinosydnonime (SIN-1) treatment was examined by MTT assay (N=12). SIN-1 was added at concentrations of 0.001 mM, 0.01 mM, 0.1 mM, 0.5 mM, and 10 mM for 24 h. MTT dye (10 µl) was added to each well for the final 4 h of the experiment. The experiment was stopped with the addition of 100 µl solubilization solution to each well and left to solubilize for 24 h. Absorbance was then measured at 570 nm. Results are presented as mean percent change of cell death relative to control ± SEM. (*$p<0.05$, **$p<0.01$). Inset: Mean corrected absorbance values ± SEM are shown.

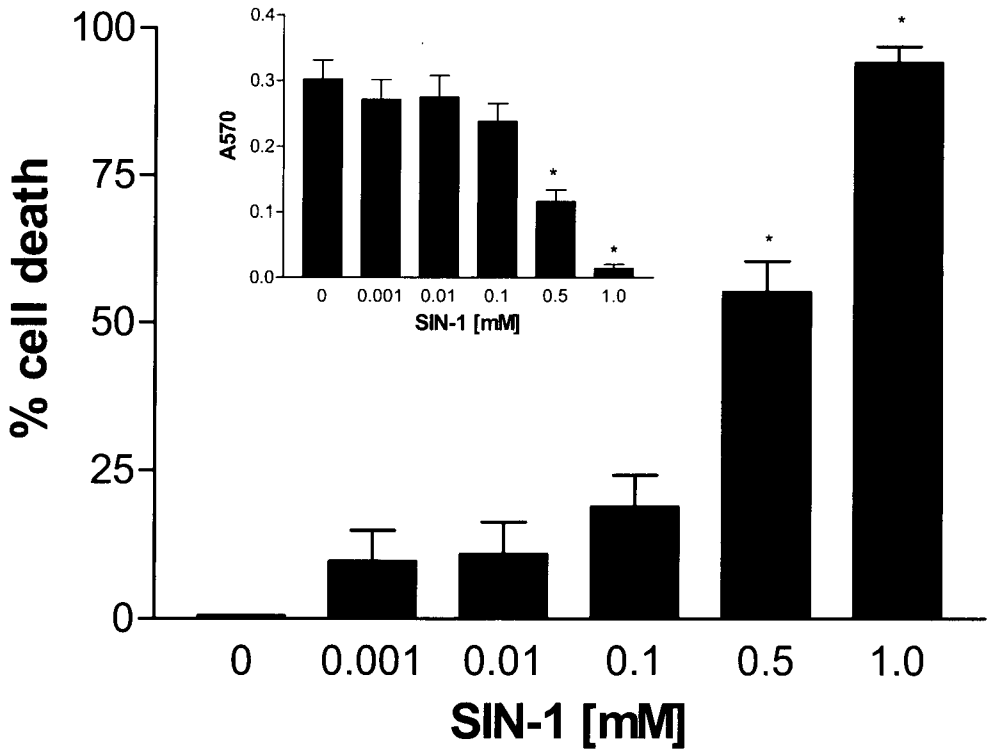

Figure 16: H_2O_2 enhances 3-morpholinosydnonime -induced cell death
Cardiomyocytes were maintained in culture for 72 h in 96-well plates. The amount of cell death following 0.5 mM 3-morpholinosydnonime (SIN-1) treatment in combination with 10 μM and 100 μM H_2O_2 for 24 h was examined by MTT assay (N=9). MTT dye (10 μl) was added to each well for the final 4 h of the experiment. The experiment was stopped with the addition of 100 μl solubilization solution to each well and left to solubilize for 24 h. Absorbance was then measured at 570 nm. Results are presented as mean percent change of cell death relative to control ± SEM. *p<0.05, **p<0.01.

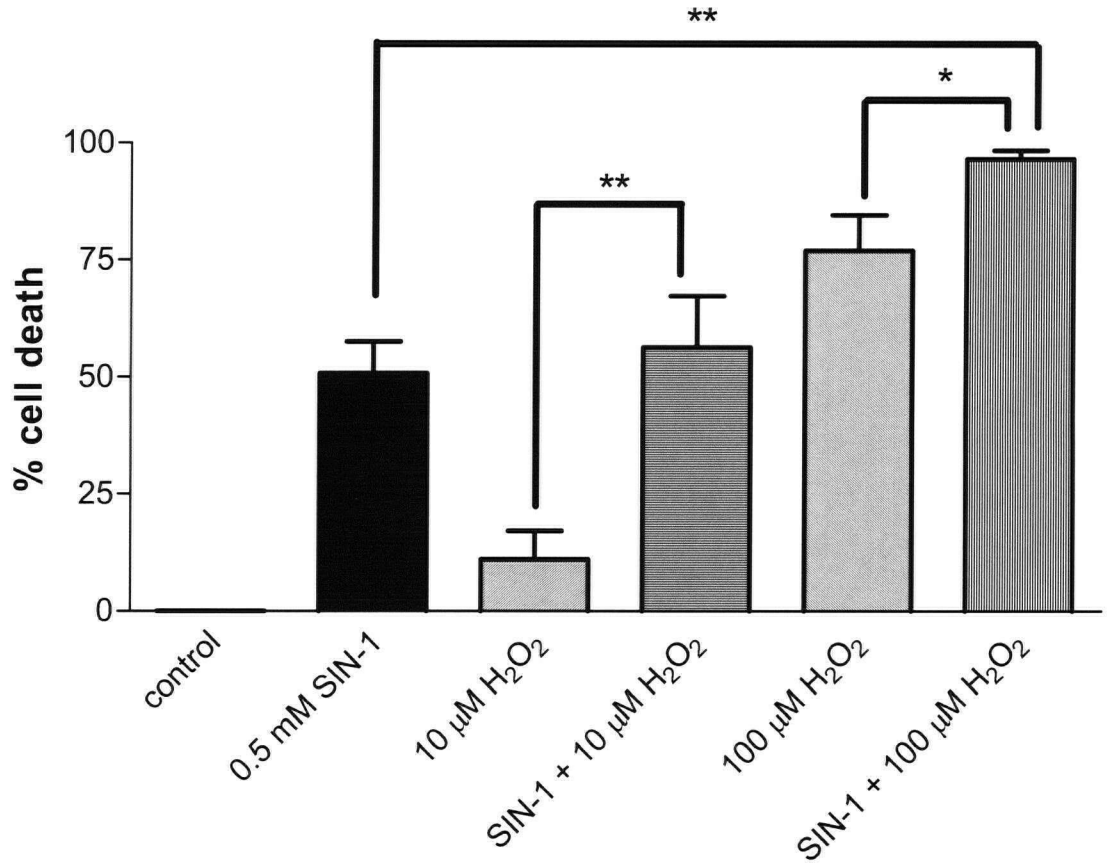

Figure 17: FeTPPS reduces 3-morpholinosydnonime-induced cell death
Cardiomyocytes were maintained in culture for 72 h in 96-well plates. The amount of cell death following 3-morpholinosydnonime (SIN-1) treatment alone and in combination with FeTPPS for 24 h was examined by MTT assay (N=9). MTT dye (10 µl) was added to each well for the final 4 h of the experiment. The experiment was stopped with the addition of 100 µl solubilization solution to each well and left to solubilize for 24 h. Absorbance was then measured at 570 nm. Results are presented as percent change of cell death relative to control (absence of SIN-1 and FeTPPS), and are expressed as mean ± SEM. (*$p<0.05$).

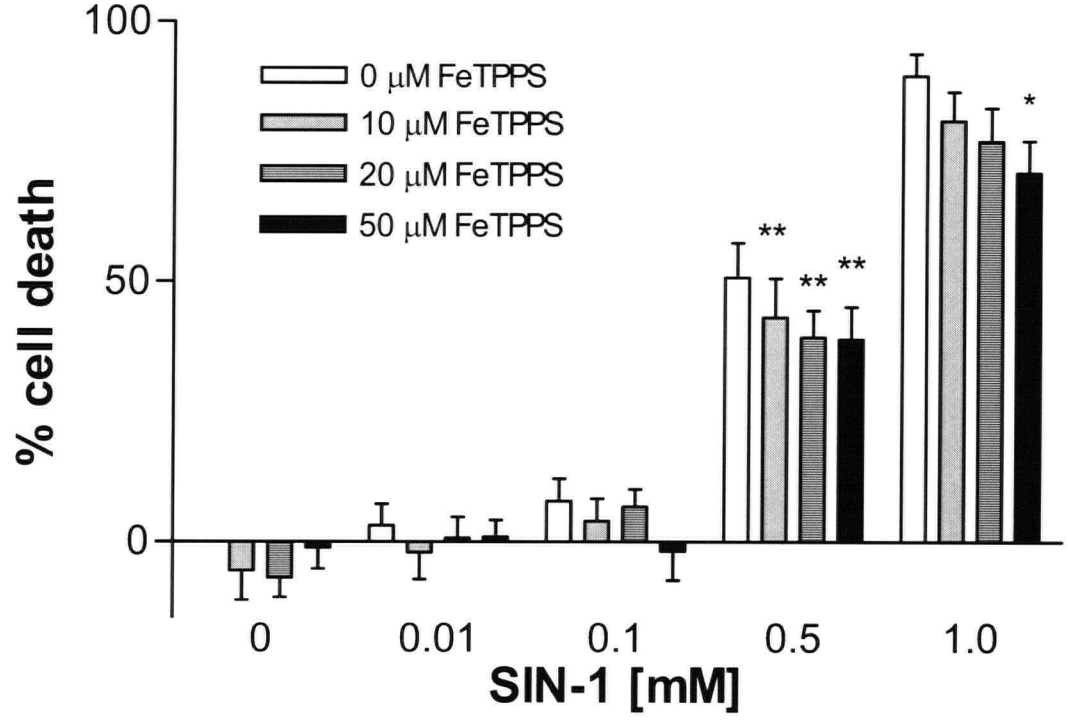

Figure 18: Nitrite in solution

Nitrite in solution was used as an indicator of the presence of nitric oxide (NO) released from the indicated treatments. Cell free culture medium was incubated for 24 h at 37°C and 5% CO_2, following treatment with the indicated combinations of 1.0 mM S-nitrosoglutathione (GSNO), 0.5 mM 3-morpholinosydnonime (SIN-1), 100 μM H_2O_2, and/or 50 μM FeTPPS (N=3). Aliquots of samples and standards (100 μl) were taken and combined with 50 μl 1% sulphanilamide and 50 μl 0.1% N'N-naphthylethylenediamine (Griess reaction) in duplicate wells of a 96-well plate. The absorbance was read at 570 nm after 10 minutes. Results are presented as concentration [uM] of nitrite, NO_2^-, in solution ± SEM. Panel A: SIN-1-mediated changes in nitrite concentration. Panel B: GSNO-mediated changes in nitrite concentration.

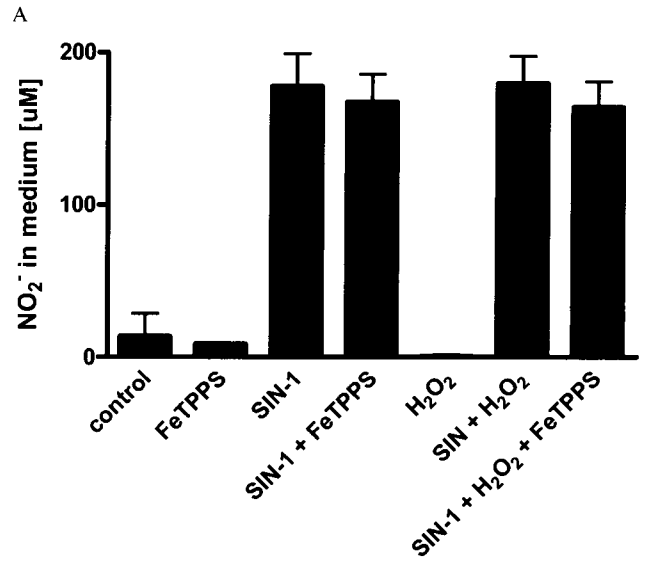

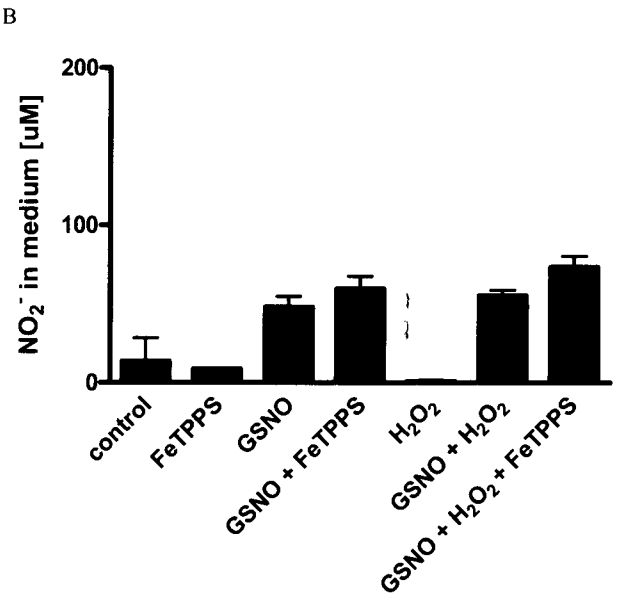

Figure 19: FeTPPS reduces 3-morpholinosydnonime/H_2O_2-induced cell death
Cardiomyocytes were maintained in culture for 72 h in 96-well plates. The amount of cell death following 3-morpholinosydnonime (SIN-1) and H_2O_2 treatments alone and in combination with FeTPPS for 24 h was examined by MTT assay (N=9). MTT dye (10 µl) was added to each well for the final 4 h of the experiment. The experiment was stopped with the addition of 100 µl solubilization solution to each well and left to solubilize for 24 h. Absorbance was then measured at 570 nm. Absorbance was measured at 570 nm. Results are presented as mean percent change of cell death relative to control ± SEM. Statistically significant differences between FeTPPS and respective controls is denoted (*$p<0.05$, **$p<0.01$).

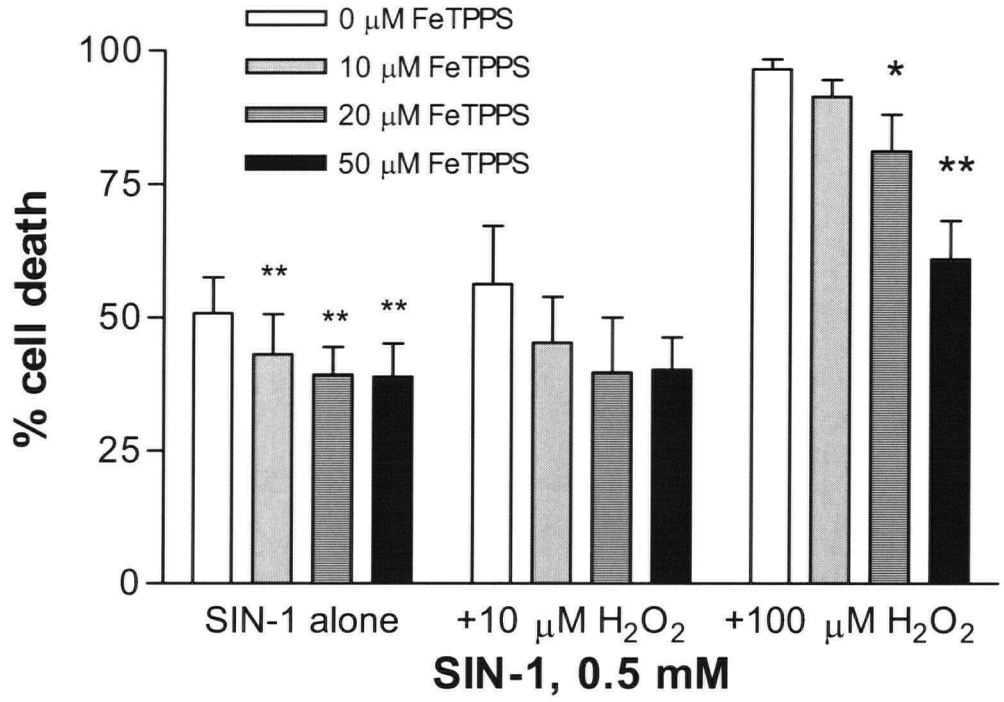

Figure 20: FeTPPS reduces S-nitrosoglutathione + H_2O_2-induced cell death, but not S-nitrosoglutathione-induced cell death

Cardiomyocytes were maintained in culture for 72 h in 96-well plates. The amount of cell death following S-nitrosoglutathione (GSNO) and H_2O_2 treatments alone and in combination with FeTPPS for 24 h was examined by MTT assay (N=17 for control, N=8 for 0.1 mM and 1.0 mM GSNO, N=14 for 100 μM H_2O_2, N=5 for both combinations of GSNO and H_2O_2). MTT dye (10 μl) was added to each well for the final 4 h of the experiment. The experiment was stopped with the addition of 100 μl solubilization solution to each well and left to solubilize for 24 h. Absorbance was then measured at 570 nm. Results are presented as mean percent change of cell death relative to control ± SEM. Statistically significant changes induced by FeTPPS are denoted (*p<0.05, **p<0.01).

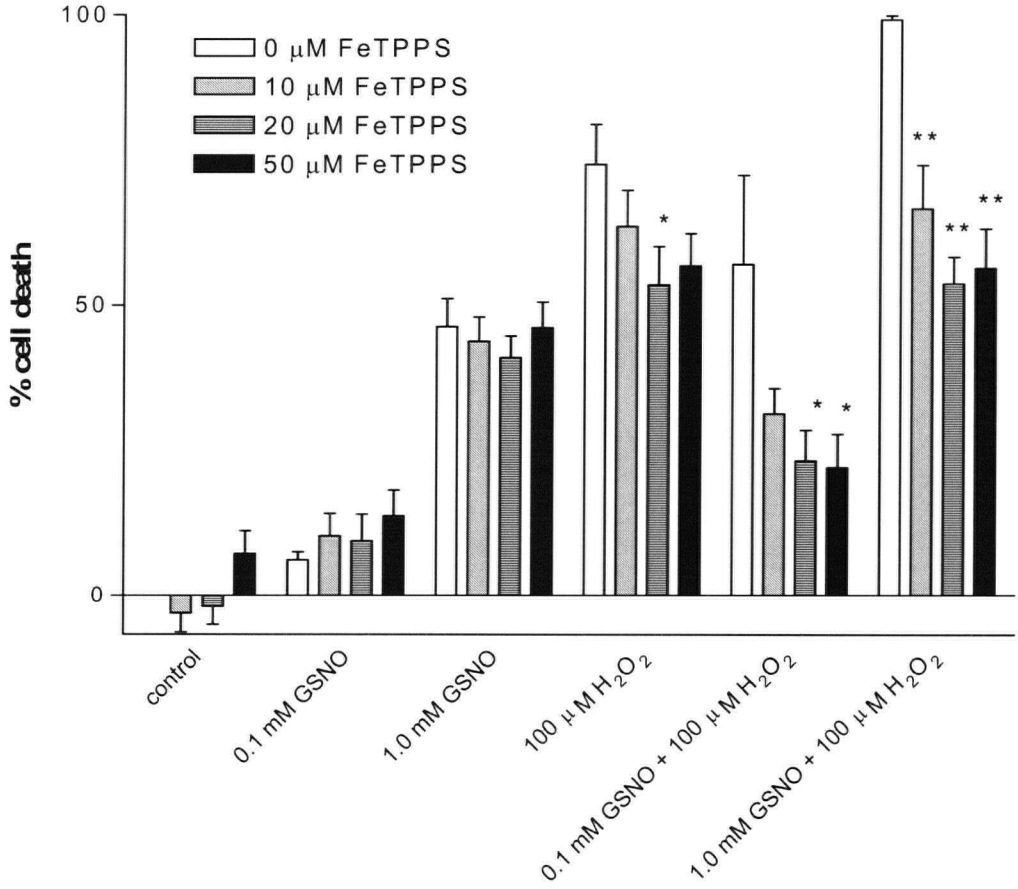

Figure 21: FeTPPS reduces H_2O_2-induced cell death

Cardiomyocytes were maintained in culture for 72 h in 96-well plates. The amount of cell death following H_2O_2 treatment alone and in combination with FeTPPS for 24 h was examined by MTT assay (N=14). MTT dye (10 µl) was added to each well for the final 4 h of the experiment. The experiment was stopped with the addition of 100 µl solubilization solution to each well and left to solubilize for 24 h. Absorbance was then measured at 570 nm. Results are presented as mean percent change of cell death relative to control ± SEM. Statistically significant changes induced by FeTPPS are denoted (*$p<0.05$).

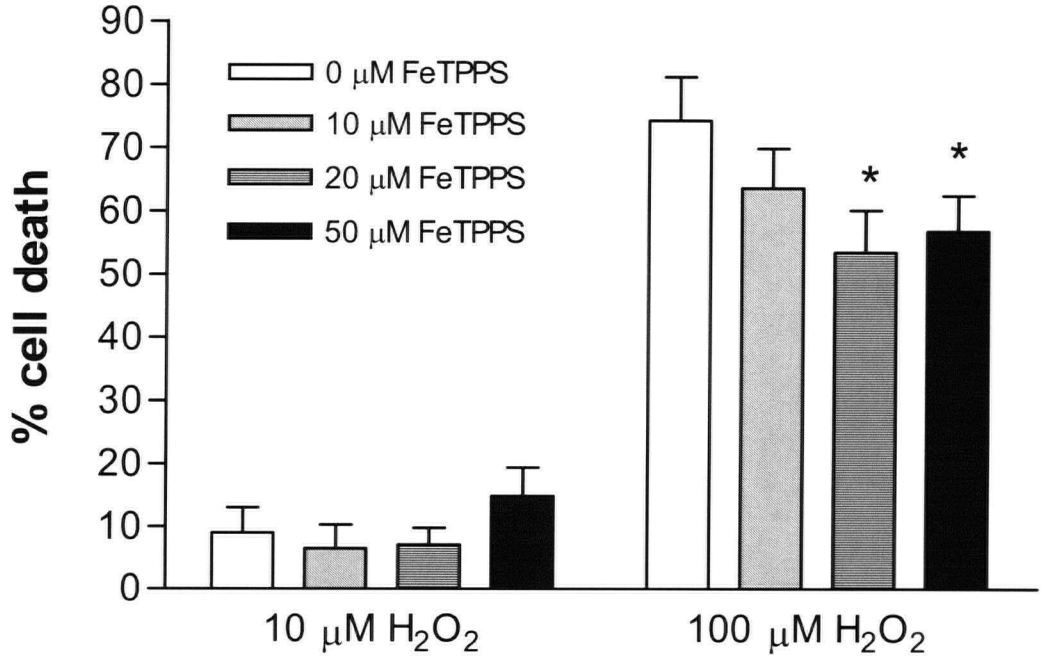

Figure 22: Pifithrin does not affect 3-morpholinosydnonime-induced cell death
Cardiomyocytes were maintained in culture for 72 h in 96-well plates. The amount of cell death following 0.1 mM and 1.0 mM 3-morpholinosydnonime (SIN-1) treatment alone and in combination with pifithrin for 24 h was examined by MTT assay (N=2). MTT dye (10 µl) was added to each well for the final 4 h of the experiment. The experiment was stopped with the addition of 100 µl solubilization solution to each well and left to solubilize for 24 h. Absorbance was then measured at 570 nm. Results are presented as mean percent change of cell death relative to control ± SEM.

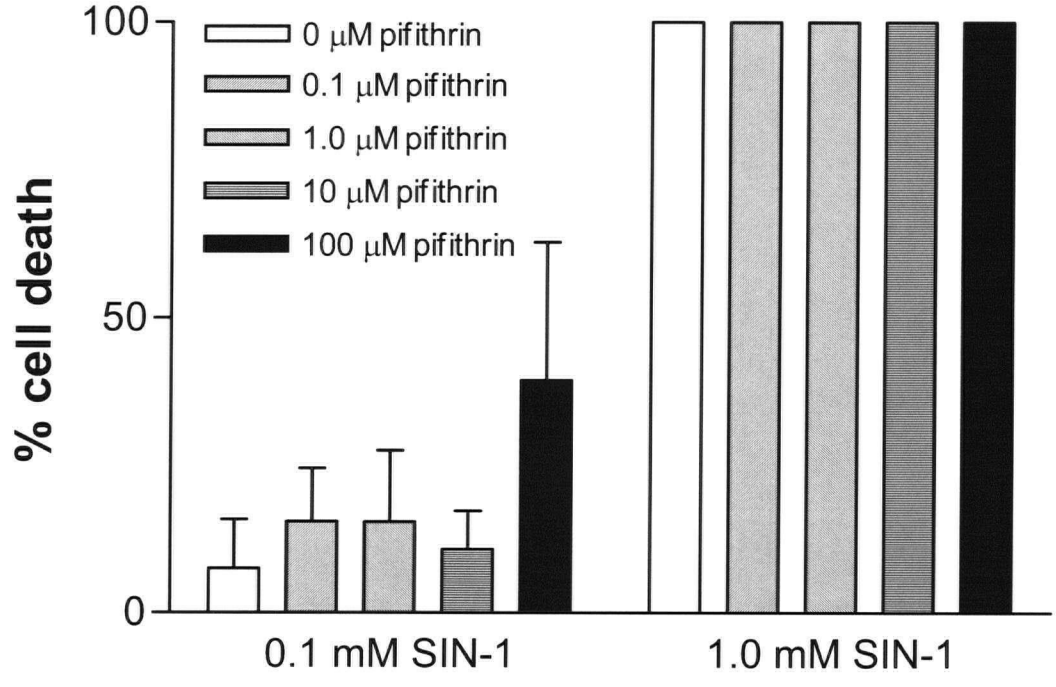

Figure 23: Cyclosporin A does not reduce 3-morpholinosydnonime-induced cell death
Cardiomyocytes were maintained in culture for 72 h in 96-well plates. The amount of cell death following 3-morpholinosydnonime (SIN-1) treatment alone or in combination with 0.1 μM or 1.0 μM cyclosporin A for 24 h was examined by MTT assay (N=12 for SIN-1 alone, N=5 for SIN-1 and both concentrations of cyclosporin A). MTT dye (10 μl) was added to each well for the final 4 h of the experiment. The experiment was stopped with the addition of 100 μl solubilization solution to each well and left to solubilize for 24 h. Absorbance was then measured at 570 nm. Results are presented as mean percent change of cell death relative to control ± SEM.

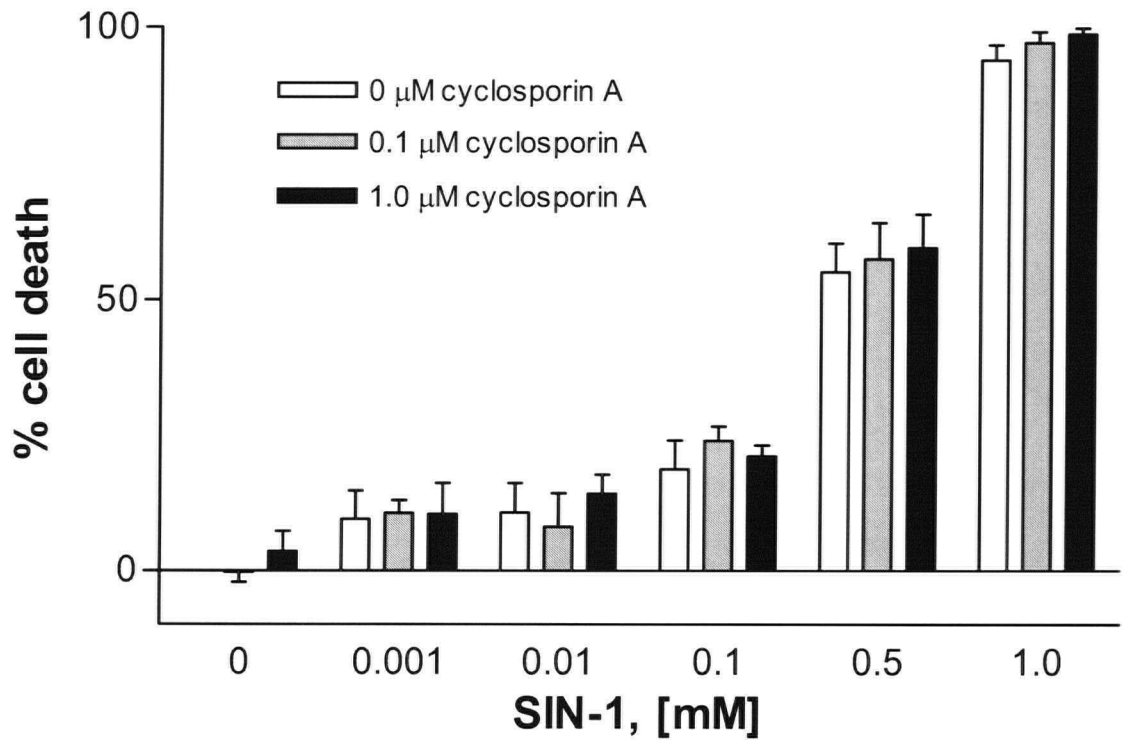

Figure 24: 3-morpholinosydnonime causes a reduction of mitochondrial transmembrane potential

Cardiomyocytes were plated directly on to glass coverslips and maintained in culture for 72 h. Cells were treated with 0.5 mM 3-morpholinosydnonime (SIN-1) with or without 50 μM FeTPPS for 24 h, or 100 μM ceramide for 24 h as a positive control. Coverslips were stained with DePsipher™ to visualize mitochondrial membrane potential. Red/orange aggregates indicate healthy mitochondria; green monomers indicate reduced mitochondrial membrane potential. Representative cells are shown (N=3).

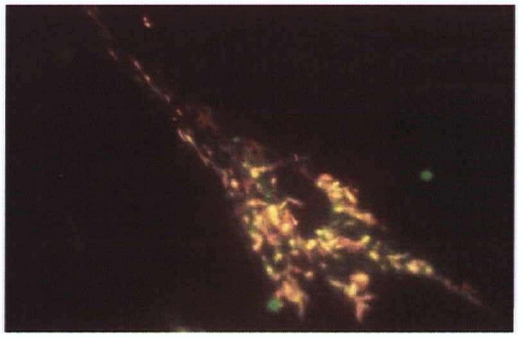

Control

SIN-1

Ceramide

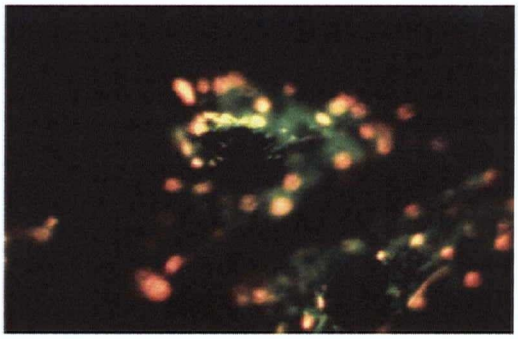

SIN-1 / FeTPPS

Figure 25: FeTPPS reduces 3-morpholinosydnonime-induced protein nitration

Panel A - Cardiomyocytes in culture for 72 h were treated with 0.5 mM 3-morpholinosydnonime (SIN-1) with and without 50 μM FeTPPS for 24 h. Panel B – Cardiomyocytes were treated with the indicated combinations of 0.5 mM SIN-1, 10 μM H_2O_2, and/or 50 μM FeTPPS. Whole cell lysates were collected in RIPA buffer. Equal amounts of protein, assessed by the Bradford assay, were loaded on to 12% SDS-PAGE gels, transferred to nitrocellulose membranes, probed with nitrotyrosine-specific antibodies and HRP-conjugated secondary antibodies, and visualized on photographic film by chemiluminescence exposure.

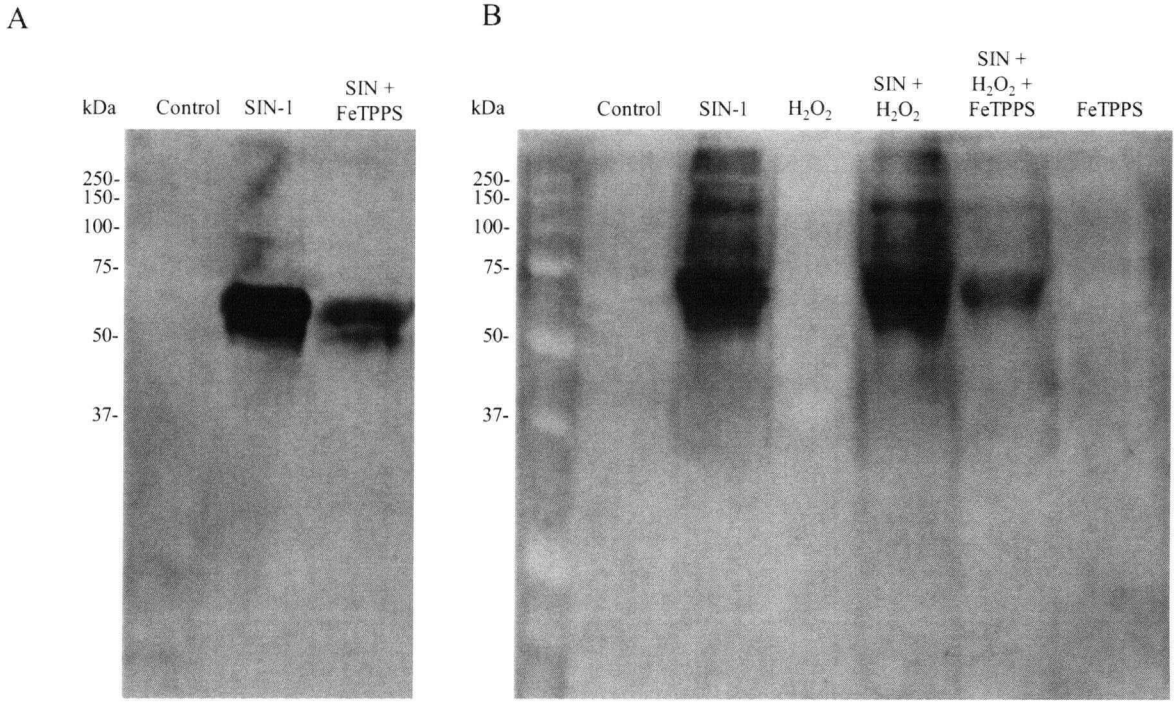

Figure 26: FeTPPS reduces 3-morpholinosydnonime-induced mitochondrial tyrosine nitration
Cardiomyocytes in culture for 72 h were treated with the indicated combinations of 0.5 mM 3-morpholinosydnonime (SIN-1), 10 μM H_2O_2, and/or 50 μM FeTPPS for 24 h (N=2). Cytosolic and mitochondrial fractions were obtained by differential centrifugation. Equal amounts of protein, assessed by the Bradford assay, were loaded on to 12% SDS-PAGE gels, transferred to nitrocellulose membranes, probed with nitrotyrosine-specific antibodies and HRP-conjugated secondary antibodies, and visualized on photographic film by chemiluminescence exposure.

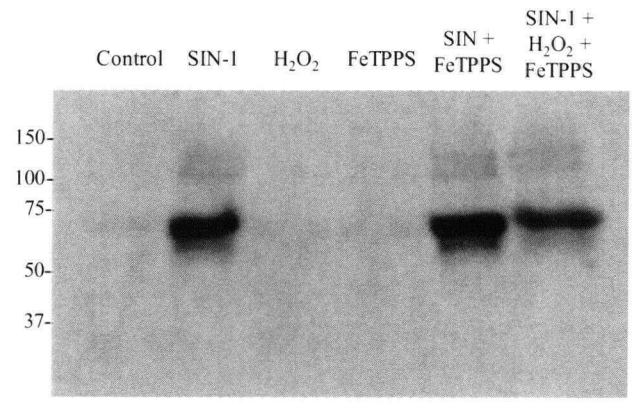

CYTOSOL

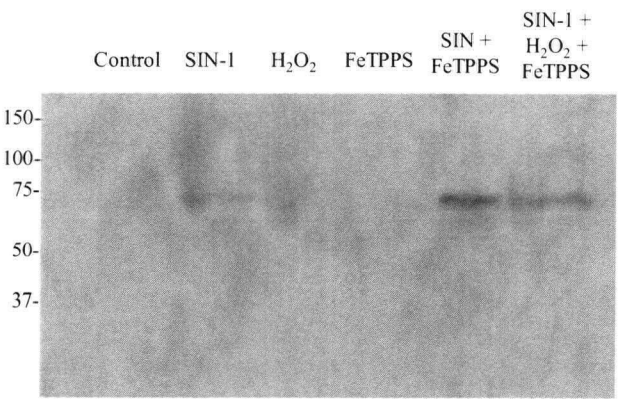

MITOCHONDRIA

Figure 27: FeTPPS reduces 3-morpholinosydnonime- and S-nitrosoglutathione-induced tyrosine nitration

Cardiomyocytes were cultured directly on to glass coverslips and maintained for 72 h. Cells were then treated with the indicated combinations of 0.5 mM 3-morpholinosydnonime (SIN-1), 1.0 mM S-nitrosoglutathione (GSNO), and 50 μM FeTPPS for 24 h. Cells were permeabilized and incubated with nitrotyrosine-specific antibodies and FITC-conjugated secondary antibodies prior to viewing on an epifluorescent microscope. Representative photomicrographs are shown for the indicated treatments.

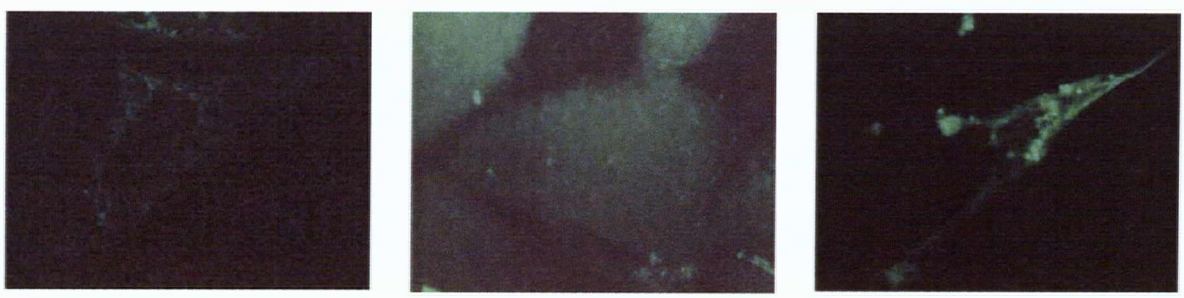

control | 0.5 mM SIN-1 | 1.0 mM GSNO

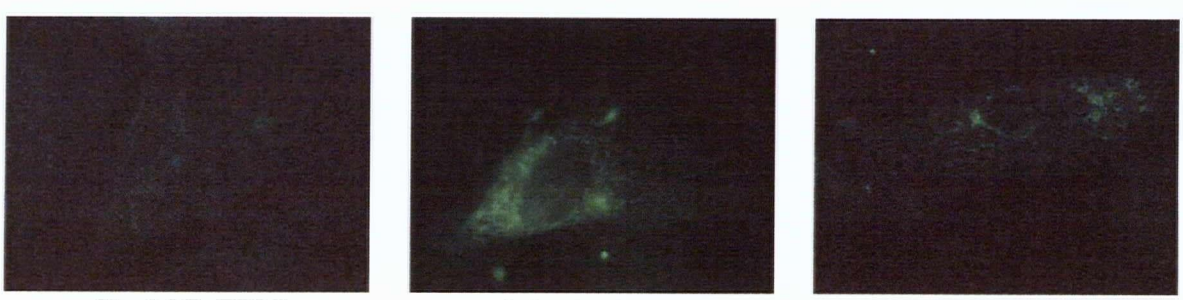

50 μM FeTPPS | 0.5 mM SIN-1 + 50 μM FeTPPS | 1.0 mM GSNO + 50 μM FeTPPS

5.0 DISCUSSION

5.1 GSNO

S-nitrosoglutathione (GSNO) is one of the most commonly used nitric oxide donors. It plays a natural role in intracellular transport and storage of NO [271]. GSNO, $C_{10}H_{16}N_4O_7S$, has a molecular weight of 336.32 g/ml and consists of an NO group covalently bound to a glutathione molecule via a thiol group. At pH 7.4 and 37°C, and in the absence of any metal ion-catalyzed decomposition, GSNO releases NO with a second order rate constant of $3x10^{-4}$ dm^3 mol^{-1} s^{-1} [272]. GSNO is relatively stable in the dark and absence of metal ions, with a half life of 2.8 h in solution [273]. However, metal ions catalyze the cleavage of the N-S bond, with the release of nitrosonium cations and subsequent transfer of an electron from an electron donor yielding NO [272].

The cellular effects of GSNO are mainly attributed to S-transnitrosylation reactions (involving the transfer of the nitrosonium ion NO^+) which occur rapidly, faster than free NO release [274-276]. The importance of transnitrosylation is demonstrated by the observation that the biological effects of GSNO do not correlate with the release of free NO into solution [277]. This was observable in our results, where 1.0 mM GSNO and 0.5 mM SIN-1 caused approximately equivalent amounts of cell death, yet 1.0 mM GSNO resulted in much less nitrite in solution than SIN-1 caused, as measured by the Griess assay, suggesting mechanisms other than free NO-mediated mechanisms, such as transnitrosylations. The s-nitrosothiols serve as a reservoir of NO that can release free NO, which itself can react with a vast set of cellular targets. It has been suggested that this release of NO may depend on thiols and the formation of disulphide linkages to displace the NO from the GSNO [278]. While the precise mechanisms governing the release of NO from nitrosothiols are not fully understood, it has been established that metal ions can efficiently catalyze the conversion [271, 279]. As most culture media contain

transition metal ions, this pathway may represent the formation of the majority of NO in solution [279].

S-transnitrosylation reactions involve the transfer of an NO (nitroso) group from an s-nitrosothiol to a thiol, which can have important consequences to the cell if this involves the modification of a critical residue or leads to altered protein activity [280]. A general mechanism for s-transnitrosylation reactions has been described (Figure 28) [274]. The recipient thiol group undergoes deprotonation to yield a negatively charged thiolate anion. This nucleophilic thiolate anion then reacts with the electrophilic nitrogen atom of the GSNO, which results in heterolytic cleavage of the N-S bond and displaces the parent thiol compound of the NO donor. Following protonation of this thiol, the overall result of the reaction is a transfer of the NO group from one thiol to the other. The rate of reaction between the two species will depend on numerous factors, such as pH, nucleophilicity, stability of the compounds, and local environmental conditions [274, 275, 281]. The functional consequences of the nitrosylation events will depend precisely on the identity of the proteins involved. It has been proposed that with some proteins, this form of modification may represent a regulatory mechanism comparable to phosphorylation [282].

5.2 SIN-1

3-Morpholinosydnonimine (SIN-1), is water-soluble, has a molecular formula of $C_6H_{10}N_4O_2$, and molecular weight of 170.08 g/mol. In solution, SIN-1 decomposes to liberate NO and generate superoxide anion (O_2^-) [283]. A mechanism for this decomposition has been proposed, whereby the sydnonimine ring is cleaved, followed by a single electron transfer to O_2 to form O_2^-, and then a final intramolecular recombination liberates NO (Figure 29) [284].

NO and O_2^- can rapidly react to form peroxynitrite, a far more potent oxidant and nitrosylating agent than NO itself. The reaction between NO and O_2^- is spontaneous and occurs near the diffusion limit, meaning that the reaction between the two components is heavily

favoured and only limited by the rate of diffusion between the two. This reaction has a rate constant of (6.7±0.9) x 10^9 M^{-1} s^{-1} [285]. At pH 7.4, peroxynitrite is protonated and has a half-life of 1.9 sec, decomposing to form a strong oxidant comparable to hydroxyl radical [286].

Protein thiols are significant targets of peroxynitrite, as the formation of s-nitrosothiols at low peroxynitrite concentrations plays a role in cellular signaling mechanisms [287]. However, peroxynitrite will also react with CO_2 or metalloproteins [288]. The mechanism for thiol nitrosylation by peroxynitrite is similar to that proposed for GSNO, whereby the protein thiol attacks the nitrogen of peroxynitrite, causing the elimination of HOO^- and subsequent protonation to form H_2O_2 (Figure 30) [287].

In addition, free NO is derived exclusively through the decomposition of these resultant s-nitrosothiol products [287]. Peroxynitrite can also oxidize protein thiols by a mechanism that involves binding of the thiol to the terminal peroxynitrite oxygen, with the concomitant elimination of nitrite (Figure 31) [9]. Cytotoxic effects of high peroxynitrite concentrations can occur through non-specific thiol oxidation or nitrosylation [9] or the liberation of excessive NO and its subsequent effects [287].

5.3 Griess reaction results

The Griess assay is a method used to quantitate the amount of nitrite present in a sample. It provides an estimate of total NO, although it does not take into account the amount of nitrate present. Therefore, it is useful as a relative comparator between samples [289], but does not provide absolute NO data. Under acidic conditions, NO_2^- forms the strong nitrosating agent NO^+, which reacts with sulphanilamide to form a diazonium ion, which then reacts with N,N'-naphthylethylenediamine to form a red azo product that can be detected spectrophotometrically at 595 nm (Figure 32) [289].

We utilized the Griess assay to demonstrate that these NO donors do indeed release NO, as they caused an accumulation of nitrite in cell-free solution. Treatment with 0.1 mM GSNO for 24 h resulted in 3.3±1.8 μM nitrite, whereas treatment with 1.0 mM resulted in 31.0±9.3 μM nitrite. Given that there is a 10-fold difference of GSNO concentrations between these two treatments, the 10-fold difference of measured nitrite between them is as would be expected. However, as the molar ratio of NO should be 1 molecule NO per molecule of GSNO, one might expect the resultant nitrite levels to more closely approach the concentrations of GSNO, ie. 0.1 mM or 1.0 mM. A possible reason for the discrepancy among our results is the formation of nitrate in addition to nitrite. More generally, however, as GSNO primarily loses its NO through transnitrosylation reactions, and our experiments were conducted in cell-free media but with in the presence of fetal calf serum to mimic culture conditions, it is possible that a significant proportion of NO was present as s-nitrosylated serum proteins.

Similarly to GSNO, the molar ratio of NO should also be 1 molecule NO per molecule SIN-1. Therefore, one might expect to find 0.5 mM SIN-1 to yield 0.5 mM nitrite. We found 0.5 mM SIN-1 for 24 h resulted in 177.0±21.6 μM nitrite in cell-free solution. Comparatively, while the concentration of 1.0 mM GSNO was higher than the concentration of SIN-1, SIN-1 caused a much greater increase in nitrite concentration. Once again, the presence of nitrate may skew these results away from representing the total amount of NO present. The neutral pH 7.4 of our experiments may also factor into the rate of SIN-1 decay, as its decomposition involves base-mediated sydnonimine ring cleavage [284]. Isomerization of the protonated form of peroxynitrite (peroxynitrous acid) results in the dominant accumulation of nitrate at low pH, as under these conditions, this isomerization occurs more rapidly than decomposition into nitrite [290]. However, when the pH is higher than 7.0 and total peroxynitrite concentration is greater than 0.1 mM, conversion to nitrite increasingly becomes the major pathway of peroxynitrite decomposition [290]. Whereas GSNO primarily decays by transnitrosylation, SIN-1 freely

releases superoxide anion and NO with concomitant peroxynitrite decomposition, independently of a binding partner for a transnitrosylation. This may factor into explaining the greater amount of nitrite measured in solution due to SIN-1 compared to GSNO.

Physiologically, basal NO levels, synthesized mainly by NOS3 in the endothelial cells, is on the order of 100 nM [291, 292], approximately 1000-fold less than the concentrations provided by the NO donors in these experiments. However, following myocardial infarction, plasma NO levels have been found much higher, on the order of 100 μM [293]. Therefore, the concentrations used here approximate NO levels in pathologic states.

5.4 GSNO induces cardiac cell death

We found that NO, derived from GSNO, induced a concentration-dependent induction of cardiomyocyte cell death. NO-induced cell death in cardiomyocytes is well recognized [103, 122, 254, 294], although under some circumstances NO can inhibit cell death [96]. The duality of the role played by NO in cell death – in its promotion or inhibition – is well known and has been attributed to the cellular concentration of NO and its interactions within the intracellular environment with other biological molecules, such as superoxide anions [295-301]. Our results have consistently shown that treatment with NO alone, from GSNO, is capable of causing cell death in cardiomyocytes.

5.5 SIN-1 induces cardiac cell death

We also found that SIN-1 induced a concentration-dependent increase in cardiomyocyte cell death. The majority of the cellular effects elicited by SIN-1 are believed to occur by the formation of peroxynitrite from the NO and superoxide anions that it generates [302, 303]. However, NO and superoxide anions may also exert toxic effects independent of each other or of peroxynitrite formation [304, 305]. As NO and superoxide are released in such close proximity

and they spontaneously react very quickly to produce peroxynitrite [284], this suggests that the observed cell death following SIN-1 treatment is likely due to peroxynitrite formation. Peroxynitrite has been recognized as being capable of eliciting toxic cellular effects due to its potency as an oxidant and nitrosylating agent that can react with a multitude of cellular targets [306]. Our results have repeatedly demonstrated that SIN-1 is capable of causing cardiomyocyte cell death, which is likely due to peroxynitrite formation.

5.6 H_2O_2 enhances GSNO-induced cell death

The NO donor sodium nitroprusside produces cell death through a mechanism that involves H_2O_2 formation, and low concentrations of exogenous H_2O_2 can enhance this cell death [254]. Caspase activation induced by DETA/NO, an NO donor that also results in formation of reactive oxygen species, also mediates its effects via H_2O_2 production [255]. These observations suggest that increased H_2O_2 concentrations may enhance NO-induced cell death.

Indeed, our observations demonstrate that H_2O_2 accentuates GSNO-induced cell death. This may occur, in part, by an increased formation of peroxynitrite [307]. Increased peroxynitrite concentration has been associated with toxicity and cell death in numerous studies [308-310]. Under normal circumstances, H_2O_2 decomposes to form water and O_2. However, alteration of the normal functioning of the mitochondrial electron transport system, perhaps through NO-mediated modification, generates excessive superoxide anions from O_2 [311]. Furthermore, a reversible NO-induced modification of cytochrome oxidase O_2 consumption also causes accumulation of reactive oxygen species (ROS) [312]. Together, these lead to increased superoxide anion concentrations, which could react with the NO generated from GSNO to form peroxynitrite and elicit greater cell damage.

While the addition of H_2O_2 caused a significant increase of GSNO- and SIN-1-induced cell death, H_2O_2 treatments alone also induced a significant amount of cell death compared to the

controls. ROS themselves are also highly reactive, and while they function in a controlled manner as signaling molecules at low concentrations, there are numerous ways in which their overproduction can adversely affect the health of the cell [313, 314]. Lipids, proteins, and DNA are all potential targets for ROS-dependent oxidative damage [315]. While the increased ROS concentration may augment the NO-based effects, it cannot be ruled out, at this point, that H_2O_2 and NO elicit harmful cellular effects by independent, additive pathways.

5.7 FeTPPS

FeTPPS (5,10,15,20-tetrakis(4-sulfonatophenyl)porphyrinato iron (III) chloride) is a useful peroxynitrite scavenger. It is water-soluble, with the molecular formula $C_{44}H_{28}ClFeN_4O_{12}S_4$ and molecular weight 1024.3 g/mol. It has been used to catalyze the isomerization of peroxynitrite to nitrate, resulting in a reduction of the damaging effects of peroxynitrite [316].

A general catalytic mechanism for iron (III)-porphyrins-mediated peroxynitrite isomerization has been proposed (Figure 33) [270, 317]. Peroxynitrite covalently binds via its distal oxygen atom to the $Fe(III)^+$ center of the porphyrin ring. The peroxynitrite O-O bond then undergoes spontaneous homolysis, resulting in the production of a free nitrogen dioxide radical and the formation of an Fe(IV)=O bond [270]. The Fe(IV) center is quickly reduced by the newly generated radical, as it either regenerates the original Fe(III)-peroxynitrite intermediate through reformation of the O-O bond, or recombines with the double-bonded O to form a new N-O bond, which readily decomposes to form nitrate, NO_3^- [270].

This ability of FeTPPS to effectively remove peroxynitrite from solution reduces the harmful effects elicited by peroxynitrite. In macrophages, FeTPPS has an EC50 for cytoprotection against peroxynitrite of 5 μM [316]. At a concentration of 300 μM, FeTPPS displayed toxic effects in a fibroblast blood-brain model, but lower concentrations demonstrated

that it reduced peroxynitrite-induced loss of integrity [318]. It also improves the viability of NO-treated cells, perhaps through a reduction of nitrotyrosine formation [303, 316, 318-320]. Importantly, FeTPPS has displayed beneficial effects in heart models, demonstrated by an improvement in cytokine-induced (NO-mediated) myocardial dysfunction [319], reduction of endotoxin-induced inhibition of myocardial contractile function [321], and a normalization of peroxynitrite-mediated increased left ventricular end diastolic pressure in hyperlipidemic rats [322].

5.8 FeTPPS reduces SIN-1-induced and GSNO plus H_2O_2-induced cell death

We used FeTPPS to reduce the amount of peroxynitrite in solution following treatments, and examined the effects on the cardiomyocytes in culture. We found that FeTPPS significantly reduced the amount of cell death induced by SIN-1. However, there was not a total elimination of cell death. Higher concentrations of FeTPPS alone reduced cell viability, so it would be difficult to differentiate between these toxic effects elicited by FeTPPS itself, and any further reduction in peroxynitrite-mediated death associated with increased availability of FeTPPS. However, the results from lower concentrations of FeTPPS substantiate the hypothesis that a reduction of peroxynitrite, by its conversion to nitrate, is sufficient to reduce the amount of cell death. Additionally, it may be suggested that there exists the possibility that SIN-1-induced toxicity is not mediated by peroxynitrite alone.

Possible reactions of the NO and superoxide anions released from SIN-1 with various cellular targets, independently of each other, may account for some toxic effects [284]. Interestingly, it has been proposed that when SIN-1 is administered in the presence of electron acceptors, the superoxide anions react with those, rather than NO, to produce O_2, thus resulting in an accumulation of NO rather than the formation of peroxynitrite [284]. In this case, the

FeTPPS would have a minimal effect on the cell, being specifically reactive with peroxynitrite and not NO.

The proposal that NO and superoxide exerting independent effects is supported by our results combining SIN-1 with H_2O_2 and FeTPPS. The increased oxidative environment formed by the H_2O_2 would presumably contain a higher superoxide anion concentration, which would encourage a greater formation of peroxynitrite from NO. An increased peroxynitrite concentration could explain the greater reduction of cell death following FeTPPS in combination with SIN-1 and H_2O_2, compared to its combination with SIN-1 alone. As FeTPPS is unable to completely reduce SIN-1-induced cell death, this suggests that in our model system, SIN-1 may produce a significant amount of NO in addition to peroxynitrite. This may possibly be mediated by components of the medium, possibly the fetal calf serum, providing a source of electron acceptors to facilitate the accumulation of NO rather than peroxynitrite [284].

The effect of FeTPPS on cell death induced by GSNO was also examined. While FeTPPS had no effect on GSNO-induced cell death, it did show a reduction upon the inclusion of H_2O_2 with GSNO. Again, this is likely explained by the interplay between ROS and NO. As GSNO is strictly an NO donor, increasing the oxidative environment with H_2O_2 could lead to the formation of peroxynitrite from the NO, which would then be isomerized by FeTPPS to reduce its toxic effects.

5.9 FeTPPS reduces H_2O_2-induced cell death

Our results also provide evidence to show that FeTPPS can significantly reduce H_2O_2-induced cell death, in the absence of any exogenously provided NO. Nitric oxide synthase enzymes produce basal levels of NO endogenously as a part of normal cellular function and signaling pathways [323, 324]. I speculate that this basal amount of NO produced naturally by the cell would react to form peroxynitrite, owing to the presence of H_2O_2-induced ROS. As

such, a part of the observed H_2O_2-induced cell death may be due to effects caused by peroxynitrite. Our observation that FeTPPS is capable of reducing H_2O_2-induced cell death supports this proposal.

5.10 GSNO produces an increase in p53 expression in the cell

Our study demonstrates that cellular p53 protein levels increase in response to NO, an effect that is associated with an increase in cell death. The role of p53 in response to cellular damage is either to induce repair and ensure cell viability or to commit the cell to death [227, 325]. When required, the normally low basal level dramatically accumulates due to the inhibition of its cytosolic degradation [326, 327]. We consistently demonstrated an overall increased expression of p53 in whole cell lysates in cardiomyocytes which is consistent with other studies performed in heart models [294, 328], as well as in a variety of different cell types [234, 241, 249, 329-333]. More specifically, NO caused a significant increase at lower concentrations, whereas higher concentrations showed a slight increase which was not statistically significant. Interestingly, these increased amounts of p53 are associated with minimal amounts of cell death, in contrast to the higher concentrations with less of an expression increase but a corresponding dramatic increase in death. This observation argues for a role for p53 in reducing the harmful effects of NO on cell viability. Similarly, it may be interpreted that the toxic effects of higher NO concentrations occur by mechanisms that are not governable by p53, and so no significant increase in p53 expression is found under those conditions.

5.11 GSNO produces an accumulation of p53 in the nucleus

We examined the subcellular compartmentalization of the p53 response and found that NO induced a significant accumulation of p53 in the nucleus. The notion of p53 in the nucleus developed from the initial observation that p53 possessed DNA-binding capability [177]. This

concept evolved into one of the now-understood functions of p53 as that of a transcription factor, to induce the expression of several specific p53-dependent genes within the nucleus. Among the multitude of genes under its regulation are the pro-apoptotic factors Bax [180], PUMA [183], Bid [184], and Apaf-1 [187], any one of which could contribute to NO-induced loss of cell viability. Nuclear import of p53 is mediated by the binding of its nuclear localization signal to the importin complex at the nuclear pore [334]. In addition to this influx, the accumulation of p53 in the nucleus following NO treatment is likely due to a combination of both a promotion of nuclear retention via NO-induced p53 phosphorylation and inhibition of Mdm2-mediated p53 nuclear export [245, 335]. The positive regulators of p53, ATM kinase and p19ARF, do not regulate the NO-mediated p53 increase [239]. While nuclear translocation and accumulation of p53 have previously been observed in response to various stimuli [336, 337], to our knowledge, this is not a well-described component of the response of cardiomyocytes to NO.

5.12 NO-induced cell death was not altered by pifithrin

Pifithrin is a reversible inhibitor of p53's transcriptional activity, and therefore, p53-dependent apoptosis [264]. While pifithrin may have an effect at other cellular sites, it is a potent inhibitor of p53-mediated transcriptional control [338]. The concentration of pifithrin was selected for its ability to reduce cell death in cardiomyocytes, as lower concentrations were less effective and higher ones demonstrated cytotoxicity [265]. Similar concentration effects were found in neural [266] and hepatic cells [267].

This is the first study to examine p53 inhibition with pifithrin in cardiomyocytes subjected to NO. We verified the efficacy of pifithrin in this model where it diminished adriamycin-induced cellular apoptotic morphology and DNA fragmentation, as adriamycin induces apoptosis in a p53-dependent mechanism [265]. However, we repeatedly found that pifithrin caused no change in the amount of cell death induced by NO, nor did it alter NO-

induced DNA damage. Numerous studies using various stimuli describe a reduction in cell death following p53 inhibition with pifithrin [266, 339, 340]. This variation in response to pifithrin may be caused by a limited specificity of its binding target.

While the nuclear accumulation mechanisms of p53 remain intact in response to GSNO, our data demonstrates that pifithrin does not reduce the amount of NO-induced cell death, caused by either GSNO or SIN-1, and so this mechanism appears independent of p53's activity. Conversely, the opposite has also been found to be true, where pifithrin reduced both p53-dependent apoptosis and the amount of p53 in the nucleus [339]. However, this study was performed in rat hepatocytes utilizing LPS to induce apoptosis, so both of these factors may account for the differences in the findings. In our study, we consistently found that pifithrin did not reduce GSNO-induced or SIN-1-induced cell death, as measured by MTT assay, nor did it reduce the amount of DNA fragmentation caused by NO treatment. These results suggest that gene transactivation by p53 is not involved in the maintenance of cell viability, despite its increased nuclear presence in response to NO.

By comparison, Y-box-binding protein YB1 physically interacts with p53 within the nucleus to inhibit transactivation of pro-death genes and cell death through a selective regulation of p53-dependent genes [331]. Our results may be interpreted to indicate that the cellular response to NO-induced cell damage is to recruit p53 to the nucleus, while YB1, or NO itself, may modify p53's ability to sufficiently handle and reduce the cell's stress appropriately, in a manner that is comparable to the actions of pifithrin.

5.13 GSNO induces DNA fragmentation

Utilizing the comet assay, we observed increased DNA fragmentation in response to NO. The comet assay has been repeatedly validated as an indicator of DNA damage as it reliably demonstrates DNA fragmentation [341, 342]. Our finding of NO-induced DNA fragmentation

can be supported by other data [234]. DNA strand breaks occur in a concentration-dependent manner in response to the NO donor SNP, in single cell suspensions from organs isolated from mice [343]. Our results suggest that NO-induced cell death was associated with an increase in p53 expression in whole cell lysates and in particular, an accumulation of p53 in the nucleus. Increased p53 expression inhibits DNA synthesis and the cell cycle following DNA damage induced by gamma radiation or actinomycin D [138].

Through the use of the comet assay, we observed an increase of DNA damage in response to increasing concentrations of NO. Our results are consistent with other studies using a variety of cell types that showed NO causes DNA damage [344-347] and inhibits repair [348]. Specifically, this result was observed in cardiomyocytes [103, 294, 349]. NO induces DNA damage by various mechanisms, such as by modification of the sugar backbone or of the DNA bases [34], resulting in strand breaks or increased susceptibility to cleavage by endonucleases [350]. As well, the interaction of NO with superoxide ions forms peroxynitrite, which is a more potent inducer of DNA strand breaks than NO itself [34]. Damaged DNA has been shown to increase p53 expression, with an increased regulation of DNA repair among its numerous roles [138, 234, 235, 328, 351].

5.14 GSNO-induced DNA damage is not altered by pifithrin

Here we are introducing the novel finding that inhibition of p53 through the use of pifithrin is not sufficient to significantly reduce the amount of cell death observed in cardiomyocytes following NO treatment, nor does it change the amount of damaged DNA induced by NO. If p53 were involved in modulating DNA repair following NO exposure, then the inhibition by pifithrin would prevent any p53-dependent "repair gene" transcription. Therefore, by blocking the transcription of repair genes, there would be a deficiency of repair machinery that could act to reduce the damage, and so DNA damage may accumulate and be

greater than if NO were administered in the absence of pifithrin. However, the inclusion of pifithrin in the treatments did not reduce death or increase DNA damage. This suggests that the repair of the observed DNA damage by NO occurs independently of p53-dependent transcription. Alternately, p53 may still be involved in regulating DNA repair through transcription-independent mechanisms, such as directly binding to damage sites to recruit repair proteins or to initiate repair itself [140]. These mechanisms could potentially function even in the presence of pifithrin, and therefore pifithrin would not affect the amount of DNA damage present or its rate of repair.

5.15 GSNO does not induce cell death through the mitochondrial death pathway

Mitochondrial fractionation studies were performed using differential centrifugation techniques. These methods have been shown to yield highly enriched mitochondrial fractions with minimal contamination with other organelles, as assessed by electron microscopy or enzyme activity assays [352, 353]. We have also demonstrated that the mitochondrial fractions contained abundant cytochrome c, which was lacking in the cytosolic components, and no detectable amount of the cytosolic marker PI-3 kinase [268].

We show that in cardiomyocytes, NO-induced cell death is unlikely to be mediated through a mitochondrial pathway. We consistently found only a minimal level of p53 associated with mitochondria, with no significant increase within mitochondrial fractions following NO treatment. Data in other cell types indicates that p53 translocates to the mitochondria during p53-dependent apoptosis [203, 204, 354-356]. Furthermore, it was determined that the specific targeting of p53 to the mitochondria, thus by-passing its nuclear import and gene transactivation activity, is sufficient to induce apoptosis [203]. Mitochondrial translocation is dependent specifically on the amino acid present at the codon 72 locus. Mutant p53 containing a proline at this position shows diminished ability to relocate, in addition to hindered apoptotic ability [207].

By comparison, arginine substitution at this location enables free and spontaneous translocation and promotes apoptosis [207]. These results implicate a p53 mitochondrial translocation as being a significant transcription-independent component of the cell death circuitry, separate from the transcriptional control mechanisms associated with p53's nuclear translocation. However, this mitochondrial translocation ability has not been examined in NO-treated cardiomyocytes, and as such, our findings suggest that translocation of p53 to mitochondria is not active in the heart in response to NO.

Furthermore, NO did not induce cytochrome c release from the mitochondria, a key step in the apoptosis process. Release of cytochrome c, from the inner mitochondrial membrane into the cytosol, is a central step in the apoptotic response. Once in the cytosol, it aids in the activation of caspase-9, thus initiating the caspase cascade leading towards the death of the cell [357]. NO has previously been recognized to induce such translocation [78, 358-361]. Of particular significance, in macrophages, NO-induced cytochrome c relocation depends upon p53 accumulation [249]. In contrast to this observation, we show here that the cardiomyocyte response does not appear to include a cytochrome c release accompanying p53 accumulation as a major role in responding to NO. However, our results suggest that there may be a minor release of cytochrome c from the mitochondria following NO treatment. Conversely, a number of studies suggest that cytochrome c release is inhibited following NO treatment [66, 111, 298, 362, 363]. These varying observations suggest that the cytochrome c release is not a general response to NO and it depends on the cell type and environmental conditions.

Contrary to studies in various model systems that demonstrated that NO-induced cell death may include an associated mitochondrial depolarization [364-367], we found that NO did not cause a reduction of the $\Delta\Psi_m$. Additionally, inhibition of the mitochondrial PTP with cyclosporin A conferred no significant protection from the effects of NO. Loss of $\Delta\Psi_m$ is thought to occur by the opening of the mitochondrial PTP, a large conductance channel that

facilitates leakage of pro-apoptotic factors and dissipation of the electrochemical gradient [368], though the point of modification by NO on this process is uncertain. In previous studies conducted in cardiomyocytes, NO did not induce a mitochondrial depolarization either, but, interestingly, prevented it from occurring altogether when administered ahead of ischemia/reperfusion, or H_2O_2 [369-371]. However, the protective effect of NO observed in these studies was reflected in the increased viability of the cells studied. By contrast, our data clearly demonstrates a negative effect of NO on cardiomyocyte viability through a mechanism independent of changes in $\Delta\Psi_m$. The role of a "mitochondrial apoptosis-induced channel," separate from the permeability transition pore, has also been proposed as a means of cytochrome c release from mitochondria without a loss of membrane integrity or depolarization [372], which may help to explain the minor leakage of cytochrome c separate from a loss of mitochondrial potential in our study.

In perfused heart studies, NO induced cytochrome c release and mitochondrial PTP opening as rapidly as 10 minutes following treatment [360]. However, their study administered the NO by perfusing the heart, whereas our experiment involved treating cell cultures in medium. This difference in NO delivery and model system may account for the differing results. Other experiments also suggest that NO induces caspase-mediated apoptosis dependent on mitochondrial PTP opening and cytochrome c release [361]. Importantly, however, is that these conclusions were drawn based on studies with isolated mitochondria, a model system that is without any of the additional interactions that occur within the cellular context of our study. Differing observations between these and our study is most likely a result of the diversity of models used in the investigations.

Taken together, our findings that NO does not translocate to mitochondria, does not alter mitochondrial transmembrane potential, does not induce a large loss of cytochrome c into the

cytosol, coupled with the inability of cyclosporin A to alter NO-induced cell death strongly suggest that NO reduces cell viability through a mechanism independent of the mitochondria.

5.16 SIN-1 causes a reduction of mitochondrial transmembrane potential

While GSNO was found to have no significant effect on $\Delta\Psi_m$, SIN-1-induced cell death was associated with a reduced potential, as shown by DePsipher staining. This difference is likely due to the nature of the donors, as SIN-1 produces peroxynitrite, whereas GSNO releases NO or participates in transnitrosylation reactions. High NO concentrations, resulting in the formation of peroxynitrite, have been found to lead to irreversible damage to complex V (ATP synthase) of the electron transport system and promote apoptosis [373]. Similarly, exogenously provided peroxynitrite resulted in inhibition of complexes I, II, and V, minor inhibition of complex IV, and no significant inhibition of complex III [130]. By contrast, NO caused reversible inhibition of the respiratory chain at complexes III and IV, leading to depletion of cellular ATP stores and apoptosis [67, 374]. Depletion of cellular ATP reduces the ability of the mitochondria to maintain a $\Delta\Psi_m$ [280]. As NO affects ATP production in a reversible manner, the concentrations of GSNO we used may not have been sufficient to induce a noticeable reduction of $\Delta\Psi_m$, whereas the irreversible effects of peroxynitrite, from SIN-1, did.

While we did not specifically measure mitochondrial proteins involved in apoptosis, I speculate that their involvement may be possible in SIN-1-induced cell death. In conjunction with the increase in p53 expression, Bax expression is increased by a p53-dependent mechanism [89], while its and p53's breakdown by the 26S proteasome is inhibited [375]. A role for Bax in our results is suggested by recent studies that have elucidated compounds that block mitochondrial channels formed by Bax insertion and oligomerization, and whose use in ischemia-induced apoptosis models has revealed a prevention of cytochrome c release, maintenance of $\Delta\Psi_m$, and reduction in apoptosis [376]. Therefore, our results may be interpreted

as NO is causing p53 accumulation, and peroxynitrite may lead to increased Bax production and insertion into the mitochondrial membrane, thus causing a loss of $\Delta\Psi_m$ and death of the cell.

5.17 NO increases cellular protein tyrosine nitration

NO modifies tyrosine residues of proteins by nitration, the covalent addition of an $-NO_2$ group to one of the *ortho* carbons of the aromatic ring [377]. Western blotting for nitrotyrosine residues demonstrated that there was an increased amount of nitrotyrosine following SIN-1 or GSNO treatment. Increasing amounts of data suggest that protein nitration may be an additional form of cell signaling, comparable to mechanisms such as phosphorylation, especially if the modified residue is critical to the function of the protein [378]. The finding of an enzyme "denitrase" activity, to reverse the nitration signal, further supports this theory [379]. Whereas specificity for phosphorylation is usually conferred by a specific peptide sequence, there does not appear to be a consensus sequence for nitration, but rather it may depend on the local environment of the particular tyrosine residue, and its overall position on the protein (ie. on the surface or buried) [377]. Evidence suggests that the tyrosine is initially oxidized through free radical reactions to form a tyrosine phenoxyl radical, followed by its reaction with a nitrogen dioxide radical formed from the breakdown of peroxynitrite [48], as peroxynitrite itself does not favourably react with tyrosine directly [380]. Alternate mechanisms suggest that the initial tyrosine radical can readily bind to NO to form a nitroso intermediate which can subsequently be oxidized to form nitrotyrosine [381], or that nitronium ions (NO_2^+) react with the tyrosine ring to directly form nitrotyrosine [10].

Our results suggest that some key proteins involved in cell viability, both in the cytosol and mitochondria, are modified by tyrosine nitration, leading to cell death. Furthermore, there also appears to be a significant accumulation of nitrotyrosine staining in the cell membrane following SIN-1 administration. As a proposal for future investigation, a literature search for

proteins with a molecular weight of approximately 75-200 (as implied by Figure 25) that may possibly play a role in cell death, and which may be subject to modification by NO, briefly includes proteins such as APAF-1 (apoptotic protease activating factor-1), CARP-1 (cell cycle and apoptosis regulator protein 1), DAPK-1 (death-associated protein kinase 1), MEKK-5 (mitogen-activated protein kinase kinase kinase 5), p160 ROCK-1 (Rho-associated protein kinase 1), α-actinin-1, -2, and -3, and SERCA-1, -2, -3 (sarcoplasmic-endoplasmic reticulum calcium ATPase-1, -2, -3).

While our results show general tyrosine nitration, several proteins have previously been identified as being targets for modification by NO [378]. Additionally, peroxynitrite causes tyrosine nitration of proteins associated with membranes [382]. Some proteins have already been specifically identified as tyrosine nitration targets. Signaling pathways can be altered, as ERK1/2 becomes activated following nitration [383], whereas NF-κB becomes inactivated following nitration [384]. Co-factor-dependent PKC activity also is inhibited by peroxynitrite-induced protein tyrosine nitration [385]. Complex I of the electron transport system displays a high degree of tyrosine nitration [130], whose inhibition may contribute to the observed loss of $\Delta\Psi_m$. Cytochrome c is also a target for nitration, following which it catalyzes the nitration of nearby proteins [386]. Importantly, tyrosine nitration by peroxynitrite has also been observed on p53, leading to a decrease in DNA-binding ability and perhaps playing a role in carcinogenesis [247, 248]. This supports our previous suggestion that p53 in the nucleus may be unable to modify transcription, due to a modification by NO. Undoubtedly, the list of known proteins that undergo tyrosine nitration, and its effect on function, will continue to increase.

5.18 Limitations of the study

Several limitations of this study should be kept in mind. For this study, we utilized embryonic chick cardiomyocytes in culture. While an examination of this study in a more

clinically comparable model system would be favourable in order to confidently extrapolate the results, the avian model possesses a high degree of homology with other vertebrates [387] and is therefore a suitable system for exploring the mechanisms of cell death, with potential application to other species. Secondly, mitochondrial $\Delta\Psi_m$ was visualized by DePsipher staining, and the effects of NO qualitatively described. However, we have demonstrated that the DePsipher staining of intact cells correlates well with detailed FACS analysis of DePsipher evaluation of $\Delta\Psi$m [263]. Thirdly, we used only the MTT assay to evaluate cell death. NO-induced cell death can occur through multiple mechanisms of cell death [255]. It is not immediately obvious whether the cell death we observed was apoptotic or necrotic, or a combination of both. Cytochrome c, a useful marker of apoptosis, was found in the cytosol in only minor amounts. However, assessment of cell death by MTT permits an assessment of total cell death so that cell death from apoptosis and necrosis are combined. Further examination of cell death pathways (eg. caspase activation, ATP synthesis) would be valuable in ascertaining if NO indeed kills by apoptosis or necrosis. Fourthly, we used the agent FeTPPS and did not measure cellular peroxynitrite concentrations. However, the ability of FeTPPS to catalyze the isomerization of peroxynitrite to nitrate is well documented [316] and its ability to reduce the damaging effects of peroxynitrite well recognized [303, 316, 318-320]. FeTPPS did not completely prevent cell death induced by SIN-1, in part due to the inherent cellular toxicity of this agent. Fifthly, another concern is that the mode of action of pifithrin on p53 remains poorly characterized. In addition to inhibiting p53-dependent gene transcription, it is also a potent aryl hydrocarbon receptor (AhR) agonist [338]. However, p53-mediated transcriptional control occurs by an AhR-independent mechanism [338], and therefore these observations do not represent the same pathway. Pifithrin has also been shown to suppress heat shock and glucocorticoid receptor signaling [388]. These results demonstrate that pifithrin has additional, potentially unidentified

cellular targets that are independent of p53 and could possibly play a role in the regulation of NO-induced cell death.

5.19 Summary

In summary, this research has contributed valuable insight into the mechanisms behind NO-induced cell death in cardiomyocytes. The effect of NO is dependent on the type of NO donor used. GSNO-derived NO was found to induce cell death in cardiomyocytes by mechanisms that appear to be independent of the mitochondria (eg. no p53/mitochondria association, no change in $\Delta\Psi_m$, cyclosporin A-insensitive, and minor cytochrome c release). In response to NO, p53 was found to increase in a concentration-dependent manner; such that lower NO was associated with higher p53 levels, and vice-versa. However, DNA damage increased with NO concentration. Inhibition of p53's gene transactivation activity by the inhibitor pifithrin was not able to reduce NO-induced cell death, nor did it play a role in modulating the extent of NO-induced DNA damage. However, in response to NO, p53 still accumulated in or translocated into the nucleus. Therefore, it seems as though p53 plays a role within the nucleus in the NO-induced death response that is independent of initiating transcription of important genes or significantly reducing DNA damage.

Peroxynitrite also induced cardiomyocyte cell death when provided by SIN-1, or by its generation from the combination of GSNO and H_2O_2, demonstrated by the reduction in cell death afforded by the peroxynitrite isomerase FeTPPS. SIN-1-induced cell death was not affected by pifithrin either, suggesting that it also occurs by mechanisms independent of p53 transactivation. H_2O_2 caused an increase in GSNO-induced cell death possibly as an additive effect, or due to a higher toxicity of peroxynitrite. However, GSNO alone caused cell death independent of peroxynitrite formation. In contrast to GSNO, SIN-1 was capable of inducing a loss of $\Delta\Psi_m$, suggesting that NO and peroxynitrite induce cell death through different

mechanisms. Immunocytochemistry also suggests that GSNO and SIN-1 cause differing effects, where both donors caused significant protein nitration, but with different cellular distributions. It is likely that these protein nitration reactions modify the target proteins' functions, and in so doing, modulate key mechanisms governing cell survival, leading to NO-induced cell death.

The following proposal speculates on a unifying explanation for my results. Normal NO metabolism results in the formation of basal peroxynitrite. At these low concentrations, peroxynitrite does not induce toxic cellular effects. At higher concentrations, it causes cell death. Peroxynitrite may do this by the nitration of key regulatory proteins, especially mitochondrial proteins, resulting in a loss of mitochondrial integrity, $\Delta\Psi_m$, and cell death. Similarly, under conditions that do not favour peroxynitrite formation, higher concentrations of NO cause the nitration of a different subset of proteins, which again influence the health of the cell. Low concentrations of NO cause a rapid increase in p53 protein, perhaps in an effort to protect the cell from NO-induced damage. Comparatively, higher concentrations of NO do not induce as large an increase of p53 expression, possibly indicating that high NO may overwhelm the protective abilities of p53. NO-induced cell death does not occur through an association of p53 with mitochondria, nor does it induce mitochondrial apoptotic mechanisms, such as release of cytochrome c or loss of $\Delta\Psi_m$. By contrast, NO causes the accumulation of p53 within the nucleus where further regulation of nuclear functions may inhibit p53's DNA binding, yet p53 may still directly participate in low level DNA repair independently of its gene transactivation capacity. The recruitment of p53 into the nucleus may be in response to NO-induced DNA damage, which occurs through several previously noted mechanisms, as a result of NO's naturally reactive chemistry. However, despite this recruitment, it appears that it is insufficient to combat the NO-induced DNA damage. Alternately, p53 may play a role separate from DNA damage regulation. In addition to effects caused by NO itself, enhanced production of peroxynitrite, that occurs when ROS derived from excess hydrogen peroxide reacts with NO

provided by an NO donor such as GSNO or even SIN-1, enhances cell death. Therefore, the modification of key proteins by nitration, as a result of heightened NO or peroxynitrite concentrations may result in the alteration of normal cellular processes that leads to NO-induced cell death.

Figures

Figure 28: S-transnitrosylation mechanism
The thiol group of the nitro-group recipient (R_1-S-H) undergoes deprotonation to yield a negatively charged thiolate anion. This nucleophilic thiolate anion then attacks the electrophilic nitrogen atom of the NO donor (R_2-S-N=O), which results in heterolytic cleavage of the N-S bond and displaces the parent thiol compound of the NO donor. Following protonation of this thiol, the overall result of the reaction is a transfer of the NO group from one thiol to the other. Figure adapted from [274].

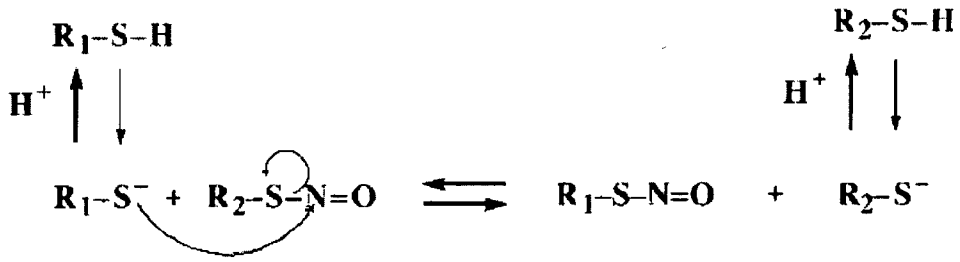

Figure 29: 3-morpholinosydnonime decomposition mechanism
In solution, the sydnonimine ring of 3-morpholinosydnonime (SIN-1) is cleaved, followed by a single electron transfer to O_2 to form O_2^-. The resulting reaction intermediate (SIN-1**) undergoes a final intramolecular recombination, which liberates NO. Figure adapted from [284].

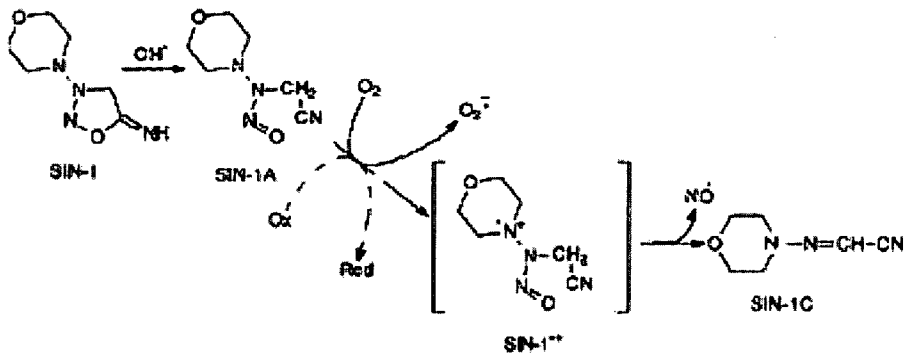

Figure 30: S-transnitrosylation by peroxynitrite

The thiol group of the nitrosylation target (R-S-H) undergoes deprotonation to yield a negatively charged thiolate anion. This nucleophilic thiolate anion then attacks the electrophilic nitrogen atom of protonated peroxynitrite (O=N-O-O-H), which results in heterolytic cleavage of the N-O bond and transfer of the NO group to the thiol. Hydrogen peroxide is also formed following protonation. Figure adapted from [287].

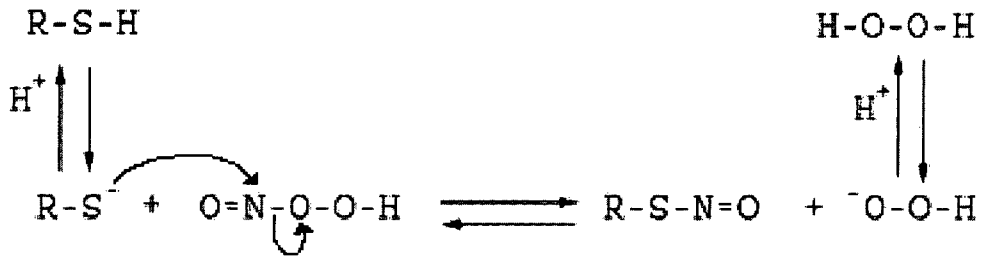

Figure 31: Thiol oxidation by peroxynitrite

The thiol group undergoes deprotonation to yield a negatively charged thiolate anion. The thiolate anion then attacks the terminal oxygen atom of peroxynitrite, with the concomitant elimination of nitrite and formation of a hydroxylated thiol. Figure adapted from [9].

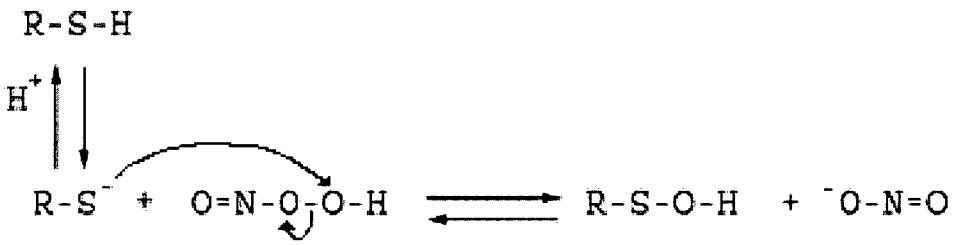

Figure 32: The Griess reaction

The Griess reaction measures nitrite, NO_2^- concentration. Under acidic conditions, NO_2^- forms the strong nitrosating agent, nitrosonium cation NO^+, which reacts with sulphanilamide to form a diazonium ion, which reacts with N,N'-naphthylethylenediamine to form a red azo product that can be detected spectrophotometrically at 595 nm. Figure adapted from [389].

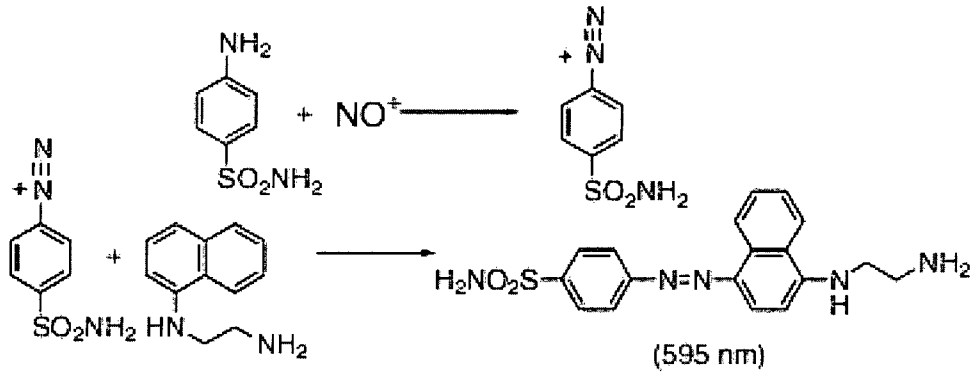

Figure 33: FeTPPS-mediated peroxynitrite isomerization

Peroxynitrite covalently binds via its distal oxygen atom to the Fe $(III)^{+}$ center of the porphyrin ring of FeTPPS. The peroxynitrite O-O bond then undergoes spontaneous homolysis, resulting in the production of a free nitrogen dioxide radical and the formation of an Fe(IV)=O bond. The Fe(IV) center is quickly reduced by the newly generated radical, as it either regenerates the original Fe(III)-peroxynitrite intermediate through reformation of the O-O bond, or recombines with the double-bonded O to form a new N-O bond, which readily decomposes to form nitrate, NO_3^- [270]. Figure adapted from [270].

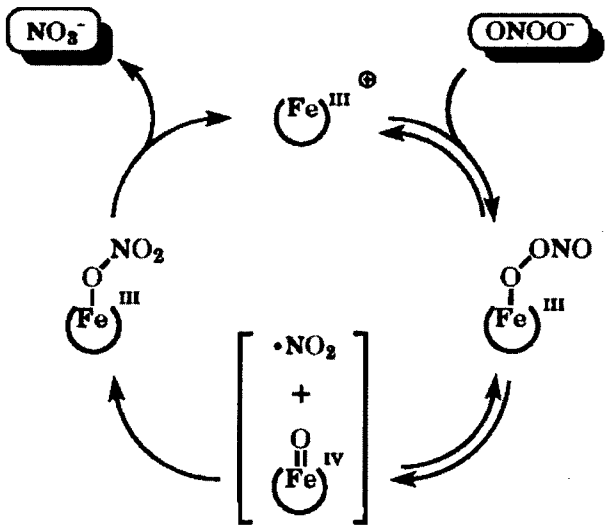

REFERENCES

[1] Poelmann RE, Gittenberger-de Groot AC. Apoptosis as an instrument in cardiovascular development. Birth Defects Res C Embryo Today 2005;75:305-313.

[2] Kroemer G, El Deiry WS, Golstein P, Peter ME, Vaux D, Vandenabeele P, et al. Classification of cell death: recommendations of the Nomenclature Committee on Cell Death. Cell Death Differ 2005;12 Suppl 2:1463-1467.

[3] Nicotera P, Leist M, Ferrando-May E. Apoptosis and necrosis: different execution of the same death. Biochem Soc Symp 1999;66:69-73.

[4] Subczynski WK, Lomnicka M, Hyde JS. Permeability of nitric oxide through lipid bilayer membranes. Free Radic Res 1996;24:343-349.

[5] Hibbs JB, Jr., Taintor RR, Vavrin Z, Rachlin EM. Nitric oxide: a cytotoxic activated macrophage effector molecule. Biochem Biophys Res Commun 1988;157:87-94.

[6] Kelm M, Schrader J. Nitric oxide release from the isolated guinea pig heart. Eur J Pharmacol 1988;155:317-321.

[7] Oyama J, Frantz S, Blais JC, Jr., Kelly RA, Bourcier T. Nitric oxide, cell death, and heart failure. Heart Fail Rev 2002;7:327-334.

[8] Gow AJ, Ischiropoulos H. Nitric oxide chemistry and cellular signaling. J Cell Physiol 2001;187:277-282.

[9] Radi R, Beckman JS, Bush KM, Freeman BA. Peroxynitrite oxidation of sulfhydryls. The cytotoxic potential of superoxide and nitric oxide. J Biol Chem 1991;266:4244-4250.

[10] Ischiropoulos H, Zhu L, Chen J, Tsai M, Martin JC, Smith CD, et al. Peroxynitrite-mediated tyrosine nitration catalyzed by superoxide dismutase. Arch Biochem Biophys 1992;298:431-437.

[11] Yermilov V, Rubio J, Becchi M, Friesen MD, Pignatelli B, Ohshima H. Formation of 8-nitroguanine by the reaction of guanine with peroxynitrite in vitro. Carcinogenesis 1995;16:2045-2050.

[12] Espey MG, Miranda KM, Feelisch M, Fukuto J, Grisham MB, Vitek MP, et al. Mechanisms of cell death governed by the balance between nitrosative and oxidative stress. Ann N Y Acad Sci 2000;899:209-221.

[13] Lewis RS, Tamir S, Tannenbaum SR, Deen WM. Kinetic analysis of the fate of nitric oxide synthesized by macrophages in vitro. J Biol Chem 1995;270:29350-29355.

[14] Eiserich JP, Cross CE, Jones AD, Halliwell B, van d, V. Formation of nitrating and chlorinating species by reaction of nitrite with hypochlorous acid. A novel mechanism for nitric oxide-mediated protein modification. J Biol Chem 1996;271:19199-19208.

[15] Alderton WK, Cooper CE, Knowles RG. Nitric oxide synthases: structure, function and inhibition. Biochem J 2001;357:593-615.

[16] Giulivi C. Functional implications of nitric oxide produced by mitochondria in mitochondrial metabolism. Biochem J 1998;332 (Pt 3):673-679.

[17] Giulivi C, Poderoso JJ, Boveris A. Production of nitric oxide by mitochondria. J Biol Chem 1998;273:11038-11043.

[18] Elfering SL, Sarkela TM, Giulivi C. Biochemistry of mitochondrial nitric-oxide synthase. J Biol Chem 2002;277:38079-38086.

[19] Palacios M, Knowles RG, Palmer RM, Moncada S. Nitric oxide from L-arginine stimulates the soluble guanylate cyclase in adrenal glands. Biochem Biophys Res Commun 1989;165:802-809.

[20] Bush PA, Gonzalez NE, Griscavage JM, Ignarro LJ. Nitric oxide synthase from cerebellum catalyzes the formation of equimolar quantities of nitric oxide and citrulline from L-arginine. Biochem Biophys Res Commun 1992;185:960-966.

[21] Silvagno F, Xia H, Bredt DS. Neuronal nitric-oxide synthase-mu, an alternatively spliced isoform expressed in differentiated skeletal muscle. J Biol Chem 1996;271:11204-11208.

[22] Xu KY, Huso DL, Dawson TM, Bredt DS, Becker LC. Nitric oxide synthase in cardiac sarcoplasmic reticulum. Proc Natl Acad Sci U S A 1999;96:657-662.

[23] Esteban FJ, Pedrosa JA, Jimenez A, Fernandez AP, Bentura ML, Martinez-Murillo R, et al. Distribution of neuronal nitric oxide synthase in the rat liver. Neurosci Lett 1997;226:99-102.

[24] Knowles RG, Palacios M, Palmer RM, Moncada S. Formation of nitric oxide from L-arginine in the central nervous system: a transduction mechanism for stimulation of the soluble guanylate cyclase. Proc Natl Acad Sci U S A 1989;86:5159-5162.

[25] Su Z, Blazing MA, Fan D, George SE. The calmodulin-nitric oxide synthase interaction. Critical role of the calmodulin latch domain in enzyme activation. J Biol Chem 1995;270:29117-29122.

[26] Venema RC, Sayegh HS, Kent JD, Harrison DG. Identification, characterization, and comparison of the calmodulin-binding domains of the endothelial and inducible nitric oxide synthases. J Biol Chem 1996;271:6435-6440.

[27] Sessa WC, Barber CM, Lynch KR. Mutation of N-myristoylation site converts endothelial cell nitric oxide synthase from a membrane to a cytosolic protein. Circ Res 1993;72:921-924.

[28] Hewett SJ, Corbett JA, McDaniel ML, Choi DW. Interferon-gamma and interleukin-1 beta induce nitric oxide formation from primary mouse astrocytes. Neurosci Lett 1993;164:229-232.

[29] Shindo T, Ikeda U, Ohkawa F, Takahashi M, Funayama H, Nishinaga M, et al. Nitric oxide synthesis in rat cardiac myocytes and fibroblasts. Life Sci 1994;55:1101-1108.

[30] Stuehr DJ, Cho HJ, Kwon NS, Weise MF, Nathan CF. Purification and characterization of the cytokine-induced macrophage nitric oxide synthase: an FAD- and FMN-containing flavoprotein. Proc Natl Acad Sci U S A 1991;88:7773-7777.

[31] Rogers NE, Ignarro LJ. Constitutive nitric oxide synthase from cerebellum is reversibly inhibited by nitric oxide formed from L-arginine. Biochem Biophys Res Commun 1992;189:242-249.

[32] Caulfield JL, Wishnok JS, Tannenbaum SR. Nitric oxide-induced deamination of cytosine and guanine in deoxynucleosides and oligonucleotides. J Biol Chem 1998;273:12689-12695.

[33] Nakano T, Katafuchi A, Shimizu R, Terato H, Suzuki T, Tauchi H, et al. Repair activity of base and nucleotide excision repair enzymes for guanine lesions induced by nitrosative stress. Nucleic Acids Res 2005;33:2181-2191.

[34] Burney S, Caulfield JL, Niles JC, Wishnok JS, Tannenbaum SR. The chemistry of DNA damage from nitric oxide and peroxynitrite. Mutat Res 1999;424:37-49.

[35] Sawa T, Ohshima H. Nitrative DNA damage in inflammation and its possible role in carcinogenesis. Nitric Oxide 2006;14:91-100.

[36] Yermilov V, Rubio J, Ohshima H. Formation of 8-nitroguanine in DNA treated with peroxynitrite in vitro and its rapid removal from DNA by depurination. FEBS Lett 1995;376:207-210.

[37] Douki T, Cadet J. Peroxynitrite mediated oxidation of purine bases of nucleosides and isolated DNA. Free Radic Res 1996;24:369-380.

[38] deRojas-Walker T, Tamir S, Ji H, Wishnok JS, Tannenbaum SR. Nitric oxide induces oxidative damage in addition to deamination in macrophage DNA. Chem Res Toxicol 1995;8:473-477.

[39] Uppu RM, Cueto R, Squadrito GL, Salgo MG, Pryor WA. Competitive reactions of peroxynitrite with 2'-deoxyguanosine and 7,8-dihydro-8-oxo-2'-deoxyguanosine (8-oxodG): relevance to the formation of 8-oxodG in DNA exposed to peroxynitrite. Free Radic Biol Med 1996;21:407-411.

[40] Koppenol WH, Moreno JJ, Pryor WA, Ischiropoulos H, Beckman JS. Peroxynitrite, a cloaked oxidant formed by nitric oxide and superoxide. Chem Res Toxicol 1992;5:834-842.

[41] Ohshima H, Gilibert I, Bianchini F. Induction of DNA strand breakage and base oxidation by nitroxyl anion through hydroxyl radical production. Free Radic Biol Med 1999;26:1305-1313.

[42] Mirza UA, Chait BT, Lander HM. Monitoring reactions of nitric oxide with peptides and proteins by electrospray ionization-mass spectrometry. J Biol Chem 1995;270:17185-17188.

[43] Broillet MC. S-nitrosylation of proteins. Cell Mol Life Sci 1999;55:1036-1042.

[44] Marshall HE, Stamler JS. Inhibition of NF-kappa B by S-nitrosylation. Biochemistry 2001;40:1688-1693.

[45] Ding H, Demple B. Direct nitric oxide signal transduction via nitrosylation of iron-sulfur centers in the SoxR transcription activator. Proc Natl Acad Sci U S A 2000;97:5146-5150.

[46] Kim PK, Kwon YG, Chung HT, Kim YM. Regulation of caspases by nitric oxide. Ann N Y Acad Sci 2002;962:42-52.

[47] Ischiropoulos H. Biological selectivity and functional aspects of protein tyrosine nitration. Biochem Biophys Res Commun 2003;305:776-783.

[48] Bartesaghi S, Ferrer-Sueta G, Peluffo G, Valez V, Zhang H, Kalyanaraman B, et al. Protein tyrosine nitration in hydrophilic and hydrophobic environments. Amino Acids 2006.

[49] Souza JM, Daikhin E, Yudkoff M, Raman CS, Ischiropoulos H. Factors determining the selectivity of protein tyrosine nitration. Arch Biochem Biophys 1999;371:169-178.

[50] Berlett BS, Friguet B, Yim MB, Chock PB, Stadtman ER. Peroxynitrite-mediated nitration of tyrosine residues in Escherichia coli glutamine synthetase mimics adenylylation: relevance to signal transduction. Proc Natl Acad Sci U S A 1996;93:1776-1780.

[51] Cassina AM, Hodara R, Souza JM, Thomson L, Castro L, Ischiropoulos H, et al. Cytochrome c nitration by peroxynitrite. J Biol Chem 2000;275:21409-21415.

[52] MacMillan-Crow LA, Thompson JA. Tyrosine modifications and inactivation of active site manganese superoxide dismutase mutant (Y34F) by peroxynitrite. Arch Biochem Biophys 1999;366:82-88.

[53] Balafanova Z, Bolli R, Zhang J, Zheng Y, Pass JM, Bhatnagar A, et al. Nitric oxide (NO) induces nitration of protein kinase Cepsilon (PKCepsilon), facilitating PKCepsilon translocation via enhanced PKCepsilon -RACK2 interactions: a novel mechanism of no-triggered activation of PKCepsilon. J Biol Chem 2002;277:15021-15027.

[54] Kim YM, Bergonia HA, Muller C, Pitt BR, Watkins WD, Lancaster JR, Jr. Loss and degradation of enzyme-bound heme induced by cellular nitric oxide synthesis. J Biol Chem 1995;270:5710-5713.

[55] Gorbunov NV, Osipov AN, Day BW, Zayas-Rivera B, Kagan VE, Elsayed NM. Reduction of ferrylmyoglobin and ferrylhemoglobin by nitric oxide: a protective mechanism against ferryl hemoprotein-induced oxidations. Biochemistry 1995;34:6689-6699.

[56] Craven PA, DeRubertis FR. Requirement for heme in the activation of purified guanylate cyclase by nitric oxide. Biochim Biophys Acta 1983;745:310-321.

[57] Mason MG, Nicholls P, Wilson MT, Cooper CE. Nitric oxide inhibition of respiration involves both competitive (heme) and noncompetitive (copper) binding to cytochrome c oxidase. Proc Natl Acad Sci U S A 2006;103:708-713.

[58] Khatsenko O, Kikkawa Y. Nitric oxide differentially affects constitutive cytochrome P450 isoforms in rat liver. J Pharmacol Exp Ther 1997;280:1463-1470.

[59] Wink DA, Osawa Y, Darbyshire JF, Jones CR, Eshenaur SC, Nims RW. Inhibition of cytochromes P450 by nitric oxide and a nitric oxide-releasing agent. Arch Biochem Biophys 1993;300:115-123.

[60] St Croix CM, Wasserloos KJ, Dineley KE, Reynolds IJ, Levitan ES, Pitt BR. Nitric oxide-induced changes in intracellular zinc homeostasis are mediated by metallothionein/thionein. Am J Physiol Lung Cell Mol Physiol 2002;282:L185-L192.

[61] Jackson TA, Yikilmaz E, Miller AF, Brunold TC. Spectroscopic and computational study of a non-heme iron [Fe-NO]7 system: exploring the geometric and electronic structures of the nitrosyl adduct of iron superoxide dismutase. J Am Chem Soc 2003;125:8348-8363.

[62] Castro L, Rodriguez M, Radi R. Aconitase is readily inactivated by peroxynitrite, but not by its precursor, nitric oxide. J Biol Chem 1994;269:29409-29415.

[63] Niquet J, Baldwin RA, Allen SG, Fujikawa DG, Wasterlain CG. Hypoxic neuronal necrosis: protein synthesis-independent activation of a cell death program. Proc Natl Acad Sci U S A 2003;100:2825-2830.

[64] Niquet J, Liu H, Wasterlain CG. Programmed neuronal necrosis and status epilepticus. Epilepsia 2005;46 Suppl 5:43-48.

[65] Almeida A, Bolanos JP. A transient inhibition of mitochondrial ATP synthesis by nitric oxide synthase activation triggered apoptosis in primary cortical neurons. J Neurochem 2001;77:676-690.

[66] Leist M, Single B, Naumann H, Fava E, Simon B, Kuhnle S, et al. Inhibition of mitochondrial ATP generation by nitric oxide switches apoptosis to necrosis. Exp Cell Res 1999;249:396-403.

[67] Cleeter MW, Cooper JM, Darley-Usmar VM, Moncada S, Schapira AH. Reversible inhibition of cytochrome c oxidase, the terminal enzyme of the mitochondrial respiratory chain, by nitric oxide. Implications for neurodegenerative diseases. FEBS Lett 1994;345:50-54.

[68] Persichini T, Mazzone V, Polticelli F, Moreno S, Venturini G, Clementi E, et al. Mitochondrial type I nitric oxide synthase physically interacts with cytochrome c oxidase. Neurosci Lett 2005;384:254-259.

[69] Cassina A, Radi R. Differential inhibitory action of nitric oxide and peroxynitrite on mitochondrial electron transport. Arch Biochem Biophys 1996;328:309-316.

[70] Pearce LL, Kanai AJ, Epperly MW, Peterson J. Nitrosative stress results in irreversible inhibition of purified mitochondrial complexes I and III without modification of cofactors. Nitric Oxide 2005;13:254-263.

[71] Larson SK, Dwyer D, Lo HH, Ghafourifar P. Mitochondrial cytochrome c reacts with nitric oxide via S-nitrosation. Biochem Biophys Res Commun 2006;342:991-995.

[72] Messmer UK, Brune B. Modification of macrophage glyceraldehyde-3-phosphate dehydrogenase in response to nitric oxide. Eur J Pharmacol 1996;302:171-182.

[73] Padgett CM, Whorton AR. S-nitrosoglutathione reversibly inhibits GAPDH by S-nitrosylation. Am J Physiol 1995;269:C739-C749.

[74] Welsh N, Sandler S. Interleukin-1 beta induces nitric oxide production and inhibits the activity of aconitase without decreasing glucose oxidation rates in isolated mouse pancreatic islets. Biochem Biophys Res Commun 1992;182:333-340.

[75] Bal-Price A, Brown GC. Nitric-oxide-induced necrosis and apoptosis in PC12 cells mediated by mitochondria. J Neurochem 2000;75:1455-1464.

[76] Zhang J, Dawson VL, Dawson TM, Snyder SH. Nitric oxide activation of poly(ADP-ribose) synthetase in neurotoxicity. Science 1994;263:687-689.

[77] Melino G, Bernassola F, Knight RA, Corasaniti MT, Nistico G, Finazzi-Agro A. S-nitrosylation regulates apoptosis. Nature 1997;388:432-433.

[78] Uchiyama T, Otani H, Okada T, Ninomiya H, Kido M, Imamura H, et al. Nitric oxide induces caspase-dependent apoptosis and necrosis in neonatal rat cardiomyocytes. J Mol Cell Cardiol 2002;34:1049-1061.

[79] Los M, Mozoluk M, Ferrari D, Stepczynska A, Stroh C, Renz A, et al. Activation and caspase-mediated inhibition of PARP: a molecular switch between fibroblast necrosis and apoptosis in death receptor signaling. Mol Biol Cell 2002;13:978-988.

[80] Regula KM, Kirshenbaum LA. Apoptosis of ventricular myocytes: a means to an end. J Mol Cell Cardiol 2005;38:3-13.

[81] Kim JS, He L, Lemasters JJ. Mitochondrial permeability transition: a common pathway to necrosis and apoptosis. Biochem Biophys Res Commun 2003;304:463-470.

[82] Vieira HL, Belzacq AS, Haouzi D, Bernassola F, Cohen I, Jacotot E, et al. The adenine nucleotide translocator: a target of nitric oxide, peroxynitrite, and 4-hydroxynonenal. Oncogene 2001;20:4305-4316.

[83] Piantadosi CA, Tatro LG, Whorton AR. Nitric oxide and differential effects of ATP on mitochondrial permeability transition. Nitric Oxide 2002;6:45-60.

[84] Novgorodov SA, Gudz TI. Permeability transition pore of the inner mitochondrial membrane can operate in two open states with different selectivities. J Bioenerg Biomembr 1996;28:139-146.

[85] Hirsch T, Marzo I, Kroemer G. Role of the mitochondrial permeability transition pore in apoptosis. Biosci Rep 1997;17:67-76.

[86] Andreka P, Tran T, Webster KA, Bishopric NH. Nitric oxide and promotion of cardiac myocyte apoptosis. Mol Cell Biochem 2004;263:35-53.

[87] Cheng EH, Wei MC, Weiler S, Flavell RA, Mak TW, Lindsten T, et al. BCL-2, BCL-X(L) sequester BH3 domain-only molecules preventing BAX- and BAK-mediated mitochondrial apoptosis. Mol Cell 2001;8:705-711.

[88] Marzo I, Brenner C, Zamzami N, Jurgensmeier JM, Susin SA, Vieira HL, et al. Bax and adenine nucleotide translocator cooperate in the mitochondrial control of apoptosis. Science 1998;281:2027-2031.

[89] Messmer UK, Reed UK, Brune B. Bcl-2 protects macrophages from nitric oxide-induced apoptosis. J Biol Chem 1996;271:20192-20197.

[90] Schneider P, Tschopp J. Apoptosis induced by death receptors. Pharm Acta Helv 2000;74:281-286.

[91] De Nadai C, Sestili P, Cantoni O, Lievremont JP, Sciorati C, Barsacchi R, et al. Nitric oxide inhibits tumor necrosis factor-alpha-induced apoptosis by reducing the generation of ceramide. Proc Natl Acad Sci U S A 2000;97:5480-5485.

[92] Thornberry NA, Lazebnik Y. Caspases: enemies within. Science 1998;281:1312-1316.

[93] Li J, Billiar TR, Talanian RV, Kim YM. Nitric oxide reversibly inhibits seven members of the caspase family via S-nitrosylation. Biochem Biophys Res Commun 1997;240:419-424.

[94] Mohr S, Zech B, Lapetina EG, Brune B. Inhibition of caspase-3 by S-nitrosation and oxidation caused by nitric oxide. Biochem Biophys Res Commun 1997;238:387-391.

[95] Zhou P, Qian L, Iadecola C. Nitric oxide inhibits caspase activation and apoptotic morphology but does not rescue neuronal death. J Cereb Blood Flow Metab 2005;25:348-357.

[96] Maejima Y, Adachi S, Morikawa K, Ito H, Isobe M. Nitric oxide inhibits myocardial apoptosis by preventing caspase-3 activity via S-nitrosylation. J Mol Cell Cardiol 2005;38:163-174.

[97] Udupi V, Yu M, Malaviya S, Saavedra JE, Shami PJ. JS-K, a nitric oxide prodrug, induces cytochrome c release and caspase activation in HL-60 myeloid leukemia cells. Leuk Res 2006.

[98] Yabuki M, Tsutsui K, Horton AA, Yoshioka T, Utsumi K. Caspase activation and cytochrome c release during HL-60 cell apoptosis induced by a nitric oxide donor. Free Radic Res 2000;32:507-514.

[99] Du C, Guan Q, Diao H, Yin Z, Jevnikar AM. Nitric oxide induces apoptosis in renal tubular epithelial cells through activation of caspase-8. Am J Physiol Renal Physiol 2006;290:F1044-F1054.

[100] Zhou X, Gordon SA, Kim YM, Hoffman RA, Chen Y, Zhang XR, et al. Nitric oxide induces thymocyte apoptosis via a caspase-1-dependent mechanism. J Immunol 2000;165:1252-1258.

[101] Cary SP, Winger JA, Derbyshire ER, Marletta MA. Nitric oxide signaling: no longer simply on or off. Trends Biochem Sci 2006;31:231-239.

[102] Blaise GA, Gauvin D, Gangal M, Authier S. Nitric oxide, cell signaling and cell death. Toxicology 2005;208:177-192.

[103] Shimojo T, Hiroe M, Ishiyama S, Ito H, Nishikawa T, Marumo F. Nitric oxide induces apoptotic death of cardiomyocytes via a cyclic-GMP-dependent pathway. Exp Cell Res 1999;247:38-47.

[104] Suenobu N, Shichiri M, Iwashina M, Marumo F, Hirata Y. Natriuretic peptides and nitric oxide induce endothelial apoptosis via a cGMP-dependent mechanism. Arterioscler Thromb Vasc Biol 1999;19:140-146.

[105] Loweth AC, Williams GT, Scarpello JH, Morgan NG. Evidence for the involvement of cGMP and protein kinase G in nitric oxide-induced apoptosis in the pancreatic B-cell line, HIT-T15. FEBS Lett 1997;400:285-288.

[106] Weller R, Schwentker A, Billiar TR, Vodovotz Y. Autologous nitric oxide protects mouse and human keratinocytes from ultraviolet B radiation-induced apoptosis. Am J Physiol Cell Physiol 2003;284:C1140-C1148.

[107] Heinloth A, Brune B, Fischer B, Galle J. Nitric oxide prevents oxidised LDL-induced p53 accumulation, cytochrome c translocation, and apoptosis in macrophages via guanylate cyclase stimulation. Atherosclerosis 2002;162:93-101.

[108] Chun SY, Eisenhauer KM, Kubo M, Hsueh AJ. Interleukin-1 beta suppresses apoptosis in rat ovarian follicles by increasing nitric oxide production. Endocrinology 1995;136:3120-3127.

[109] Fiscus RR, Yuen JP, Chan SL, Kwong JH, Chew SB. Nitric oxide and cyclic GMP as pro- and anti-apoptotic agents. J Card Surg 2002;17:336-339.

[110] Genaro AM, Hortelano S, Alvarez A, Martinez C, Bosca L. Splenic B lymphocyte programmed cell death is prevented by nitric oxide release through mechanisms involving sustained Bcl-2 levels. J Clin Invest 1995;95:1884-1890.

[111] Kim YM, Kim TH, Seol DW, Talanian RV, Billiar TR. Nitric oxide suppression of apoptosis occurs in association with an inhibition of Bcl-2 cleavage and cytochrome c release. J Biol Chem 1998;273:31437-31441.

[112] Kim YM, Chung HT, Kim SS, Han JA, Yoo YM, Kim KM, et al. Nitric oxide protects PC12 cells from serum deprivation-induced apoptosis by cGMP-dependent inhibition of caspase signaling. J Neurosci 1999;19:6740-6747.

[113] Takuma K, Phuagphong P, Lee E, Mori K, Baba A, Matsuda T. Anti-apoptotic effect of cGMP in cultured astrocytes: inhibition by cGMP-dependent protein kinase of mitochondrial permeable transition pore. J Biol Chem 2001;276:48093-48099.

[114] Ciani E, Virgili M, Contestabile A. Akt pathway mediates a cGMP-dependent survival role of nitric oxide in cerebellar granule neurones. J Neurochem 2002;81:218-228.

[115] Tejedo JR, Cahuana GM, Ramirez R, Esbert M, Jimenez J, Sobrino F, et al. nitric oxide triggers the phosphatidylinositol 3-kinase/Akt survival pathway in insulin-producing RINm5F cells by arousing Src to activate insulin receptor substrate-1. Endocrinology 2004;145:2319-2327.

[116] Palmer RM, Ferrige AG, Moncada S. Nitric oxide release accounts for the biological activity of endothelium-derived relaxing factor. Nature 1987;327:524-526.

[117] Sears CE, Bryant SM, Ashley EA, Lygate CA, Rakovic S, Wallis HL, et al. Cardiac neuronal nitric oxide synthase isoform regulates myocardial contraction and calcium handling. Circ Res 2003;92:e52-e59.

[118] Herring N, Paterson DJ. Nitric oxide-cGMP pathway facilitates acetylcholine release and bradycardia during vagal nerve stimulation in the guinea-pig in vitro. J Physiol 2001;535:507-518.

[119] Balligand JL, Kelly RA, Marsden PA, Smith TW, Michel T. Control of cardiac muscle cell function by an endogenous nitric oxide signaling system. Proc Natl Acad Sci U S A 1993;90:347-351.

[120] Radomski MW, Salas E. Nitric oxide--biological mediator, modulator and factor of injury: its role in the pathogenesis of atherosclerosis. Atherosclerosis 1995;118 Suppl:S69-S80.

[121] Luscher TF. Imbalance of endothelium-derived relaxing and contracting factors. A new concept in hypertension? Am J Hypertens 1990;3:317-330.

[122] Ing DJ, Zang J, Dzau VJ, Webster KA, Bishopric NH. Modulation of cytokine-induced cardiac myocyte apoptosis by nitric oxide, Bak, and Bcl-x. Circ Res 1999;84:21-33.

[123] Sam F, Sawyer DB, Xie Z, Chang DL, Ngoy S, Brenner DA, et al. Mice lacking inducible nitric oxide synthase have improved left ventricular contractile function and reduced apoptotic cell death late after myocardial infarction. Circ Res 2001;89:351-356.

[124] Pinsky DJ, Cai B, Yang X, Rodriguez C, Sciacca RR, Cannon PJ. The lethal effects of cytokine-induced nitric oxide on cardiac myocytes are blocked by nitric oxide synthase antagonism or transforming growth factor beta. J Clin Invest 1995;95:677-685.

[125] Koglin J, Granville DJ, Glysing-Jensen T, Mudgett JS, Carthy CM, McManus BM, et al. Attenuated acute cardiac rejection in NOS2 -/- recipients correlates with reduced apoptosis. Circulation 1999;99:836-842.

[126] Mani AR, Ippolito S, Ollosson R, Moore KP. Nitration of cardiac proteins is associated with abnormal cardiac chronotropic responses in rats with biliary cirrhosis. Hepatology 2006;43:847-856.

[127] Turko IV, Murad F. Protein nitration in cardiovascular diseases. Pharmacol Rev 2002;54:619-634.

[128] Turko IV, Li L, Aulak KS, Stuehr DJ, Chang JY, Murad F. Protein tyrosine nitration in the mitochondria from diabetic mouse heart. Implications to dysfunctional mitochondria in diabetes. J Biol Chem 2003;278:33972-33977.

[129] Kanski J, Behring A, Pelling J, Schoneich C. Proteomic identification of 3-nitrotyrosine-containing rat cardiac proteins: effects of biological aging. Am J Physiol Heart Circ Physiol 2005;288:H371-H381.

[130] Murray J, Taylor SW, Zhang B, Ghosh SS, Capaldi RA. Oxidative damage to mitochondrial complex I due to peroxynitrite: identification of reactive tyrosines by mass spectrometry. J Biol Chem 2003;278:37223-37230.

[131] Mihm MJ, Bauer JA. Peroxynitrite-induced inhibition and nitration of cardiac myofibrillar creatine kinase. Biochimie 2002;84:1013-1019.

[132] Mihm MJ, Yu F, Reiser PJ, Bauer JA. Effects of peroxynitrite on isolated cardiac trabeculae: selective impact on myofibrillar energetic controllers. Biochimie 2003;85:587-596.

[133] Lokuta AJ, Maertz NA, Meethal SV, Potter KT, Kamp TJ, Valdivia HH, et al. Increased nitration of sarcoplasmic reticulum Ca2+-ATPase in human heart failure. Circulation 2005;111:988-995.

[134] Borbely A, Toth A, Edes I, Virag L, Papp JG, Varro A, et al. Peroxynitrite-induced alpha-actinin nitration and contractile alterations in isolated human myocardial cells. Cardiovasc Res 2005;67:225-233.

[135] Bachmaier K, Neu N, Pummerer C, Duncan GS, Mak TW, Matsuyama T, et al. iNOS expression and nitrotyrosine formation in the myocardium in response to inflammation is controlled by the interferon regulatory transcription factor 1. Circulation 1997;96:585-591.

[136] Cesselli D, Jakoniuk I, Barlucchi L, Beltrami AP, Hintze TH, Nadal-Ginard B, et al. Oxidative stress-mediated cardiac cell death is a major determinant of ventricular dysfunction and failure in dog dilated cardiomyopathy. Circ Res 2001;89:279-286.

[137] Liu P, Hock CE, Nagele R, Wong PY. Formation of nitric oxide, superoxide, and peroxynitrite in myocardial ischemia-reperfusion injury in rats. Am J Physiol 1997;272:H2327-H2336.

[138] Kastan MB, Onyekwere O, Sidransky D, Vogelstein B, Craig RW. Participation of p53 protein in the cellular response to DNA damage. Cancer Res 1991;51:6304-6311.

[139] Yu J, Zhang L. The transcriptional targets of p53 in apoptosis control. Biochem Biophys Res Commun 2005;331:851-858.

[140] Liu Y, Kulesz-Martin M. p53 protein at the hub of cellular DNA damage response pathways through sequence-specific and non-sequence-specific DNA binding. Carcinogenesis 2001;22:851-860.

[141] Shieh SY, Ikeda M, Taya Y, Prives C. DNA damage-induced phosphorylation of p53 alleviates inhibition by MDM2. Cell 1997;91:325-334.

[142] Chowdary DR, Dermody JJ, Jha KK, Ozer HL. Accumulation of p53 in a mutant cell line defective in the ubiquitin pathway. Mol Cell Biol 1994;14:1997-2003.

[143] Gu W, Roeder RG. Activation of p53 sequence-specific DNA binding by acetylation of the p53 C-terminal domain. Cell 1997;90:595-606.

[144] Chuikov S, Kurash JK, Wilson JR, Xiao B, Justin N, Ivanov GS, et al. Regulation of p53 activity through lysine methylation. Nature 2004;432:353-360.

[145] Gostissa M, Hengstermann A, Fogal V, Sandy P, Schwarz SE, Scheffner M, et al. Activation of p53 by conjugation to the ubiquitin-like protein SUMO-1. EMBO J 1999;18:6462-6471.

[146] Xirodimas DP, Saville MK, Bourdon JC, Hay RT, Lane DP. Mdm2-mediated NEDD8 conjugation of p53 inhibits its transcriptional activity. Cell 2004;118:83-97.

[147] Oren M. Regulation of the p53 tumor suppressor protein. J Biol Chem 1999;274:36031-36034.

[148] Rogel A, Popliker M, Webb CG, Oren M. p53 cellular tumor antigen: analysis of mRNA levels in normal adult tissues, embryos, and tumors. Mol Cell Biol 1985;5:2851-2855.

[149] Giannakakou P, Sackett DL, Ward Y, Webster KR, Blagosklonny MV, Fojo T. p53 is associated with cellular microtubules and is transported to the nucleus by dynein. Nat Cell Biol 2000;2:709-717.

[150] Lo KW, Kan HM, Chan LN, Xu WG, Wang KP, Wu Z, et al. The 8-kDa dynein light chain binds to p53-binding protein 1 and mediates DNA damage-induced p53 nuclear accumulation. J Biol Chem 2005;280:8172-8179.

[151] Galigniana MD, Harrell JM, O'Hagen HM, Ljungman M, Pratt WB. Hsp90-binding immunophilins link p53 to dynein during p53 transport to the nucleus. J Biol Chem 2004;279:22483-22489.

[152] Pratt WB, Galigniana MD, Harrell JM, DeFranco DB. Role of hsp90 and the hsp90-binding immunophilins in signalling protein movement. Cell Signal 2004;16:857-872.

[153] Zylicz M, King FW, Wawrzynow A. Hsp70 interactions with the p53 tumour suppressor protein. EMBO J 2001;20:4634-4638.

[154] Murphy ME, Leu JI, George DL. p53 moves to mitochondria: a turn on the path to apoptosis. Cell Cycle 2004;3:836-839.

[155] Momand J, Zambetti GP, Olson DC, George D, Levine AJ. The mdm-2 oncogene product forms a complex with the p53 protein and inhibits p53-mediated transactivation. Cell 1992;69:1237-1245.

[156] Haupt Y, Maya R, Kazaz A, Oren M. Mdm2 promotes the rapid degradation of p53. Nature 1997;387:296-299.

[157] Kubbutat MH, Jones SN, Vousden KH. Regulation of p53 stability by Mdm2. Nature 1997;387:299-303.

[158] Rodriguez MS, Desterro JM, Lain S, Lane DP, Hay RT. Multiple C-terminal lysine residues target p53 for ubiquitin-proteasome-mediated degradation. Mol Cell Biol 2000;20:8458-8467.

[159] Perry ME, Piette J, Zawadzki JA, Harvey D, Levine AJ. The mdm-2 gene is induced in response to UV light in a p53-dependent manner. Proc Natl Acad Sci U S A 1993;90:11623-11627.

[160] Mayo LD, Turchi JJ, Berberich SJ. Mdm-2 phosphorylation by DNA-dependent protein kinase prevents interaction with p53. Cancer Res 1997;57:5013-5016.

[161] Shvarts A, Steegenga WT, Riteco N, van Laar T, Dekker P, Bazuine M, et al. MDMX: a novel p53-binding protein with some functional properties of MDM2. EMBO J 1996;15:5349-5357.

[162] Marine JC, Jochemsen AG. Mdmx as an essential regulator of p53 activity. Biochem Biophys Res Commun 2005;331:750-760.

[163] Jackson MW, Berberich SJ. MdmX protects p53 from Mdm2-mediated degradation. Mol Cell Biol 2000;20:1001-1007.

[164] Stad R, Ramos YF, Little N, Grivell S, Attema J, Der Eb AJ, et al. Hdmx stabilizes Mdm2 and p53. J Biol Chem 2000;275:28039-28044.

[165] Canman CE, Lim DS. The role of ATM in DNA damage responses and cancer. Oncogene 1998;17:3301-3308.

[166] Siliciano JD, Canman CE, Taya Y, Sakaguchi K, Appella E, Kastan MB. DNA damage induces phosphorylation of the amino terminus of p53. Genes Dev 1997;11:3471-3481.

[167] Khosravi R, Maya R, Gottlieb T, Oren M, Shiloh Y, Shkedy D. Rapid ATM-dependent phosphorylation of MDM2 precedes p53 accumulation in response to DNA damage. Proc Natl Acad Sci U S A 1999;96:14973-14977.

[168] Hirao A, Kong YY, Matsuoka S, Wakeham A, Ruland J, Yoshida H, et al. DNA damage-induced activation of p53 by the checkpoint kinase Chk2. Science 2000;287:1824-1827.

[169] Kapoor M, Lozano G. Functional activation of p53 via phosphorylation following DNA damage by UV but not gamma radiation. Proc Natl Acad Sci U S A 1998;95:2834-2837.

[170] Lozano G, Zambetti GP. What have animal models taught us about the p53 pathway? J Pathol 2005;205:206-220.

[171] Bruins W, Zwart E, Attardi LD, Iwakuma T, Hoogervorst EM, Beems RB, et al. Increased sensitivity to UV radiation in mice with a p53 point mutation at Ser389. Mol Cell Biol 2004;24:8884-8894.

[172] Kamijo T, Weber JD, Zambetti G, Zindy F, Roussel MF, Sherr CJ. Functional and physical interactions of the ARF tumor suppressor with p53 and Mdm2. Proc Natl Acad Sci U S A 1998;95:8292-8297.

[173] DiGiammarino EL, Filippov I, Weber JD, Bothner B, Kriwacki RW. Solution structure of the p53 regulatory domain of the p19Arf tumor suppressor protein. Biochemistry 2001;40:2379-2386.

[174] Tao W, Levine AJ. P19(ARF) stabilizes p53 by blocking nucleo-cytoplasmic shuttling of Mdm2. Proc Natl Acad Sci U S A 1999;96:6937-6941.

[175] Honda R, Yasuda H. Association of p19(ARF) with Mdm2 inhibits ubiquitin ligase activity of Mdm2 for tumor suppressor p53. EMBO J 1999;18:22-27.

[176] Nister M, Tang M, Zhang XQ, Yin C, Beeche M, Hu X, et al. p53 must be competent for transcriptional regulation to suppress tumor formation. Oncogene 2005;24:3563-3573.

[177] Kern SE, Kinzler KW, Bruskin A, Jarosz D, Friedman P, Prives C, et al. Identification of p53 as a sequence-specific DNA-binding protein. Science 1991;252:1708-1711.

[178] Foster BA, Coffey HA, Morin MJ, Rastinejad F. Pharmacological rescue of mutant p53 conformation and function. Science 1999;286:2507-2510.

[179] Fridman JS, Lowe SW. Control of apoptosis by p53. Oncogene 2003;22:9030-9040.

[180] Miyashita T, Krajewski S, Krajewska M, Wang HG, Lin HK, Liebermann DA, et al. Tumor suppressor p53 is a regulator of bcl-2 and bax gene expression in vitro and in vivo. Oncogene 1994;9:1799-1805.

[181] Miyashita T, Reed JC. Tumor suppressor p53 is a direct transcriptional activator of the human bax gene. Cell 1995;80:293-299.

[182] Oda E, Ohki R, Murasawa H, Nemoto J, Shibue T, Yamashita T, et al. Noxa, a BH3-only member of the Bcl-2 family and candidate mediator of p53-induced apoptosis. Science 2000;288:1053-1058.

[183] Nakano K, Vousden KH. PUMA, a novel proapoptotic gene, is induced by p53. Mol Cell 2001;7:683-694.

[184] Sax JK, Fei P, Murphy ME, Bernhard E, Korsmeyer SJ, El Deiry WS. BID regulation by p53 contributes to chemosensitivity. Nat Cell Biol 2002;4:842-849.

[185] Owen-Schaub LB, Zhang W, Cusack JC, Angelo LS, Santee SM, Fujiwara T, et al. Wild-type human p53 and a temperature-sensitive mutant induce Fas/APO-1 expression. Mol Cell Biol 1995;15:3032-3040.

[186] Wu GS, Burns TF, McDonald ER, III, Jiang W, Meng R, Krantz ID, et al. KILLER/DR5 is a DNA damage-inducible p53-regulated death receptor gene. Nat Genet 1997;17:141-143.

[187] Moroni MC, Hickman ES, Lazzerini DE, Caprara G, Colli E, Cecconi F, et al. Apaf-1 is a transcriptional target for E2F and p53. Nat Cell Biol 2001;3:552-558.

[188] MacLachlan TK, El Deiry WS. Apoptotic threshold is lowered by p53 transactivation of caspase-6. Proc Natl Acad Sci U S A 2002;99:9492-9497.

[189] Attardi LD, Reczek EE, Cosmas C, Demicco EG, McCurrach ME, Lowe SW, et al. PERP, an apoptosis-associated target of p53, is a novel member of the PMP-22/gas3 family. Genes Dev 2000;14:704-718.

[190] Lin Y, Ma W, Benchimol S. Pidd, a new death-domain-containing protein, is induced by p53 and promotes apoptosis. Nat Genet 2000;26:122-127.

[191] Tinel A, Tschopp J. The PIDDosome, a protein complex implicated in activation of caspase-2 in response to genotoxic stress. Science 2004;304:843-846.

[192] Okamura S, Arakawa H, Tanaka T, Nakanishi H, Ng CC, Taya Y, et al. p53DINP1, a p53-inducible gene, regulates p53-dependent apoptosis. Mol Cell 2001;8:85-94.

[193] Oda K, Arakawa H, Tanaka T, Matsuda K, Tanikawa C, Mori T, et al. p53AIP1, a potential mediator of p53-dependent apoptosis, and its regulation by Ser-46-phosphorylated p53. Cell 2000;102:849-862.

[194] Hwang PM, Bunz F, Yu J, Rago C, Chan TA, Murphy MP, et al. Ferredoxin reductase affects p53-dependent, 5-fluorouracil-induced apoptosis in colorectal cancer cells. Nat Med 2001;7:1111-1117.

[195] Stambolic V, MacPherson D, Sas D, Lin Y, Snow B, Jang Y, et al. Regulation of PTEN transcription by p53. Mol Cell 2001;8:317-325.

[196] Stambolic V, Suzuki A, de la Pompa JL, Brothers GM, Mirtsos C, Sasaki T, et al. Negative regulation of PKB/Akt-dependent cell survival by the tumor suppressor PTEN. Cell 1998;95:29-39.

[197] Zilfou JT, Hoffman WH, Sank M, George DL, Murphy M. The corepressor mSin3a interacts with the proline-rich domain of p53 and protects p53 from proteasome-mediated degradation. Mol Cell Biol 2001;21:3974-3985.

[198] Murphy M, Ahn J, Walker KK, Hoffman WH, Evans RM, Levine AJ, et al. Transcriptional repression by wild-type p53 utilizes histone deacetylases, mediated by interaction with mSin3a. Genes Dev 1999;13:2490-2501.

[199] Hoffman WH, Biade S, Zilfou JT, Chen J, Murphy M. Transcriptional repression of the anti-apoptotic survivin gene by wild type p53. J Biol Chem 2002;277:3247-3257.

[200] Mirza A, McGuirk M, Hockenberry TN, Wu Q, Ashar H, Black S, et al. Human survivin is negatively regulated by wild-type p53 and participates in p53-dependent apoptotic pathway. Oncogene 2002;21:2613-2622.

[201] Ho JS, Ma W, Mao DY, Benchimol S. p53-Dependent transcriptional repression of c-myc is required for G1 cell cycle arrest. Mol Cell Biol 2005;25:7423-7431.

[202] Ambs S, Hussain SP, Harris CC. Interactive effects of nitric oxide and the p53 tumor suppressor gene in carcinogenesis and tumor progression. FASEB J 1997;11:443-448.

[203] Marchenko ND, Zaika A, Moll UM. Death signal-induced localization of p53 protein to mitochondria. A potential role in apoptotic signaling. J Biol Chem 2000;275:16202-16212.

[204] Sansome C, Zaika A, Marchenko ND, Moll UM. Hypoxia death stimulus induces translocation of p53 protein to mitochondria. Detection by immunofluorescence on whole cells. FEBS Lett 2001;488:110-115.

[205] Mihara M, Erster S, Zaika A, Petrenko O, Chittenden T, Pancoska P, et al. p53 has a direct apoptogenic role at the mitochondria. Mol Cell 2003;11:577-590.

[206] Talos F, Petrenko O, Mena P, Moll UM. Mitochondrially targeted p53 has tumor suppressor activities in vivo. Cancer Res 2005;65:9971-9981.

[207] Dumont P, Leu JI, Della PA, III, George DL, Murphy M. The codon 72 polymorphic variants of p53 have markedly different apoptotic potential. Nat Genet 2003;33:357-365.

[208] Crow MT, Mani K, Nam YJ, Kitsis RN. The mitochondrial death pathway and cardiac myocyte apoptosis. Circ Res 2004;95:957-970.

[209] Dejean LM, Martinez-Caballero S, Guo L, Hughes C, Teijido O, Ducret T, et al. Oligomeric Bax is a component of the putative cytochrome c release channel MAC, mitochondrial apoptosis-induced channel. Mol Biol Cell 2005;16:2424-2432.

[210] Petros AM, Nettesheim DG, Wang Y, Olejniczak ET, Meadows RP, Mack J, et al. Rationale for Bcl-xL/Bad peptide complex formation from structure, mutagenesis, and biophysical studies. Protein Sci 2000;9:2528-2534.

[211] Chipuk JE, Bouchier-Hayes L, Kuwana T, Newmeyer DD, Green DR. PUMA couples the nuclear and cytoplasmic proapoptotic function of p53. Science 2005;309:1732-1735.

[212] Leu JI, Dumont P, Hafey M, Murphy ME, George DL. Mitochondrial p53 activates Bak and causes disruption of a Bak-Mcl1 complex. Nat Cell Biol 2004;6:443-450.

[213] Chipuk JE, Kuwana T, Bouchier-Hayes L, Droin NM, Newmeyer DD, Schuler M, et al. Direct activation of Bax by p53 mediates mitochondrial membrane permeabilization and apoptosis. Science 2004;303:1010-1014.

[214] Antonsson B, Montessuit S, Sanchez B, Martinou JC. Bax is present as a high molecular weight oligomer/complex in the mitochondrial membrane of apoptotic cells. J Biol Chem 2001;276:11615-11623.

[215] Rosse T, Olivier R, Monney L, Rager M, Conus S, Fellay I, et al. Bcl-2 prolongs cell survival after Bax-induced release of cytochrome c. Nature 1998;391:496-499.

[216] Antonsson B, Montessuit S, Lauper S, Eskes R, Martinou JC. Bax oligomerization is required for channel-forming activity in liposomes and to trigger cytochrome c release from mitochondria. Biochem J 2000;345 Pt 2:271-278.

[217] Jacotot E, Costantini P, Laboureau E, Zamzami N, Susin SA, Kroemer G. Mitochondrial membrane permeabilization during the apoptotic process. Ann N Y Acad Sci 1999;887:18-30.

[218] Shimizu S, Narita M, Tsujimoto Y. Bcl-2 family proteins regulate the release of apoptogenic cytochrome c by the mitochondrial channel VDAC. Nature 1999;399:483-487.

[219] Narita M, Shimizu S, Ito T, Chittenden T, Lutz RJ, Matsuda H, et al. Bax interacts with the permeability transition pore to induce permeability transition and cytochrome c release in isolated mitochondria. Proc Natl Acad Sci U S A 1998;95:14681-14686.

[220] Harper JW, Adami GR, Wei N, Keyomarsi K, Elledge SJ. The p21 Cdk-interacting protein Cip1 is a potent inhibitor of G1 cyclin-dependent kinases. Cell 1993;75:805-816.

[221] El Deiry WS, Tokino T, Velculescu VE, Levy DB, Parsons R, Trent JM, et al. WAF1, a potential mediator of p53 tumor suppression. Cell 1993;75:817-825.

[222] Gartel AL, Serfas MS, Tyner AL. p21--negative regulator of the cell cycle. Proc Soc Exp Biol Med 1996;213:138-149.

[223] Li R, Waga S, Hannon GJ, Beach D, Stillman B. Differential effects by the p21 CDK inhibitor on PCNA-dependent DNA replication and repair. Nature 1994;371:534-537.

[224] Taylor WR, Stark GR. Regulation of the G2/M transition by p53. Oncogene 2001;20:1803-1815.

[225] Mhawech P. 14-3-3 proteins--an update. Cell Res 2005;15:228-236.

[226] Hermeking H, Lengauer C, Polyak K, He TC, Zhang L, Thiagalingam S, et al. 14-3-3 sigma is a p53-regulated inhibitor of G2/M progression. Mol Cell 1997;1:3-11.

[227] Sengupta S, Harris CC. p53: traffic cop at the crossroads of DNA repair and recombination. Nat Rev Mol Cell Biol 2005;6:44-55.

[228] Lane DP. p53, guardian of the genome. Nature 1992;358:15-16.

[229] Wang XW, Yeh H, Schaeffer L, Roy R, Moncollin V, Egly JM, et al. p53 modulation of TFIIH-associated nucleotide excision repair activity. Nat Genet 1995;10:188-195.

[230] Rubbi CP, Milner J. p53 is a chromatin accessibility factor for nucleotide excision repair of DNA damage. EMBO J 2003;22:975-986.

[231] Gaiddon C, Moorthy NC, Prives C. Ref-1 regulates the transactivation and pro-apoptotic functions of p53 in vivo. EMBO J 1999;18:5609-5621.

[232] Sturzbecher HW, Donzelmann B, Henning W, Knippschild U, Buchhop S. p53 is linked directly to homologous recombination processes via RAD51/RecA protein interaction. EMBO J 1996;15:1992-2002.

[233] Mummenbrauer T, Janus F, Muller B, Wiesmuller L, Deppert W, Grosse F. p53 Protein exhibits 3'-to-5' exonuclease activity. Cell 1996;85:1089-1099.

[234] Messmer UK, Ankarcrona M, Nicotera P, Brune B. p53 expression in nitric oxide-induced apoptosis. FEBS Lett 1994;355:23-26.

[235] Forrester K, Ambs S, Lupold SE, Kapust RB, Spillare EA, Weinberg WC, et al. Nitric oxide-induced p53 accumulation and regulation of inducible nitric oxide synthase expression by wild-type p53. Proc Natl Acad Sci U S A 1996;93:2442-2447.

[236] Ambs S, Ogunfusika MO, Merriam WG, Bennett WP, Billiar TR, Harris CC. Up-regulation of inducible nitric oxide synthase expression in cancer-prone p53 knockout mice. Proc Natl Acad Sci U S A 1998;95:8823-8828.

[237] Messmer UK, Brune B. Nitric oxide-induced apoptosis: p53-dependent and p53-independent signalling pathways. Biochem J 1996;319 (Pt 1):299-305.

[238] Brune B, Golkel C, von Knethen A. Cytokine and low-level nitric oxide prestimulation block p53 accumulation and apoptosis of RAW 264.7 macrophages. Biochem Biophys Res Commun 1996;229:396-401.

[239] Wang X, Michael D, de Murcia G, Oren M. p53 Activation by nitric oxide involves down-regulation of Mdm2. J Biol Chem 2002;277:15697-15702.

[240] Schonhoff CM, Daou MC, Jones SN, Schiffer CA, Ross AH. Nitric oxide-mediated inhibition of Hdm2-p53 binding. Biochemistry 2002;41:13570-13574.

[241] Kaji T, Kaieda I, Hisatsune T, Kaminogawa S. 3-Morpholinosydnonimine hydrochloride induces p53-dependent apoptosis in murine primary neural cells: a critical role for p21(ras)-MAPK-p19(ARF) pathway. Nitric Oxide 2002;6:125-134.

[242] Kim SJ, Hwang SG, Shin DY, Kang SS, Chun JS. p38 kinase regulates nitric oxide-induced apoptosis of articular chondrocytes by accumulating p53 via NFkappa B-

dependent transcription and stabilization by serine 15 phosphorylation. J Biol Chem 2002;277:33501-33508.

[243] McLaughlin LM, Demple B. Nitric oxide-induced apoptosis in lymphoblastoid and fibroblast cells dependent on the phosphorylation and activation of p53. Cancer Res 2005;65:6097-6104.

[244] Ho YS, Wang YJ, Lin JK. Induction of p53 and p21/WAF1/CIP1 expression by nitric oxide and their association with apoptosis in human cancer cells. Mol Carcinog 1996;16:20-31.

[245] Schneiderhan N, Budde A, Zhang Y, Brune B. Nitric oxide induces phosphorylation of p53 and impairs nuclear export. Oncogene 2003;22:2857-2868.

[246] Nakaya N, Lowe SW, Taya Y, Chenchik A, Enikolopov G. Specific pattern of p53 phosphorylation during nitric oxide-induced cell cycle arrest. Oncogene 2000;19:6369-6375.

[247] Chazotte-Aubert L, Hainaut P, Ohshima H. Nitric oxide nitrates tyrosine residues of tumor-suppressor p53 protein in MCF-7 cells. Biochem Biophys Res Commun 2000;267:609-613.

[248] Cobbs CS, Samanta M, Harkins LE, Gillespie GY, Merrick BA, MacMillan-Crow LA. Evidence for peroxynitrite-mediated modifications to p53 in human gliomas: possible functional consequences. Arch Biochem Biophys 2001;394:167-172.

[249] Brockhaus F, Brune B. p53 accumulation in apoptotic macrophages is an energy demanding process that precedes cytochrome c release in response to nitric oxide. Oncogene 1999;18:6403-6410.

[250] Li CQ, Robles AI, Hanigan CL, Hofseth LJ, Trudel LJ, Harris CC, et al. Apoptotic signaling pathways induced by nitric oxide in human lymphoblastoid cells expressing wild-type or mutant p53. Cancer Res 2004;64:3022-3029.

[251] Ishida A, Sasaguri T, Miwa Y, Kosaka C, Taba Y, Abumiya T. Tumor suppressor p53 but not cGMP mediates NO-induced expression of p21(Waf1/Cip1/Sdi1) in vascular smooth muscle cells. Mol Pharmacol 1999;56:938-946.

[252] Yang F, von Knethen A, Brune B. Modulation of nitric oxide-evoked apoptosis by the p53-downstream target p21(WAF1/CIP1). J Leukoc Biol 2000;68:916-922.

[253] Palmero I, Pantoja C, Serrano M. p19ARF links the tumour suppressor p53 to Ras. Nature 1998;395:125-126.

[254] Rabkin SW, Kong JY. Nitroprusside induces cardiomyocyte death: interaction with hydrogen peroxide. Am J Physiol Heart Circ Physiol 2000;279:H3089-H3100.

[255] Borutaite V, Brown GC. Nitric oxide induces apoptosis via hydrogen peroxide, but necrosis via energy and thiol depletion. Free Radic Biol Med 2003;35:1457-1468.

[256] Singh NP, McCoy MT, Tice RR, Schneider EL. A simple technique for quantitation of low levels of DNA damage in individual cells. Exp Cell Res 1988;175:184-191.

[257] Tsang MY, Cowie SE, Rabkin SW. Palmitate increases nitric oxide synthase activity that is involved in palmitate-induced cell death in cardiomyocytes. Nitric Oxide 2004;10:11-19.

[258] Kong JY, Rabkin SW. Palmitate-induced apoptosis in cardiomyocytes is mediated through alterations in mitochondria: prevention by cyclosporin A. Biochim Biophys Acta 2000;1485:45-55.

[259] Kroemer G, Dallaporta B, Resche-Rigon M. The mitochondrial death/life regulator in apoptosis and necrosis. Annu Rev Physiol 1998;60:619-642.

[260] Zamzami N, Susin SA, Marchetti P, Hirsch T, Gomez-Monterrey I, Castedo M, et al. Mitochondrial control of nuclear apoptosis. J Exp Med 1996;183:1533-1544.

[261] Smiley ST, Reers M, Mottola-Hartshorn C, Lin M, Chen A, Smith TW, et al. Intracellular heterogeneity in mitochondrial membrane potentials revealed by a J-aggregate-forming lipophilic cation JC-1. Proc Natl Acad Sci U S A 1991;88:3671-3675.

[262] Mathur A, Hong Y, Kemp BK, Barrientos AA, Erusalimsky JD. Evaluation of fluorescent dyes for the detection of mitochondrial membrane potential changes in cultured cardiomyocytes. Cardiovasc Res 2000;46:126-138.

[263] Kong JY, Rabkin SW. Mitochondrial effects with ceramide-induced cardiac apoptosis are different from those of palmitate. Arch Biochem Biophys 2003;412:196-206.

[264] Komarov PG, Komarova EA, Kondratov RV, Christov-Tselkov K, Coon JS, Chernov MV, et al. A chemical inhibitor of p53 that protects mice from the side effects of cancer therapy. Science 1999;285:1733-1737.

[265] Liu X, Chua CC, Gao J, Chen Z, Landy CL, Hamdy R, et al. Pifithrin-alpha protects against doxorubicin-induced apoptosis and acute cardiotoxicity in mice. Am J Physiol Heart Circ Physiol 2004;286:H933-H939.

[266] Strosznajder RP, Jesko H, Banasik M, Tanaka S. Effects of p53 inhibitor on survival and death of cells subjected to oxidative stress. J Physiol Pharmacol 2005;56 Suppl 4:215-221.

[267] El Gibaly AM, Scheuer C, Menger MD, Vollmar B. Improvement of rat liver graft quality by pifithrin-alpha-mediated inhibition of hepatocyte necrapoptosis. Hepatology 2004;39:1553-1562.

[268] Kong JY, Klassen SS, Rabkin SW. Ceramide activates a mitochondrial p38 mitogen-activated protein kinase: a potential mechanism for loss of mitochondrial transmembrane potential and apoptosis. Mol Cell Biochem 2005;278:39-51.

[269] Schluter KD, Weber M, Schraven E, Piper HM. NO donor SIN-1 protects against reoxygenation-induced cardiomyocyte injury by a dual action. Am J Physiol 1994;267:H1461-H1466.

[270] Stern Michael K, Jensen Michael P, Kramer Keith. Peroxynitrite Decomposition Catalysts. J Am Chem Soc 1996;118:8735-8736.

[271] Singh RJ, Hogg N, Joseph J, Kalyanaraman B. Mechanism of nitric oxide release from S-nitrosothiols. J Biol Chem 1996;271:18596-18603.

[272] Smith JN, Dasgupta TP. Kinetics and mechanism of the decomposition of S-nitrosoglutathione by l-ascorbic acid and copper ions in aqueous solution to produce nitric oxide. Nitric Oxide 2000;4:57-66.

[273] Sun J, Xu L, Eu JP, Stamler JS, Meissner G. Nitric oxide, NOC-12, and S-nitrosoglutathione modulate the skeletal muscle calcium release channel/ryanodine receptor by different mechanisms. An allosteric function for O2 in S-nitrosylation of the channel. J Biol Chem 2003;278:8184-8189.

[274] Tsikas D, Sandmann J, Rossa S, Gutzki FM, Frolich JC. Investigations of S-transnitrosylation reactions between low- and high-molecular-weight S-nitroso compounds and their thiols by high-performance liquid chromatography and gas chromatography-mass spectrometry. Anal Biochem 1999;270:231-241.

[275] Arnelle DR, Stamler JS. NO+, NO, and NO- donation by S-nitrosothiols: implications for regulation of physiological functions by S-nitrosylation and acceleration of disulfide formation. Arch Biochem Biophys 1995;318:279-285.

[276] Dasgupta TP, Aquart DV. Transfer of nitric oxide from nitrovasodilators to free thiols--evidence of two distinct stages. Biochem Biophys Res Commun 2005;335:730-733.

[277] Mathews WR, Kerr SW. Biological activity of S-nitrosothiols: the role of nitric oxide. J Pharmacol Exp Ther 1993;267:1529-1537.

[278] Zeng H, Spencer NY, Hogg N. Metabolism of S-nitrosoglutathione by endothelial cells. Am J Physiol Heart Circ Physiol 2001;281:H432-H439.

[279] Hogg N. Biological chemistry and clinical potential of S-nitrosothiols. Free Radic Biol Med 2000;28:1478-1486.

[280] Wu EY, Smith MT, Bellomo G, Di Monte D. Relationships between the mitochondrial transmembrane potential, ATP concentration, and cytotoxicity in isolated rat hepatocytes. Arch Biochem Biophys 1990;282:358-362.

[281] Liu Z, Rudd MA, Freedman JE, Loscalzo J. S-Transnitrosation reactions are involved in the metabolic fate and biological actions of nitric oxide. J Pharmacol Exp Ther 1998;284:526-534.

[282] Stamler JS, Simon DI, Osborne JA, Mullins ME, Jaraki O, Michel T, et al. S-nitrosylation of proteins with nitric oxide: synthesis and characterization of biologically active compounds. Proc Natl Acad Sci U S A 1992;89:444-448.

[283] Feelisch M, Ostrowski J, Noack E. On the mechanism of NO release from sydnonimines. J Cardiovasc Pharmacol 1989;14 Suppl 11:S13-S22.

[284] Singh RJ, Hogg N, Joseph J, Konorev E, Kalyanaraman B. The peroxynitrite generator, SIN-1, becomes a nitric oxide donor in the presence of electron acceptors. Arch Biochem Biophys 1999;361:331-339.

[285] Huie RE, Padmaja S. The reaction of no with superoxide. Free Radic Res Commun 1993;18:195-199.

[286] Beckman JS, Beckman TW, Chen J, Marshall PA, Freeman BA. Apparent hydroxyl radical production by peroxynitrite: implications for endothelial injury from nitric oxide and superoxide. Proc Natl Acad Sci U S A 1990;87:1620-1624.

[287] van d, V, Hoen PA, Wong PS, Bast A, Cross CE. Formation of S-nitrosothiols via direct nucleophilic nitrosation of thiols by peroxynitrite with elimination of hydrogen peroxide. J Biol Chem 1998;273:30255-30262.

[288] Radi R. Kinetic analysis of reactivity of peroxynitrite with biomolecules. Methods Enzymol 1996;269:354-366.

[289] Nagano T. Practical methods for detection of nitric oxide. Luminescence 1999;14:283-290.

[290] Kissner R, Koppenol WH. Product distribution of peroxynitrite decay as a function of pH, temperature, and concentration. J Am Chem Soc 2002;124:234-239.

[291] Trochu JN, Bouhour JB, Kaley G, Hintze TH. Role of endothelium-derived nitric oxide in the regulation of cardiac oxygen metabolism: implications in health and disease. Circ Res 2000;87:1108-1117.

[292] Gerova M. Nitric oxide-compromised hypertension: facts and enigmas. Physiol Res 2000;49:27-35.

[293] Feng Q, Lu X, Jones DL, Shen J, Arnold JM. Increased inducible nitric oxide synthase expression contributes to myocardial dysfunction and higher mortality after myocardial infarction in mice. Circulation 2001;104:700-704.

[294] Pinsky DJ, Aji W, Szabolcs M, Athan ES, Liu Y, Yang YM, et al. Nitric oxide triggers programmed cell death (apoptosis) of adult rat ventricular myocytes in culture. Am J Physiol 1999;277:H1189-H1199.

[295] Brune B, von Knethen A, Sandau KB. Nitric oxide and its role in apoptosis. Eur J Pharmacol 1998;351:261-272.

[296] Kolb JP. Mechanisms involved in the pro- and anti-apoptotic role of NO in human leukemia. Leukemia 2000;14:1685-1694.

[297] Melino G, Catani MV, Corazzari M, Guerrieri P, Bernassola F. Nitric oxide can inhibit apoptosis or switch it into necrosis. Cell Mol Life Sci 2000;57:612-622.

[298] Leist M, Single B, Naumann H, Fava E, Simon B, Kuhnle S, et al. Nitric oxide inhibits execution of apoptosis at two distinct ATP-dependent steps upstream and downstream of mitochondrial cytochrome c release. Biochem Biophys Res Commun 1999;258:215-221.

[299] Umansky V, Schirrmacher V. Nitric oxide-induced apoptosis in tumor cells. Adv Cancer Res 2001;82:107-131.

[300] Stefanelli C, Pignatti C, Tantini B, Stanic I, Bonavita F, Muscari C, et al. Nitric oxide can function as either a killer molecule or an antiapoptotic effector in cardiomyocytes. Biochim Biophys Acta 1999;1450:406-413.

[301] Weiland U, Haendeler J, Ihling C, Albus U, Scholz W, Ruetten H, et al. Inhibition of endogenous nitric oxide synthase potentiates ischemia-reperfusion-induced myocardial apoptosis via a caspase-3 dependent pathway. Cardiovasc Res 2000;45:671-678.

[302] Holm P, Kankaanranta H, Metsa-Ketela T, Moilanen E. Radical releasing properties of nitric oxide donors GEA 3162, SIN-1 and S-nitroso-N-acetylpenicillamine. Eur J Pharmacol 1998;346:97-102.

[303] Trackey JL, Uliasz TF, Hewett SJ. SIN-1-induced cytotoxicity in mixed cortical cell culture: peroxynitrite-dependent and -independent induction of excitotoxic cell death. J Neurochem 2001;79:445-455.

[304] Li JM, Shah AM. Endothelial cell superoxide generation: regulation and relevance for cardiovascular pathophysiology. Am J Physiol Regul Integr Comp Physiol 2004;287:R1014-R1030.

[305] Lieberthal W, Triaca V, Koh JS, Pagano PJ, Levine JS. Role of superoxide in apoptosis induced by growth factor withdrawal. Am J Physiol 1998;275:F691-F702.

[306] Pryor WA, Squadrito GL. The chemistry of peroxynitrite: a product from the reaction of nitric oxide with superoxide. Am J Physiol 1995;268:L699-L722.

[307] McBride AG, Borutaite V, Brown GC. Superoxide dismutase and hydrogen peroxide cause rapid nitric oxide breakdown, peroxynitrite production and subsequent cell death. Biochim Biophys Acta 1999;1454:275-288.

[308] Arstall MA, Sawyer DB, Fukazawa R, Kelly RA. Cytokine-mediated apoptosis in cardiac myocytes: the role of inducible nitric oxide synthase induction and peroxynitrite generation. Circ Res 1999;85:829-840.

[309] Gow AJ, Thom SR, Ischiropoulos H. Nitric oxide and peroxynitrite-mediated pulmonary cell death. Am J Physiol 1998;274:L112-L118.

[310] Leist M, Fava E, Montecucco C, Nicotera P. Peroxynitrite and nitric oxide donors induce neuronal apoptosis by eliciting autocrine excitotoxicity. Eur J Neurosci 1997;9:1488-1498.

[311] Cadenas E, Davies KJ. Mitochondrial free radical generation, oxidative stress, and aging. Free Radic Biol Med 2000;29:222-230.

[312] Sarkela TM, Berthiaume J, Elfering S, Gybina AA, Giulivi C. The modulation of oxygen radical production by nitric oxide in mitochondria. J Biol Chem 2001;276:6945-6949.

[313] Freeman BA, Crapo JD. Biology of disease: free radicals and tissue injury. Lab Invest 1982;47:412-426.

[314] Paravicini TM, Touyz RM. Redox signaling in hypertension. Cardiovasc Res 2006;71:247-258.

[315] Madamanchi NR, Vendrov A, Runge MS. Oxidative stress and vascular disease. Arterioscler Thromb Vasc Biol 2005;25:29-38.

[316] Misko TP, Highkin MK, Veenhuizen AW, Manning PT, Stern MK, Currie MG, et al. Characterization of the cytoprotective action of peroxynitrite decomposition catalysts. J Biol Chem 1998;273:15646-15653.

[317] Jensen MP, Riley DP. Peroxynitrite decomposition activity of iron porphyrin complexes. Inorg Chem 2002;41:4788-4797.

[318] Tan KH, Harrington S, Purcell WM, Hurst RD. Peroxynitrite mediates nitric oxide-induced blood-brain barrier damage. Neurochem Res 2004;29:579-587.

[319] Ferdinandy P, Danial H, Ambrus I, Rothery RA, Schulz R. Peroxynitrite is a major contributor to cytokine-induced myocardial contractile failure. Circ Res 2000;87:241-247.

[320] Heigold S, Sers C, Bechtel W, Ivanovas B, Schafer R, Bauer G. Nitric oxide mediates apoptosis induction selectively in transformed fibroblasts compared to nontransformed fibroblasts. Carcinogenesis 2002;23:929-941.

[321] Lancel S, Tissier S, Mordon S, Marechal X, Depontieu F, Scherpereel A, et al. Peroxynitrite decomposition catalysts prevent myocardial dysfunction and inflammation in endotoxemic rats. J Am Coll Cardiol 2004;43:2348-2358.

[322] Onody A, Csonka C, Giricz Z, Ferdinandy P. Hyperlipidemia induced by a cholesterol-rich diet leads to enhanced peroxynitrite formation in rat hearts. Cardiovasc Res 2003;58:663-670.

[323] Forstermann U, Closs EI, Pollock JS, Nakane M, Schwarz P, Gath I, et al. Nitric oxide synthase isozymes. Characterization, purification, molecular cloning, and functions. Hypertension 1994;23:1121-1131.

[324] Giulivi C. Characterization and function of mitochondrial nitric-oxide synthase. Free Radic Biol Med 2003;34:397-408.

[325] Gomez-Lazaro M, Fernandez-Gomez FJ, Jordan J. p53: twenty five years understanding the mechanism of genome protection. J Physiol Biochem 2004;60:287-307.

[326] Maki CG, Huibregtse JM, Howley PM. In vivo ubiquitination and proteasome-mediated degradation of p53(1). Cancer Res 1996;56:2649-2654.

[327] Freedman DA, Levine AJ. Nuclear export is required for degradation of endogenous p53 by MDM2 and human papillomavirus E6. Mol Cell Biol 1998;18:7288-7293.

[328] Tian B, Liu J, Bitterman PB, Bache RJ. Mechanisms of cytokine induced NO-mediated cardiac fibroblast apoptosis. Am J Physiol Heart Circ Physiol 2002;283:H1958-H1967.

[329] Muhl H, Sandau K, Brune B, Briner VA, Pfeilschifter J. Nitric oxide donors induce apoptosis in glomerular mesangial cells, epithelial cells and endothelial cells. Eur J Pharmacol 1996;317:137-149.

[330] Fehsel K, Kroncke KD, Meyer KL, Huber H, Wahn V, Kolb-Bachofen V. Nitric oxide induces apoptosis in mouse thymocytes. J Immunol 1995;155:2858-2865.

[331] Homer C, Knight DA, Hananeia L, Sheard P, Risk J, Lasham A, et al. Y-box factor YB1 controls p53 apoptotic function. Oncogene 2005;24:8314-8325.

[332] Lee MH, Jang MH, Kim EK, Han SW, Cho SY, Kim CJ. Nitric oxide induces apoptosis in mouse C2C12 myoblast cells. J Pharmacol Sci 2005;97:369-376.

[333] Yung HW, Bal-Price AK, Brown GC, Tolkovsky AM. Nitric oxide-induced cell death of cerebrocortical murine astrocytes is mediated through p53- and Bax-dependent pathways. J Neurochem 2004;89:812-821.

[334] Liang SH, Clarke MF. Regulation of p53 localization. Eur J Biochem 2001;268:2779-2783.

[335] Wang X, Zalcenstein A, Oren M. Nitric oxide promotes p53 nuclear retention and sensitizes neuroblastoma cells to apoptosis by ionizing radiation. Cell Death Differ 2003;10:468-476.

[336] Dasgupta G, Momand J. Geldanamycin prevents nuclear translocation of mutant p53. Exp Cell Res 1997;237:29-37.

[337] Scotto C, Delphin C, Deloulme JC, Baudier J. Concerted regulation of wild-type p53 nuclear accumulation and activation by S100B and calcium-dependent protein kinase C. Mol Cell Biol 1999;19:7168-7180.

[338] Hoagland MS, Hoagland EM, Swanson HI. The p53 inhibitor pifithrin-alpha is a potent agonist of the aryl hydrocarbon receptor. J Pharmacol Exp Ther 2005;314:603-610.

[339] Schafer T, Scheuer C, Roemer K, Menger MD, Vollmar B. Inhibition of p53 protects liver tissue against endotoxin-induced apoptotic and necrotic cell death. FASEB J 2003;17:660-667.

[340] Culmsee C, Zhu X, Yu QS, Chan SL, Camandola S, Guo Z, et al. A synthetic inhibitor of p53 protects neurons against death induced by ischemic and excitotoxic insults, and amyloid beta-peptide. J Neurochem 2001;77:220-228.

[341] Ostling O, Johanson KJ. Microelectrophoretic study of radiation-induced DNA damages in individual mammalian cells. Biochem Biophys Res Commun 1984;123:291-298.

[342] Gopalakrishna P, Khar A. Comet assay to measure DNA damage in apoptotic cells. J Biochem Biophys Methods 1995;30:69-73.

[343] Lin W, Wei X, Xue H, Kelimu M, Tao R, Song Y, et al. Study on DNA strand breaks induced by sodium nitroprusside, a nitric oxide donor, in vivo and in vitro. Mutat Res 2000;466:187-195.

[344] Delaney CA, Green MH, Lowe JE, Green IC. Endogenous nitric oxide induced by interleukin-1 beta in rat islets of Langerhans and HIT-T15 cells causes significant DNA damage as measured by the 'comet' assay. FEBS Lett 1993;333:291-295.

[345] Bentz BG, Hammer ND, Radosevich JA, Haines GK, III. Nitrosative stress induces DNA strand breaks but not caspase mediated apoptosis in a lung cancer cell line. J Carcinog 2004;3:16.

[346] Doulias PT, Barbouti A, Galaris D, Ischiropoulos H. SIN-1-induced DNA damage in isolated human peripheral blood lymphocytes as assessed by single cell gel electrophoresis (comet assay). Free Radic Biol Med 2001;30:679-685.

[347] Eizirik DL, Delaney CA, Green MH, Cunningham JM, Thorpe JR, Pipeleers DG, et al. Nitric oxide donors decrease the function and survival of human pancreatic islets. Mol Cell Endocrinol 1996;118:71-83.

[348] Chien YH, Bau DT, Jan KY. Nitric oxide inhibits DNA-adduct excision in nucleotide excision repair. Free Radic Biol Med 2004;36:1011-1017.

[349] Taimor G, Hofstaetter B, Piper HM. Apoptosis induction by nitric oxide in adult cardiomyocytes via cGMP-signaling and its impairment after simulated ischemia. Cardiovasc Res 2000;45:588-594.

[350] Lindahl T, Andersson A. Rate of chain breakage at apurinic sites in double-stranded deoxyribonucleic acid. Biochemistry 1972;11:3618-3623.

[351] Kitamura Y, Kamoshima W, Shimohama S, Nomura Y, Taniguchi T. Nitric oxide donor-induced p53-sensitive cell death is enhanced by Bcl-2 reduction in human neuroblastoma cells. Neurochem Int 1998;32:93-102.

[352] Reid E, Williamson R. Centrifugation. Methods Enzymol 1974;31:713-733.

[353] Botla R, Spivey JR, Aguilar H, Bronk SF, Gores GJ. Ursodeoxycholate (UDCA) inhibits the mitochondrial membrane permeability transition induced by glycochenodeoxycholate: a mechanism of UDCA cytoprotection. J Pharmacol Exp Ther 1995;272:930-938.

[354] Nemajerova A, Wolff S, Petrenko O, Moll UM. Viral and cellular oncogenes induce rapid mitochondrial translocation of p53 in primary epithelial and endothelial cells early in apoptosis. FEBS Lett 2005;579:6079-6083.

[355] Mihara M, Moll UM. Detection of mitochondrial localization of p53. Methods Mol Biol 2003;234:203-209.

[356] Ortega-Camarillo C, Guzman-Grenfell AM, Garcia-Macedo R, Rosales-Torres AM, Avalos-Rodriguez A, Duran-Reyes G, et al. Hyperglycemia induces apoptosis and p53 mobilization to mitochondria in RINm5F cells. Mol Cell Biochem 2006;281:163-171.

[357] Liu X, Kim CN, Yang J, Jemmerson R, Wang X. Induction of apoptotic program in cell-free extracts: requirement for dATP and cytochrome c. Cell 1996;86:147-157.

[358] Uehara T, Kikuchi Y, Nomura Y. Caspase activation accompanying cytochrome c release from mitochondria is possibly involved in nitric oxide-induced neuronal apoptosis in SH-SY5Y cells. J Neurochem 1999;72:196-205.

[359] Tejedo J, Bernabe JC, Ramirez R, Sobrino F, Bedoya FJ. NO induces a cGMP-independent release of cytochrome c from mitochondria which precedes caspase 3 activation in insulin producing RINm5F cells. FEBS Lett 1999;459:238-243.

[360] Jekabsone A, Dapkunas Z, Brown GC, Borutaite V. S-nitrosothiol-induced rapid cytochrome c release, caspase activation and mitochondrial permeability transition in perfused heart. Biochem Pharmacol 2003;66:1513-1519.

[361] Borutaite V, Morkuniene R, Brown GC. Nitric oxide donors, nitrosothiols and mitochondrial respiration inhibitors induce caspase activation by different mechanisms. FEBS Lett 2000;467:155-159.

[362] Li J, Bombeck CA, Yang S, Kim YM, Billiar TR. Nitric oxide suppresses apoptosis via interrupting caspase activation and mitochondrial dysfunction in cultured hepatocytes. J Biol Chem 1999;274:17325-17333.

[363] Rossig L, Haendeler J, Hermann C, Malchow P, Urbich C, Zeiher AM, et al. Nitric oxide down-regulates MKP-3 mRNA levels: involvement in endothelial cell protection from apoptosis. J Biol Chem 2000;275:25502-25507.

[364] Li PF, Dietz R, von Harsdorf R. p53 regulates mitochondrial membrane potential through reactive oxygen species and induces cytochrome c-independent apoptosis blocked by Bcl-2. EMBO J 1999;18:6027-6036.

[365] Figueroa S, Oset-Gasque MJ, Arce C, Martinez-Honduvilla CJ, Gonzalez MP. Mitochondrial involvement in nitric oxide-induced cellular death in cortical neurons in culture. J Neurosci Res 2006;83:441-449.

[366] Li MH, Jang JH, Surh YJ. Nitric oxide induces apoptosis via AP-1-driven upregulation of COX-2 in rat pheochromocytoma cells. Free Radic Biol Med 2005;39:890-899.

[367] Ho WP, Chen TL, Chiu WT, Tai YT, Chen RM. Nitric Oxide Induces Osteoblast Apoptosis through a Mitochondria-Dependent Pathway. Ann N Y Acad Sci 2005;1042:460-470.

[368] Ly JD, Grubb DR, Lawen A. The mitochondrial membrane potential (deltapsi(m)) in apoptosis; an update. Apoptosis 2003;8:115-128.

[369] Smart N, Mojet MH, Latchman DS, Marber MS, Duchen MR, Heads RJ. IL-6 induces PI 3-kinase and nitric oxide-dependent protection and preserves mitochondrial function in cardiomyocytes. Cardiovasc Res 2006;69:164-177.

[370] Xu Z, Park SS, Mueller RA, Bagnell RC, Patterson C, Boysen PG. Adenosine produces nitric oxide and prevents mitochondrial oxidant damage in rat cardiomyocytes. Cardiovasc Res 2005;65:803-812.

[371] Wang G, Liem DA, Vondriska TM, Honda HM, Korge P, Pantaleon DM, et al. Nitric oxide donors protect murine myocardium against infarction via modulation of mitochondrial permeability transition. Am J Physiol Heart Circ Physiol 2005;288:H1290-H1295.

[372] Martinez-Caballero S, Dejean LM, Jonas EA, Kinnally KW. The role of the mitochondrial apoptosis induced channel MAC in cytochrome c release. J Bioenerg Biomembr 2005;37:155-164.

[373] Brown GC. Nitric oxide and mitochondrial respiration. Biochim Biophys Acta 1999;1411:351-369.

[374] Poderoso JJ, Carreras MC, Lisdero C, Riobo N, Schopfer F, Boveris A. Nitric oxide inhibits electron transfer and increases superoxide radical production in rat heart mitochondria and submitochondrial particles. Arch Biochem Biophys 1996;328:85-92.

[375] Glockzin S, von Knethen A, Scheffner M, Brune B. Activation of the cell death program by nitric oxide involves inhibition of the proteasome. J Biol Chem 1999;274:19581-19586.

[376] Hetz C, Vitte PA, Bombrun A, Rostovtseva TK, Montessuit S, Hiver A, et al. Bax channel inhibitors prevent mitochondrion-mediated apoptosis and protect neurons in a model of global brain ischemia. J Biol Chem 2005;280:42960-42970.

[377] Gow AJ, Farkouh CR, Munson DA, Posencheg MA, Ischiropoulos H. Biological significance of nitric oxide-mediated protein modifications. Am J Physiol Lung Cell Mol Physiol 2004;287:L262-L268.

[378] Hess DT, Matsumoto A, Kim SO, Marshall HE, Stamler JS. Protein S-nitrosylation: purview and parameters. Nat Rev Mol Cell Biol 2005;6:150-166.

[379] Kamisaki Y, Wada K, Bian K, Balabanli B, Davis K, Martin E, et al. An activity in rat tissues that modifies nitrotyrosine-containing proteins. Proc Natl Acad Sci U S A 1998;95:11584-11589.

[380] Alvarez B, Ferrer-Sueta G, Freeman BA, Radi R. Kinetics of peroxynitrite reaction with amino acids and human serum albumin. J Biol Chem 1999;274:842-848.

[381] Eiserich JP, Butler J, van d, V, Cross CE, Halliwell B. Nitric oxide rapidly scavenges tyrosine and tryptophan radicals. Biochem J 1995;310 (Pt 3):745-749.

[382] Bartesaghi S, Valez V, Trujillo M, Peluffo G, Romero N, Zhang H, et al. Mechanistic studies of peroxynitrite-mediated tyrosine nitration in membranes using the hydrophobic probe N-t-BOC-L-tyrosine tert-butyl ester. Biochemistry 2006;45:6813-6825.

[383] Pinzar E, Wang T, Garrido MR, Xu W, Levy P, Bottari SP. Angiotensin II induces tyrosine nitration and activation of ERK1/2 in vascular smooth muscle cells. FEBS Lett 2005;579:5100-5104.

[384] Park SW, Huq MD, Hu X, Wei LN. Tyrosine nitration on p65: a novel mechanism to rapidly inactivate nuclear factor-kappaB. Mol Cell Proteomics 2005;4:300-309.

[385] Knapp LT, Kanterewicz BI, Hayes EL, Klann E. Peroxynitrite-induced tyrosine nitration and inhibition of protein kinase C. Biochem Biophys Res Commun 2001;286:764-770.

[386] Castro L, Eiserich JP, Sweeney S, Radi R, Freeman BA. Cytochrome c: a catalyst and target of nitrite-hydrogen peroxide-dependent protein nitration. Arch Biochem Biophys 2004;421:99-107.

[387] Fernandez PA, Rotello RJ, Rangini Z, Doupe A, Drexler HC, Yuan J. Expression of a specific marker of avian programmed cell death in both apoptosis and necrosis. Proc Natl Acad Sci U S A 1994;91:8641-8645.

[388] Komarova EA, Neznanov N, Komarov PG, Chernov MV, Wang K, Gudkov AV. p53 inhibitor pifithrin alpha can suppress heat shock and glucocorticoid signaling pathways. J Biol Chem 2003;278:15465-15468.

[389] Reviews. Dojin News 108. 2003. 5-11-2006.